

Using metabolomics as a tool to identify critical attributes of tissue engineered cartilaginous microtissues

Niki LOVERDOU

Supervisors:

Prof. dr.ir. Liesbet Geris (U.Liège), supervisor

Prof. dr.ir Kristel Bernaerts (KU Leuven), supervisor

Prof. dr.ir Ioannis Papantoniou (KU Leuven), co-supervisor

Dissertation presented in partial fulfillment of the requirements for the degree of Doctor of Engineering Science:
Mechanical Engineering (PhD)

Using metabolomics as a tool to identify critical attributes of tissue engineered cartilaginous microtissues

Niki LOVERDOU

Examination Committee:

Prof. dr. ir. Jean Lambermont (KU Leuven), chair

Prof. dr.ir. Liesbet Geris (U.Liège), **supervisor**

Prof. dr.ir Kristel Bernaerts (KU Leuven), **supervisor**

Prof. dr.ir Ioannis Papantoniou (KU Leuven), **co-supervisor**

Prof. dr.ir. Jean-Marie Aerts (KU Leuven)

Prof. dr. Geert Carmeliet (KU Leuven)

Prof. dr. Sarah-Maria Fendt (KU Leuven)

Prof. dr.ir. Dominique Teye (U.Liège)

Prof. dr.ir. Eirini Velliou (University College London)

Dissertation presented in partial fulfillment of the requirements for the degree of Doctor of Engineering Science:
Mechanical Engineering (PhD)

© KU Leuven – Faculty of Engineering

Celestijnenlaan 300C box 2419, B-3001 Heverlee (Belgium)

© U.Liège - Faculty of Applied Sciences

Quartier de l'Hôpital, Avenue de l'Hôpital 11 B34, B-4000 Liege (Belgium)

Alle rechten voorbehouden. Niets uit deze uitgave mag worden vermenigvuldigd en/of openbaar gemaakt worden door middel van druk, fotokopie, microfilm, elektronisch of op welke andere wijze ook zonder voorafgaande schriftelijke toestemming van de uitgever.

Tous droits réservés. Aucun extrait de cet ouvrage ne peut être reproduit, ni saisi dans une banque de données, ni communiqué au public, sous quelque forme que ce soit, électronique, mécanique, par photocopie, film ou autre, sans le consentement écrit et préalable de l'éditeur.

All rights reserved. No part of the publication may be reproduced in any form by print, photoprint, microfilm, or any other means without written permission from the publisher.

Acknowledgements

Abstract

Delayed and non-union fractures represent a largely unmet medical need as current treatment options such as bone grafting are not fully efficient, especially for large bone defects. Skeletal tissue engineering, inspired by developmental processes, shows promise for bone and cartilage regeneration, potentially addressing this clinical gap. Despite progress in the field, challenges remain in identifying critical quality attributes that predict the functionality of tissue-engineered products, as well as in scaling up bioprocesses for clinical application. This PhD research investigates metabolomics as a tool for characterizing the differentiation of cartilaginous microtissues in static as well as dynamic culture (bioreactor) setups supporting future scale-up.

The first phase of this PhD focused on metabolic profiling during chondrogenic differentiation of human periosteum-derived cells (hPDCs) into microtissues, a process that has demonstrated success in regenerating critical size tibial defects in small animal models. Stable isotope tracer analysis and exometabolomics were used to map the metabolic changes during differentiation, identifying pathways such as glutamine metabolism, which plays a role in early extracellular matrix (ECM) production and later matrix remodeling. These metabolic profiles align with existing knowledge of growth plate chondrocytes and support the recapitulation of native cartilage features. Notably, the project uncovered a previously underexplored metabolic pathway in this context—glucose-dependent *de novo* fatty acid synthesis—which increased progressively during microtissue differentiation. This pathway's role was further investigated through chemical inhibition experiments, which demonstrated its importance for the differentiation process and subsequent bone formation capacity of the microtissues *in vivo*.

The second phase of the project involved the development and validation of a novel microbioreactor system for the dynamic culture of cartilaginous microtissues in suspension. Dynamic culture conditions, characterized by intermittent shear stress, were found to accelerate chondrogenic differentiation, promoting early commitment to hypertrophy, which is crucial for endochondral ossification. Computational modeling helped optimize the mechanical environment within the bioreactor to prevent shear damage while promoting efficient tissue formation. The dynamic culture also resulted in distinct metabolic signatures obtained from the culture medium, which may serve as non-destructive markers for monitoring tissue quality during scale-up processes. This work suggested that suspension culture in bioreactors could be a scalable platform for producing clinically relevant quantities of tissue-engineered constructs in the future.

Samenvatting

Vertraagde en niet-helende fracturen vormen een grotendeels onvervulde medische behoefte, aangezien huidige behandelingsopties zoals bottransplantatie niet volledig efficiënt zijn, vooral bij grote botdefecten. Skeletale weefselbouwkunde (weefsel engineering), geïnspireerd door ontwikkelingsprocessen, toont potentieel voor de regeneratie van bot en kraakbeen, en kan mogelijk deze klinische lacune opvullen. Ondanks vooruitgang in het veld blijven er uitdagingen bestaan in het identificeren van kritieke kwaliteitskenmerken die de functionaliteit van weefsel-geëngineerde producten voorspellen, evenals in het opschalen van bioprocessen voor klinische toepassingen. Dit doctoraat onderzoekt metabolomics-profielen als een hulpmiddel voor het karakteriseren van de differentiatie van kraakbeenachtige microweefsels in zowel statische als dynamische culturomgevingen (bioreactor), ter ondersteuning van toekomstige opschaling.

De eerste fase van dit doctoraatsonderzoek richtte zich op metabolische profilering tijdens chondrogene differentiatie van menselijke periost-gederiveerde cellen (hPDC's) naar microweefsels, een proces dat succesvol is gebleken bij de regeneratie van kritische tibiale defecten in kleine diermodellen. Stabiele isotoop tracer analyse en exometabolomics werden gebruikt om de metabolische veranderingen tijdens differentiatie in kaart te brengen, waarbij paden zoals glutamine metabolisme werden geïdentificeerd, hetgeen een rol speelt bij vroege extracellulaire matrix (ECM) productie en latere matrix remodellering. Deze metabole profielen komen overeen met de bestaande kennis over groeischijf chondrocyten en ondersteunen het nabootsen van de kenmerken van natuurlijk kraakbeen. Opmerkelijk is dat het project een tot dusver weinig onderzochte metabole route in deze context identificeerde — glucose-afhankelijke de novo vetzuren synthese — die progressief toenam tijdens microweefsel differentiatie. De rol van dit pad werd verder onderzocht door middel van chemische inhibitie-experimenten, die het belang ervan voor het differentiatieproces en het daaropvolgende botvormingsvermogen van de microweefsels in vivo aantoonde.

De tweede fase van het project betrof de ontwikkeling en validatie van een nieuw microbioreactorsysteem voor de dynamische cultuur van kraakbeenachtige microweefsels in suspensie. Dynamische culturomstandigheden, gekenmerkt door intermitterende schuifspanning, versnelden de chondrogene differentiatie, wat leidde tot een vroege aanzet van hypertrofie, cruciaal voor endochondrale ossificatie. Computationale modellering hielp bij het optimaliseren van de mechanische omgeving in de bioreactor om schuifschade te voorkomen en tegelijkertijd efficiënte weefselvorming te bevorderen. Het dynamische

kweekproces resulteerde ook in onderscheidende metabole signaturen die uit het kweekmedium werden verkregen, en die mogelijk kunnen dienen als niet-destructieve merkers voor het monitoren van de weefselkwaliteit tijdens opschaling. Dit onderzoek suggereerde dat suspensiecultuur in bioreactors een schaalbaar platform kan zijn voor de productie van klinisch relevante hoeveelheden van weefsel-geëngineerde constructen in de toekomst.

Résumé

Les fractures retardées et les pseudarthroses représentent un besoin médical largement non satisfait, car les options de traitement actuelles, telles que la greffe osseuse, ne sont pas totalement efficaces, en particulier pour les grands défauts osseux. L'ingénierie tissulaire squelettique, inspirée par les processus de développement, montre des perspectives prometteuses pour la régénération des os et des cartilages, ce qui pourrait combler cette lacune clinique. Malgré les progrès réalisés dans ce domaine, des défis subsistent quant à l'identification des attributs de qualité critiques qui prédisent la fonctionnalité des produits issus de l'ingénierie tissulaire, ainsi que dans la mise à l'échelle des bioprocédés pour les applications cliniques. Cette recherche doctorale explore le profilage métabolomique comme outil de caractérisation de la différenciation de micro-tissus cartilagineux dans des environnements de culture statique et dynamique (bioprocédés), pour soutenir les futurs processus de mise à l'échelle.

La première phase de cette thèse s'est concentrée sur le profil métabolique au cours de la différenciation chondrogénique des cellules dérivées du périoste humain (hPDC) en micro-tissus, un processus qui a démontré son succès dans la régénération de défauts critiques du tibia dans des modèles animaux de petite taille. L'analyse par traceur isotopique stable et l'exométabolomique ont été utilisées pour cartographier les changements métaboliques au cours de la différenciation, identifiant des voies telles que le métabolisme de la glutamine, qui joue un rôle dans la production précoce de matrice extracellulaire (ECM) et dans le remodelage ultérieur de cette matrice. Ces profils métaboliques correspondent aux connaissances existantes sur les chondrocytes de la plaque de croissance et soutiennent la recréation des caractéristiques du cartilage natif. Fait notable, ce projet a mis en évidence une voie métabolique encore peu explorée dans ce contexte — la synthèse de novo des acides gras dépendante du glucose — qui a augmenté progressivement pendant la différenciation des micro-tissus. Le rôle de cette voie a été davantage étudié à travers des expériences d'inhibition chimique, démontrant son importance pour le processus de différenciation et la capacité de formation osseuse des micro-tissus *in vivo*.

La deuxième phase du projet a impliqué le développement et la validation d'un nouveau système de microbioprocédés pour la culture dynamique de micro-tissus cartilagineux en suspension. Les conditions de culture dynamique, caractérisées par un stress de cisaillement intermittent, ont accéléré la différenciation chondrogénique, favorisant un engagement précoce vers l'hypertrophie, essentielle à l'ossification endochondrale. La modélisation informatique a aidé à optimiser l'environnement mécanique à l'intérieur du bioprocédé pour éviter les dommages dus au cisaillement tout en favorisant la formation efficace des tissus. La

culture dynamique a également révélé des signatures métaboliques distinctes provenant du milieu de culture, qui pourraient servir de marqueurs non destructifs pour surveiller la qualité des tissus lors des processus de mise à l'échelle. Ce travail a suggéré que la culture en suspension dans des bioprocédés pourrait constituer une plateforme évolutive pour produire des quantités cliniquement pertinentes de constructions issues de l'ingénierie tissulaire à l'avenir.

List of abbreviations

2HG	2-hydroxyglutaric acid
ACC	Acetyl coenzyme A carboxylase
Acetyl-CoA	Acetyl coenzyme A
ACSL4	Acyl-CoA synthetase long-chain family member 4
ALP	Alkaline phosphatase
APC	Axin and adenomatous polyposis coli
ATMP	Advanced therapy medicinal product
BMSCs	Bone Marrow stromal cells
BMP	Bone Morphogenic proteins
COL-II	Type II collagen
COL-X	Type X collagen
CPT ½	Carnitine palmitoyltransferase ½
CQA	Critical Quality Attribute
DMEM	Dulbecco's modified eagle medium
DNA	Deoxyribonucleic acid
FAO	Fatty acid oxidation
FAS	Fatty acid synthesis
FASN	Fatty acid synthase
FGF	Fibroblast growth factors
FGFR	Fibroblast growth factors receptor
FOXO	Forkhead Box O
GLS1	Glutaminase 1
GLUT1	Glucose transporter
HIF2A	Hypoxia inducible factor 2, alpha subunit
HP	Hypertrophic
HPDC	Human periosteum-derived cell
IGFBP	Insulin-like growth factor binding protein.
IGF-I	Insulin-like growth factor 1
IGF-IR	Insulin-like growth factor 1 receptor
IHH	Indian hedgehog
MEF2C	Myocyte enhancer factor 2C
MMPs	Matrix metalloproteinases
mRNA	Messenger ribonucleic acid
PPP	Pentose phosphate pathway

PPR	Parathyroid hormone receptors
PTHrP	Parathyroid hormone-related protein
ROCK	Rho-associated coiled-coil-containing protein kinases
RT-qPCR	Real-time quantitative polymerase chain reaction
RUNX2	Runt-related transcription factor 2
ROS	Reactive Oxygen Species
SOX9	Sex determining region Y (SRY)-box 9
TE	Tissue engineering
TGF	Transforming growth factor
TCA	Tricarboxylic acid
TNF- α	Tumor necrosis factor alpha
UDP-GlcNAc	Uridine diphosphate N-acetylglucosamine
VEGF	Vascular endothelial growth factor
WNT	Wingless-type MMTV integration site family
YAP	Yes-associated protein

Content

Acknowledgements	vi
Abstract	vii
Samenvatting	viii
Résumé	x
List of abbreviations	xii
Content	xiv
Chapter 1. General introduction	1
1.1 <i>Cell-based bone regeneration. Opportunities and challenges</i>	2
1.1.1 Bone tissue engineering: A solution to the unmet clinical need of repairing non-unions?	2
1.1.2 Bone developmental engineering	2
1.1.3 Cellular metabolism as the missing link in developmental engineering strategies for bone regeneration.....	5
1.2 <i>Towards biomanufacturing of cartilaginous microtissues</i>	12
1.2.1 The need for scaling up to clinically relevant biomanufacturing of cartilaginous microtissues	12
Chapter 2. Objectives of the research	25
2.1 <i>General aim</i>	26
2.2 <i>Specific objectives</i>	26
Chapter 3. The use of metabolomics to identify quality attributes and drivers for tissue engineered cartilage to bone transition	28
3.1 <i>Abstract</i>	29
3.2 <i>Introduction</i>	30
3.3 <i>Materials and methods</i>	32
3.3.1 Cell expansion.....	32
3.3.2 Micro-tissue formation	32
3.3.3 <i>In vitro</i> treatment (Chemical Inhibition of FAS).....	33

3.3.4 DNA quantification and gene expression analysis	33
3.3.5 Cell Viability Assay	33
3.3.6 Cell Proliferation Assay	34
3.3.7 Exometabolomics	34
3.3.8 Metabolic analysis	34
3.3.9 Metabolite measurement via GC-MS.....	34
3.3.10 Metabolite measurement via LC-MS.....	35
3.3.11 Total synthesis of collagen and protein.....	35
3.3.12 Fatty Acid Synthesis.....	35
3.3.13 Transcriptomics analysis	36
3.3.14 Formation of microtissue-based implants	36
3.3.15 <i>In vivo</i> implantation and analysis	37
3.3.16 Histology and immunohistochemistry.....	37
3.3.17 Statistical analysis	37
3.4 Results	38
3.4.1 Long term culture of bone forming hPDC microtissues led to significant changes in metabolic pathways.....	38
3.4.2 Chemical inhibition of Fatty Acid Synthase led to downregulation of genes related to endochondral ossification	45
3.4.3 Chemical inhibition of FASN led to poor survival of the TE constructs after implantation.....	48
3.5 Discussion.....	50
3.6 Conclusion	52

Chapter 4. Stirred culture of cartilaginous microtissues promotes chondrogenic hypertrophy through exposure to intermittent shear stress58

4.2 Introduction	60
4.3 Materials and Methods	61
4.3.1 Cell expansion.....	61
4.3.2 Microtissue formation	62
4.3.3 Bioreactor design and culture.....	62
4.3.4 Microtissue characterization	63
4.3.5 DNA quantification and gene expression analysis	63
4.3.6 Formation of microtissue-based implants	64
4.3.7 <i>In vivo</i> implantation analysis	64
4.3.8 Sampling and metabolite extraction.....	65

4.3.9 Liquid chromatography-mass spectrometry (LC–MS) analysis	65
4.3.10 Statistical analysis	65
4.3.11 Computational model of cartilaginous microtissues in the miniBR	65
4.4 Results.....	66
4.4.1 In-silico characterization of the dynamic process environment in mini-bioreactors	66
4.4.2 Cartilaginous differentiation in dynamic and static culture environments	67
4.4.3 Exometabolomics of chondrogenic differentiation.....	73
4.5 Discussion.....	76
4.6 Conclusion	78
Chapter 5. General Discussion.....	84
5.1 Main conclusions and contributions.....	85
5.1.1 Metabolic profiling of callus microtissues during their chondrogenic differentiation in vitro.	86
5.1.2 Investigating the role of <i>de novo</i> fatty acid synthesis during cartilaginous microtissue differentiation <i>in vitro</i> and the functionality of microtissue-based constructs <i>in vivo</i>	87
5.1.3 Stirred culture of cartilaginous microtissues promotes chondrogenic hypertrophy through exposure to intermittent shear stress.	88
5.2 Perspectives and future research.....	88
5.3 General perspectives	91
5.4 Conclusion	92
Appendix A.....	96
Appendix B.....	99
Scientific acknowledgement.....	102
Curriculum Vitae.....	103

Chapter 1. General introduction

Partially based on:

Turning Nature's own processes into design strategies for living bone implant biomanufacturing: a decade of Developmental Engineering. *I. Papantoniou, G. Nilsson Hall, N. Loverdou, R. Lesage, T. Herpelinck, L. Mendes, L. Geris, r. Adv. Drug Deliv. Rev. 169* (2021), pp. 22–39.

1.1 Cell-based bone regeneration. Opportunities and challenges

1.1.1 Bone tissue engineering: A solution to the unmet clinical need of repairing non-unions?

The skeletal system allows movement of the human body and it plays an important role in hematopoiesis and the protection of internal organs^{1,2,3}. Bone has the unique ability to regenerate without the formation of scar tissue. In the occasion of fracture, the first step of the bone healing process is inflammation. The next step is the formation of a cartilage callus and woven bone. Finally, the bone healing process is completed by the remodeling of the bony callus⁴.

Despite this ability, bone diseases and traumatic injuries, in addition to co-morbidities such as diabetes and obesity hinder fracture healing and lead to large bone defects that are unable to regenerate. More specifically, in 5-10 % of bone defects bone healing is impaired, resulting in a delayed or non-union⁴. Current clinical treatments for these bone defects include different strategies. The golden standard is autografts where bone from the patient is used to fill the defect site. Some of the problems of this treatment are the limited availability of healthy bone tissue but also the added burden of co-morbidities⁵. Another option, for avoiding these downsides is the use of biocompatible biomaterials such as calcium phosphate ceramics. However, in this option, the lack of cells results in limited success in fracture healing⁶. Additionally, the use of Growth factors such as bone morphogenetic proteins (BMPs) are used for the treatment of non-union fractures. A major hurdle is the side effects of supraphysiological doses of BMPs, such as heterotopic ossification⁷. Therefore, there is a clear need for more efficient treatment strategies.

First introduced during the late 80s, during the last years tissue engineering has been extensively explored for the regeneration of several types of tissues, such as liver and skin. Bone tissue engineering is widely considered a viable alternative therapeutic strategy for repairing non-union fractures and bone defects, aiming in the implantation of cell-based constructs to achieve successful bone regeneration.

1.1.2 Bone developmental engineering

A little over a decade ago, a paradigm shift was proposed from classical TE towards developmental engineering (DE), taking developmental processes as blueprints for regeneration of tissue and organs⁸. Developmental cascades are tightly regulated, semi-autonomous, and robust. By following a biomimetic approach, there is potential to replicate the

successful formation of tissues and organs and incorporate desirable process-related characteristics such as regulation, autonomy and robustness. Since the term 'developmental engineering' was introduced just over a decade ago, research in this area has significantly increased across all organ systems.

The endochondral ossification process as a promising developmental engineering strategy for bone regeneration

The bones in the body form through two separate mechanisms. For example, flat bones like those in the skull develop through a process called intramembranous ossification. This involves mesenchymal condensation followed by differentiation into osteoblasts, which then create bone tissue. Most of the bones, such as long bones, form through a process called endochondral ossification (Figure 1), in which mesenchymal cells condense and transform into chondrocytes to produce a cartilage template. The chondrocytes then develop into hypertrophic chondrocytes and secrete metalloproteinases, that break down the collagenous extracellular matrix, along with growth factors like VEGF, that draw in blood vessels. The growth plates are composed of a gradient of chondrocytes with distinctive genetic expressions, transitioning from proliferative (Sox9, Col2a1) to prehypertrophic (Sox9, Foxa2/3, Mef2c, Ihh), and finally, hypertrophic chondrocytes (Runx2/3, Sp7, Mmp13, Spp1) that facilitate longitudinal bone growth⁹. Cartilage, a flexible connective tissue, serves as a temporary scaffold during bone formation. As the cartilage template matures, it undergoes remodeling, which involves the gradual replacement of cartilage with bone tissue. This remodeling process is necessary for the formation of strong, mineralized bone tissue. Interestingly, the process of endochondral ossification is also observed during fracture healing through the formation of cartilaginous callus¹⁰. Recapitulation of endochondral ossification has therefore been suggested as a promising developmental engineering strategy for treating long bone defects through the creation of cell-based cartilage intermediate constructs¹¹.

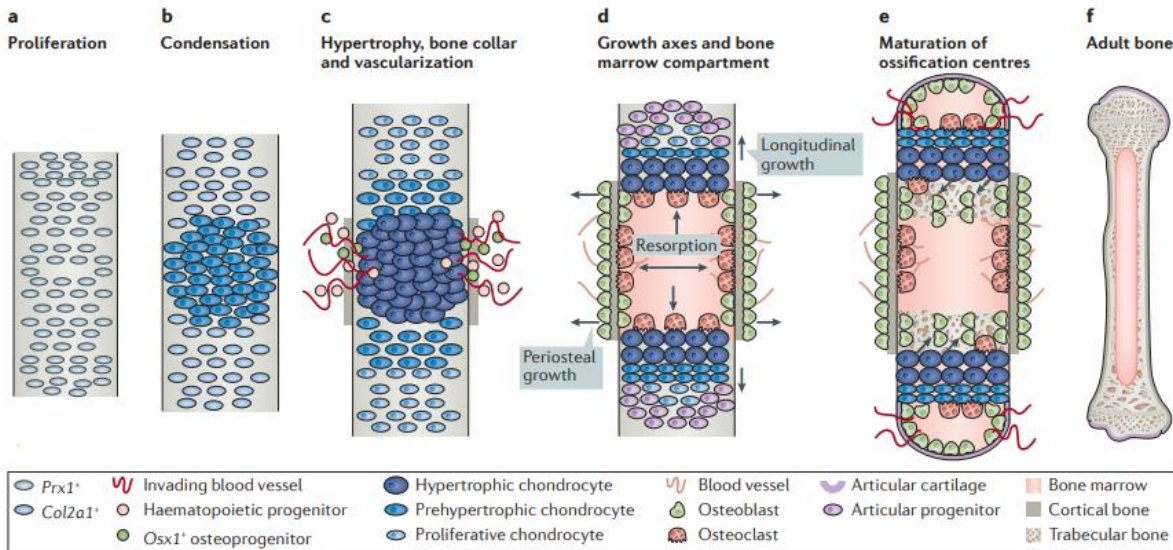


Figure 1. Endochondral ossification during bone development.

a,b) Mesenchymal cells proliferate, condense, and differentiate towards c) hypertrophy, which is followed by vascular invasion and d,e,f) bone formation. Adapted from Kronenberg *et al*⁸.

In the last 5 years, we saw a progressive increase in studies using *in vitro* engineered DE constructs for challenging long bone defects^{12,13,14,15}. Following the bottom-up approach in tissue engineering¹⁶, a common strategy is to seed hundreds of thousands of cells that aggregate and form millimeter sized scaffold-free pellets or micromasses, recapitulating cellular condensation during endochondral skeletal development. This strategy has further been optimized in our lab (Figure 2) by forming micro-sized spheroids (~100 μm in diameter) to tackle difficulties of diffusion limitations and modularity, and subsequently merging them to form millimeter-sized implants^{12,17,18,19}. These differentiated spheroids have been demonstrated to be bone forming units (“callus organoids” or “microtissues”) which, upon assembly, form bone organs without fibrotic tissue ectopically and lead to successful regeneration in long bone defects¹².

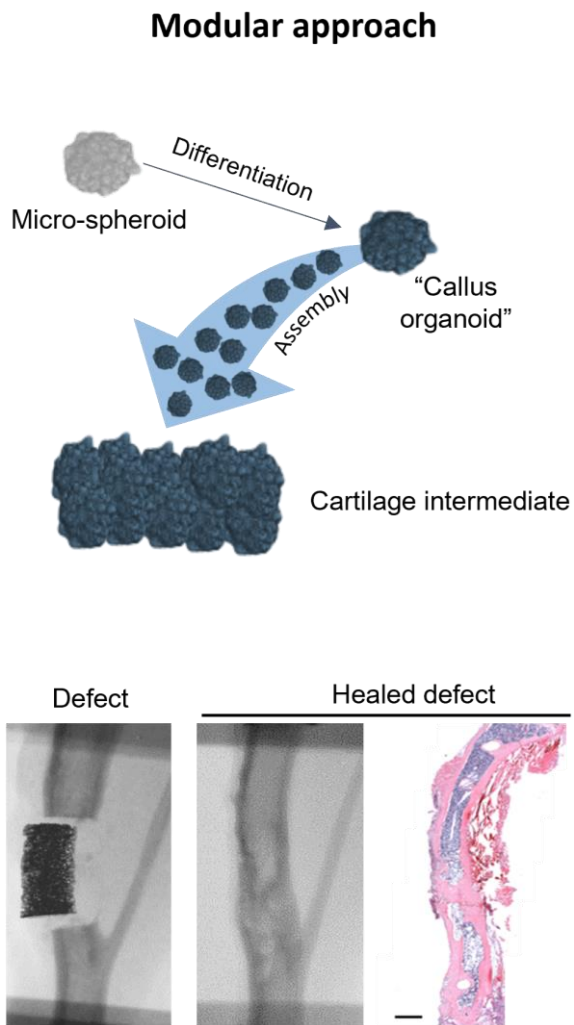


Figure 2. Developmental engineering approach in bone tissue engineering.

In our lab we developed a modular approach with “callus organoids” which heals murine critical-size long bone defects. Adapted from Papantoniou *et al*²².

Besides spheroids, the DE building blocks can be produced in the form of cell sheets¹³ tissue strands or pellets^{20,21}.

Despite these examples of successful bone formation through endochondral ossification, there are still some major challenges in the translation of these lab-based studies to preclinical studies and the production of advanced therapy medicinal products (ATMP) for human use. In the case of the cartilaginous microtissues, developed in our lab, millions to tens of millions of such microtissue modules will need to be produced to reach clinically relevant implant volumes. Therefore, scaling up the process is of pivotal importance and dynamic culture conditions of cartilaginous microtissues should be further investigated (as discussed in section 1.2.1). Variation of the *in vivo* outcome of the abovementioned studies is another bottleneck highlighting the need for better *in vitro* quality controls. Current quality controls linked with *in vivo* bone forming capacity mainly include bulk gene expression, which is inadequate to characterize the *in vitro* physiological state of cells.

1.1.3 Cellular metabolism as the missing link in developmental engineering strategies for bone regeneration.

Apart from providing cells with the required energy and the building blocks for cellular processes, there is increasing evidence that metabolism plays an important role in defining cellular properties²²⁻²⁴. Metabolomics has been of such crucial importance for the advancement of insights in the cancer field that cancer is now increasingly considered to be a metabolic disease. For regenerative processes, the systematic study of the impact of metabolism is only a recent phenomenon.

Despite the fact that metabolic research in the field of developmental biology and developmental engineering is still in its infancy, the first studies discussing the important role of metabolism in development are almost a century old²⁵. In these early studies, there were indications of spatiotemporal regulation of metabolism during development as metabolic features were shown to be tightly connected to developmental patterning^{25,26}. With recent advances in mass spectrometry, a detailed description of metabolic signatures during development is now possible, resulting in a plethora of mechanistic studies into the role of metabolic changes as drivers of (patho)physiological processes. Taking bone regeneration as an example, metabolic alterations appear to be strong drivers of the regenerative process of defect healing^{27,28}.

Here we summarize current knowledge for skeletal cell metabolism with an emphasis on the metabolism of chondrocytes and the link with different processes such as proliferation, chondrogenic differentiation, and hypertrophy. For more detailed information on skeletal cell metabolism and metabolic regulation of skeletal cell fate we refer to reviews by van Gestel *et al.*²⁸ and Devignes *et al.*⁵⁰.

Cell metabolism

Glucose is the main energy source in mammalian cells as well as the main source for generating metabolites with various anabolic functions. These pathways include the pentose phosphate pathway (PPP) for nucleotide and lipid synthesis and the hexosamine biosynthetic pathway (HBP) for protein glycosylation²⁹.

Glycolysis. Glucose is catabolized through nine sequential steps of glycolysis and converted into two molecules of pyruvate while in parallel 2 molecules of ATP are generated. When glucose enters the cell, via the glucose transporters (GLUTs), it undergoes a first irreversible conversion into glucose-6 phosphate (G6P). G6P can be stored in the form of glycogen or further metabolized to provide energy and building blocks. G6P can enter the PPP and provide ribose-5 phosphate (R5P) to the cells, a precursor for nucleotide synthesis. G6P can also be converted to fructose-6-phosphate (F6P) and follow the hexosamine synthesis pathway (HBP) that generates UDP-GlcNAc necessary for protein glycosylation, as mentioned above. F6P can further be processed in the glycolysis pathway to generate 2 molecules of pyruvate and ATP. 3-phosphoglycerate (3PG) can also be used in the pathway of serine and one carbon metabolism, which are important for nucleotide, lipid, and amino acids synthesis. During glycolysis, pyruvate converts to lactate via the lactate dehydrogenase (LDH). In this process, NAD⁺ is converted to NADH.

Pyruvate can alternatively enter the mitochondria via pyruvate dehydrogenase (PDH) and generate acetyl-CoA, which enters the tricarboxylic acid (TCA) cycle. Pyruvate can also be converted to oxaloacetate via pyruvate carboxylase (PC). This process uses these molecules and O_2 to produce ATP and is known as oxidative phosphorylation. It is the most energy-efficient use of glucose since leads to the generation of 36-38 ATP molecules per glucose molecule³⁰.

Glutamine metabolism. Glutamine is the most abundant non-essential amino acid in circulation³¹. Glutamine is an important energy source but has also diverse functions. Glutamine can be converted to glutamate, which further converts to α KG. Via α KG glutamine is linked to the TCA cycle and energy production. Additionally, glutamate can participate in glutathione synthesis³².

Fatty acid metabolism. Apart from glucose and amino acids such as glutamine, mammalian cells can produce energy via the breakdown of fatty acids into acetyl-CoA and its oxidation in the TCA cycle. The process is termed fatty acids oxidation (FAO). Apart from being an energy source, fatty acids have pleiotropic functions, including being essential components of cellular membranes and facilitating signaling and post-translational modifications. Fatty acids can be produced from acetyl-CoA and NADPH through the fatty acid synthases. This process takes place in the cytoplasm of the cell. Most of the acetyl-CoA which is converted into fatty acids is derived from carbohydrates via the glycolytic pathway. Glucose is converted to acetyl-CoA and via acetyl-CoA carboxylase (ACC) and fatty acid synthase (FASN) palmitate is produced. Palmitate can be further metabolized to longer fatty acids via the elongation of very long chain fatty acids (ELOVL) enzymes.

Skeletal Stem Cell metabolism

The term skeletal stem cells (SSCs) describes the broader stem cell populations found in the bone (bone marrow, periosteum, growth plate). The different mature skeletal cell types derive from these stem cells populations known as SSCs³³. The knowledge of SSCs metabolism is still quite limited²⁸. This is mainly because the majority of the current findings come from studying bone marrow cells or periosteal-derived cells in 2D *in vitro* cultures²⁸. Apart from the heterogeneity of these cell populations²⁸, the 2D culture fails to fully recapitulate the cells' *in vivo* state. Another major bottleneck is the limited number of *in vivo* studies, with most studies focusing on mouse skeletal stem cells²⁸.

Skeletal progenitors are characterized as highly glycolytic^{28,34}. While glycolysis does contribute to ATP production, it also serves as a source of carbon for supporting the proliferation of cells and the generation of biomass³⁵. There is a lack of studies examining the role of glucose oxidation in periosteum derived cells (PDCs) especially in *in vivo* settings. Hypoxia has a critical role in regulation of the glycolytic phenotype for BMSCs and PDCs^{28,36}. Furthermore, Stegen *et al.* 2016 showed that silencing of the transcription factor hypoxia-inducible factor 1a (HIF-1 α) impairs the survival and bone development of mouse PDCs after *in vivo* transplantation³⁷. Additionally to the abovementioned pathways, there are other relevant to glucose metabolic pathways (e.g. pentose phosphate pathway). However, the roles of these pathways in SSCs have not yet been explored in depth.

As far as fatty acid metabolism is concerned, there are limited studies regarding the roles of fatty acid oxidation (FAO) in SSCs. Human BMSCs engage in FAO while cultured but this process only accounts for less than 0.5% of ATP production^{28,38}. A study by van Gestel and colleagues found that mouse bone marrow SSCs and PDCs express genes related to FAO enzymes, such as carnitine palmitoyltransferase 1a (CPT1a), and are able to undergo FAO *in vitro*^{28,39}. However, the loss of CPT1a *in vitro* and *in vivo* did not affect the viability of SSCs, suggesting that their metabolism does not primarily depend on FAO^{28,39}.

Amino acid metabolism is crucial in cellular energetics and biosynthesis⁴⁰. The majority of studies regarding amino acid metabolism in skeletal stem cells refer to glutamine whereas the roles of other individual amino acids remain largely unexplored²⁸. There are both *in vitro* and *in vivo* studies highlighting the importance of glutamine for skeletal stem cell function²⁸. In human and mouse BMSCs as well as mouse PDCs glutamine uptake is high *in vitro*^{28,41,42}. In BMSCs and PDCs *in vitro*, glutamine fuels the mitochondrial TCA cycle, amino acid synthesis and glutathione biosynthesis^{28,42}. Moreover, the importance of glutamine metabolism in SSCs was further shown in a study where inhibition of glutamate transaminases (GLS1) resulted in decreased proliferation⁴².

Chondrocyte metabolism

In early studies, it had been shown that cartilage metabolism is mainly characterized by anaerobic glycolysis²⁶. However, around 20% of glucose may be used through the Pentose Phosphate Pathway (PPP)⁴³. Lee *et al.* 2018 demonstrated that glycolysis, and more specifically glucose uptake via GLUT1, is critical for the proper functioning of chondrocytes and that BMP signaling, a key pathway in cartilage development, regulates GLUT1 expression⁴⁴. Apart from glycolysis, which is the main pathway for energy production (over 60 %), a recent study revealed that mouse growth plate chondrocytes also use glucose

oxidation⁴⁵. When glucose oxidation has been decreased, the result was skeletal dysplasia, characterized by decreased proliferation and impaired collagen biosynthesis⁴⁵. An overview of the main glycolytic pathways in chondrocytes is provided in Figure 2.

Glutamine is another important compound for chondrocyte function (Figure 3). Handley *et al* showed that glutamine is a substrate of nitrogen donor in glucosaminoglycan synthesis in chondrocytes⁴⁶. Although glutamine does not contribute to ATP production, it plays a significant role in chondrocyte proliferation and extracellular matrix production⁴¹. More specifically, in the study of Stegen *et al*, the fate of glutamine and its role in chondrocyte function has been examined extensively. It was shown that glutamine enriches aspartate synthesis, which in turn facilitates chondrocyte function and matrix synthesis⁴¹. Another important finding was that glutamine led to glutathione synthesis, suggesting a protective mechanism against oxidative stress⁴⁵. Finally, the same study linked the HIF signaling with increased glutamine-derived α -ketoglutarate and post-modification of collagen, leading to endochondral ossification⁴⁵.

Fatty acid metabolism has not been investigated in depth in chondrocytes (Figure 4). There are studies examining the role of fatty acids uptake and fatty acid oxidation (FAO) in energy production which revealed that in chondrocytes, FAO does not play a crucial role^{39,47}. Chondrocytes have minimal FAO enzyme levels⁴⁷, resulting in a very limited ATP production through FAO. In mouse chondrocytes fatty acids don't play a crucial role in their growth and survival. Moreover, increased extracellular lipids inhibit the differentiation of SSCs into chondrocytes by reducing Sox9 expression³⁹.

Fatty acids also play important roles in signaling and post-translational modifications and therefore we believe that mechanistic studies could reveal important information on metabolic regulation of chondrogenic differentiation. Due to the avascular nature of the environment of chondrocytes have limited access to lipids, and given diffusion difficulties for such big molecules, it is possible that they need *de novo* lipogenesis to fulfill their needs, as had been demonstrated in cancer cells^{28,48}. Interestingly, there is one study that has shown that deletion of ELOVL6, an enzyme involved in fatty acid elongation during *de novo* lipogenesis, led to reduced proliferation and accelerated differentiation of chondrocytes^{28,49}. Taken together, it is of great interest to investigate the role of fatty acid synthesis in chondrocyte function.

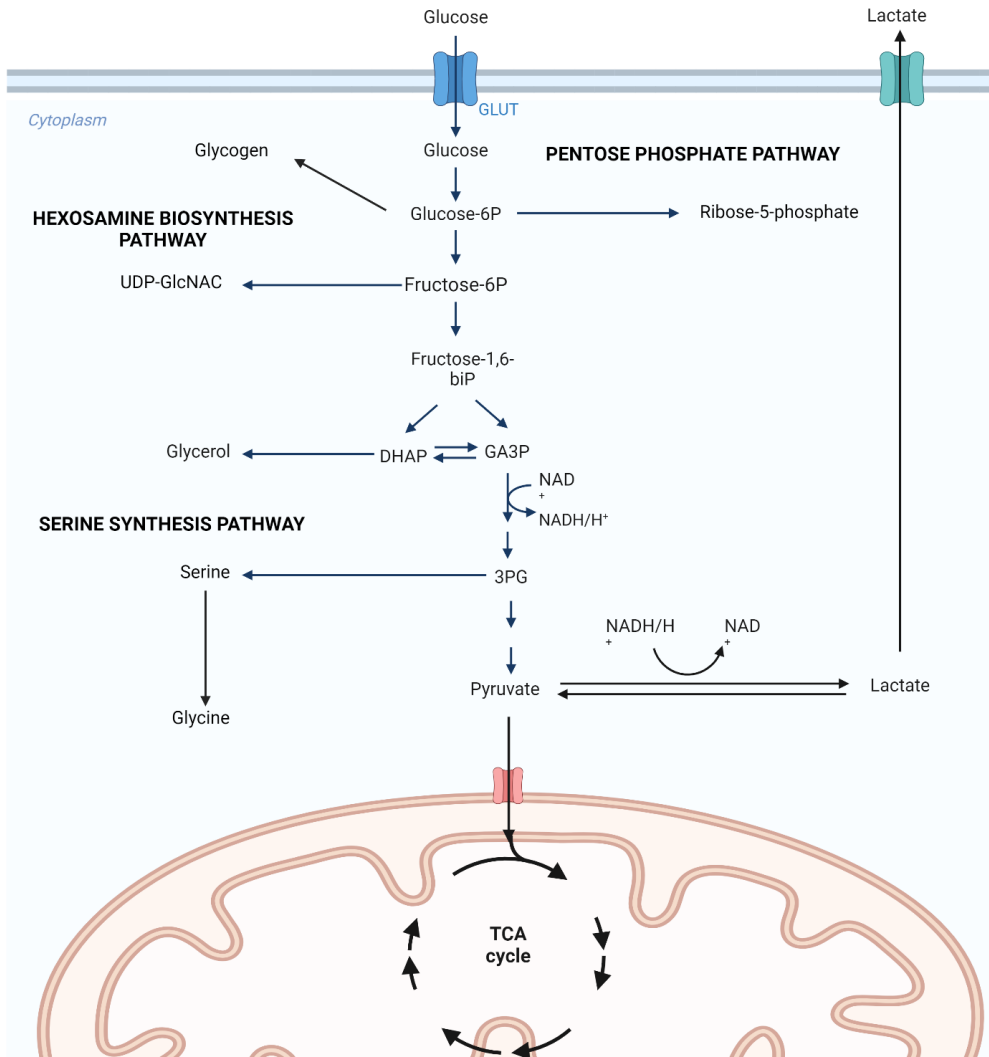


Figure 3. Overview of the main glycolytic pathways in chondrocytes according to our current knowledge.
 Figure created with Biorender

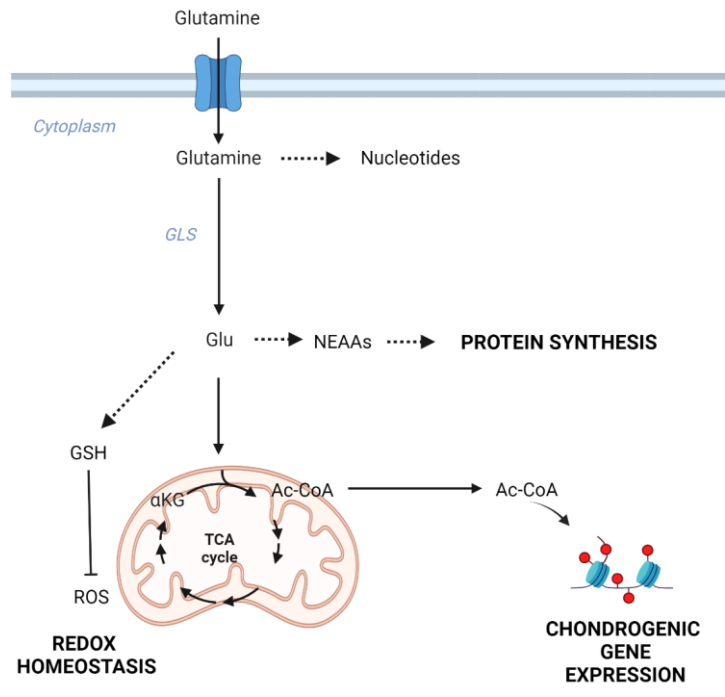


Figure 4. Overview of glutamine related pathways in chondrocytes.

Schematics showing the main cellular processes (bold) supported by glutamine metabolism in chondrocytes. Adapted from Devignes *et al*⁶⁰. Figure created with Biorender

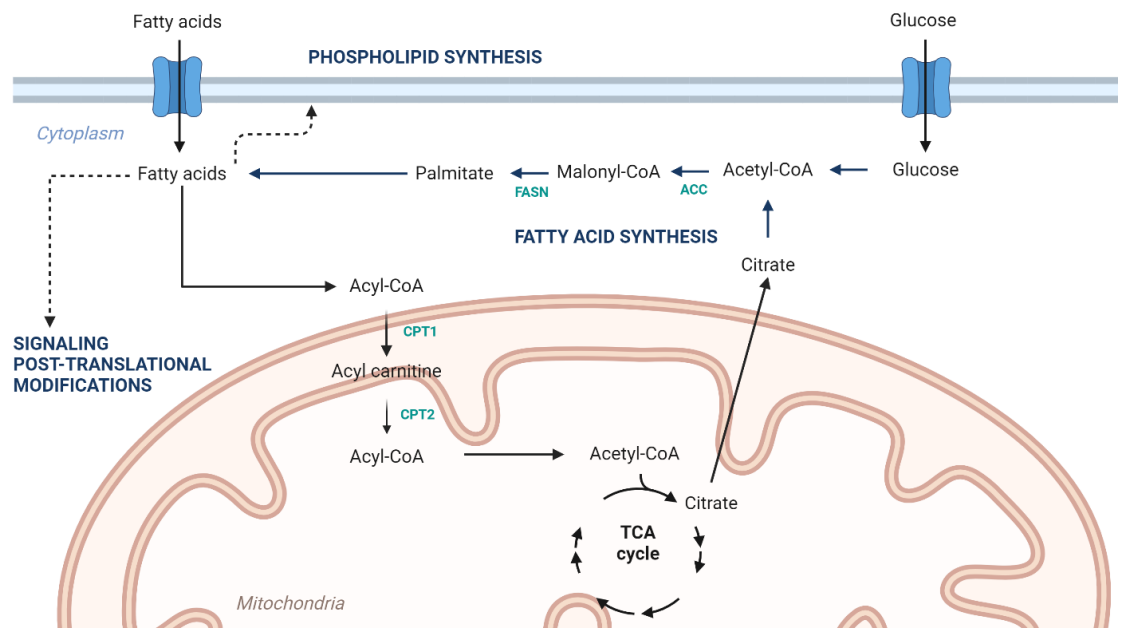


Figure 5. Overview of current knowledge of fatty acid metabolism in chondrocytes.

Figure created with Biorender

Linking metabolism and developmental engineering

Following developmental engineering-inspired cell-based bone regeneration, it is of pivotal importance to identify the metabolic signatures from undifferentiated state to the proliferative and hypertrophic state. Most studies as illustrated by the examples above, regard the metabolic profile in relation to proliferation and extracellular matrix production. There are only very few studies focusing on the metabolic signature of hypertrophic chondrocytes both from *in vitro* and *in vivo* perspective. An early study performed by Silverton et al⁴³ showed that PPP activity was the highest in the hypertrophic chondrocytes and the lowest in the resting ones. A recent study highlighted that murine chondrocytes have unique glucose metabolism signature changes moving from the proliferative to the hypertrophic state, and they are characterized by a metabolic shift to oxidative phosphorylation and subsequent upregulation of the PPP⁵¹.

While single cell techniques in transcriptomics are in rapid growth, single cell metabolomics is still in its infancy although a number of studies have demonstrated the feasibility of this technology⁵²⁻⁵⁶. In the coming years, with the experimental and computational advancements⁵³, single cell metabolomics integrated with single cell transcriptomics and proteomics, is expected to reveal important knowledge that is currently missing regarding the heterogeneity of developmental modules and their spatiotemporal regulation. This will provide crucial information on how the environment influences the developmental phenotype and will provide tools for quality control of developmentally inspired manufacturing processes.

1.2 Towards biomanufacturing of cartilaginous microtissues

1.2.1 The need for scaling up to clinically relevant biomanufacturing of cartilaginous microtissues

As developmental engineering approaches have become increasingly successful over the last decade, there is also an increasing need for translation of laboratory scale experiments into industrial processes. In the case of the cartilaginous microtissues developed in our lab, millions to tens of millions of such microtissue modules will need to be produced to reach clinically relevant implant volumes. In this challenge, the transition to bioreactor platforms enables scalability and offers the ability to monitor and control the culture and differentiation process of cells⁵⁷.

Many bioreactor types, scales, and control parameters are now available for Cell Therapy manufacturing⁵⁸ (Fig.5). Several different bioreactor systems have been investigated for the

expansion of progenitor cells, such as multi-layer and hollow-fiber bioreactors⁵⁹⁻⁶¹. There exist several types of suspension culture strategies using microcarriers in stirred bioreactors^{62,63} such as vertical wheel systems^{64,65}, wave bags⁶⁶ and mostly small scale stirred systems (typically spinner flasks of 100-200 ml)^{67,68}. Studies showing that BM-MSCs can be expanded in 5L stirred tanks⁶⁹ and 50L Mobius® bioreactors demonstrate that large scale production of single cell progenitor cells is feasible and could provide adequate quantities of cells for further differentiation.

Although the abovementioned studies showed successful examples of expansion of progenitor cells, the bioreactor culture of microtissues is still relatively limited and faces some important challenges. There are several studies discussing the use of shaken⁷⁰ or stirred systems^{71,72} for microtissues, although microtissue aggregation remains a big challenge⁷³. We will review here the use of stirred tank bioreactors, given the fact that they have become a widely used vessel type for the culture of microtissues. These platforms create a regulated and effective setting for the expansion and differentiation of cells⁷⁴. They offer numerous benefits like the capacity to increase production scale, uniform mixing of cells and nutrients, and the ability to control various process variables such as temperature, pH, and dissolved oxygen levels⁷⁵. Furthermore, stirred tank bioreactors also present an opportunity for ongoing cultivation that facilitates uninterrupted cell expansion leading to enhanced productivity⁷⁶. There is research work investigating the expansion and differentiation of induced pluripotent stem cells (iPSCs) microtissues-organoids into cardiac^{77,78}, neural⁷⁹, and kidney⁸⁰ cell types. These studies have shown that stirred tank bioreactors have the potential to produce functional adult progenitor cells and microtissues with enhanced maturation compared to cells differentiated in static conditions.

In the context of chondrogenic differentiation, few studies have focused on chondrocyte microtissues production in a stirred culture environment⁷⁹. In a previous study from our lab, a microcarrier-based stirred tank suspension process for expansion and differentiation of human periosteal derived cells has been investigated. Although this study was valuable as a proof of concept for integrated expansion and differentiation of hPDCs, we observed incomplete chondrogenic differentiation, as a result of limited cell condensation on the microcarrier surface⁶². Moreover, the abovementioned studies include limited process characterization whereas there is no consensus on the initial cell density (ranging from 2×10^4 cells/mL to 1×10^6 cells/mL) or stirring rate used (ranging from 30rpm to 110rpm). Furthermore, a key aspect of dynamic suspension culture is the impact of shear stresses generated by fluid on the progenitor cells or microtissues in the culture. There is currently insufficient understanding of the effects of shear stresses generated during the process on the maturation of

cartilaginous microtissues in suspension cultures, specifically towards hypertrophy. Finally, it is of note that the majority of these investigations focus on microtissues in an undifferentiated state. Therefore, there is still a need for specific research delving into the development of differentiated (chondrogenic) microtissues in suspension systems suitable for use in a developmental engineering setting.

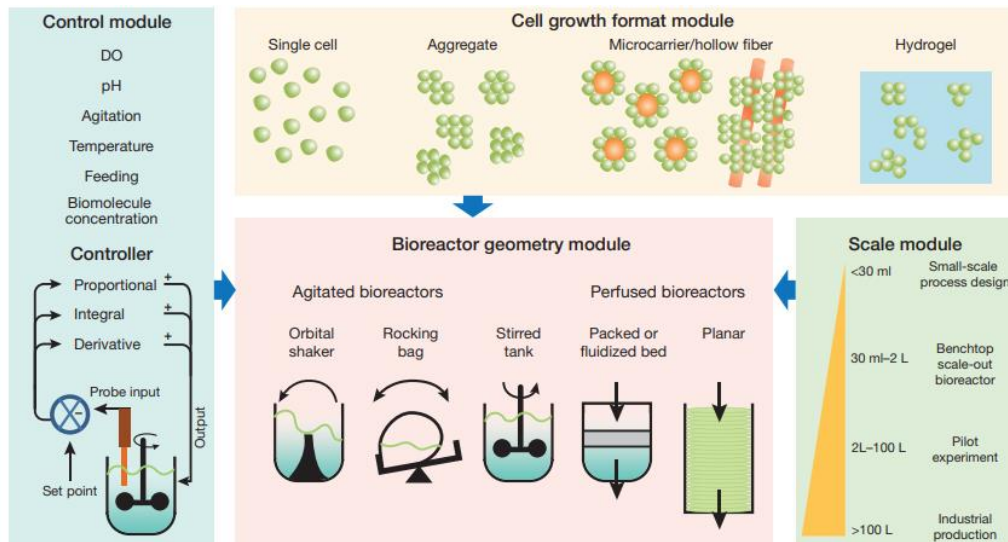


Figure 6. Bioreactor systems available in Cell Therapy Manufacturing.

Top: cells can be grown in various formats, including microtissues. Lower right: bioreactor size ranges from small-scale screening devices to benchtop, pilot, and industrial-scale devices. Lower center: Different types of bioreactors using agitated or perfused geometries. Left: parameters currently controllable in bioreactors include agitation, pH, dissolved oxygen, temperature, feeding, and biomolecule concentration, using proportional-integral-derivative controllers. DO, dissolved oxygen. Figure adapted from Lipsitz *et al*⁴¹.

The use of microbioreactors as an essential step for scaling up

Microbioreactors offer a solution to the need of scaling up by enabling small-scale, precise cultivation of cells⁸⁰. These miniature bioreactors replicate the conditions found in larger bioreactors, providing a more realistic environment for cell growth and production. This allows researchers and manufacturers to analyze and enhance cell culture conditions on a smaller scale prior to expanding to larger bioreactors for commercial production. Through the use of microbioreactors, researchers are able to gain better insights into how microenvironmental variations affect cell growth and cell state. Microbioreactors also bring benefits in terms of cost, space, and time efficiency⁸¹. They require smaller quantities of media and reagents, lowering expenses; moreover, they occupy less lab space compared to their larger counterparts while facilitating more frequent experimentation and data collection due to shorter turnaround times.

1.2.2 Metabolomics in the service of Quality by Design manufacturing of cartilaginous microtissues

With the term Quality by Design (QbD), we refer to a “*scientific, risk-based framework for process design based on relating product and process attributes to product quality*”⁵⁸. The first step in the QbD process is the identification of the “*desired product quality characteristics*”⁵⁸ (quality target product profile; QTPP). The next step is the identification of attributes that “*directly influence the safety and efficacy of the product*” (critical quality attributes) as well as the parameters that influence these attributes⁵⁸ (critical process parameters). Based on these parameters, a design space is developed in order to quantify the influence of parameter variability on quality attributes⁵⁸. In the final step, a control strategy is established to keep process parameters within a range guaranteeing product quality, and the process is monitored in a continuous way to ensure the QTPP⁵⁸.

In the context of identifying the critical quality attributes, metabolomics is a promising method due to its ability to comprehensively characterize the cell state, with additional applications in determining identity, purity, and potency characteristics (Figure 7). In skeletal tissue engineering in particular, although some markers of chondrogenesis and osteogenesis have been identified⁸², there is still a lack of meaningful *in vitro* molecular signatures linked to the cell state, able to predict the *in vivo* output. Therefore, the knowledge gained from metabolomics can be of unprecedented value for the quality control of skeletal tissue-engineered cell products.

Cell types can be characterized by distinct and unique metabolic profiles^{22,23} and although the integration of metabolomics in the biomanufacturing of cell-based products is still in its infancy, there are some interesting studies highlighting their great potential. Recent studies proposed that understanding specific metabolic needs can be used for the design of strategies for the efficient purification of cardiomyocytes by exposing them to the appropriate medium⁸³. Another study revealed the critical role of metabolic pathways in regulating cell maturation as the induction of a specific metabolic pathway led to enhanced maturation of hPSCs derived cardiomyocytes⁸⁴. The deeper understanding of cell identity of a cell product gained by metabolic studies together with other omics data sets, can be the starting point for QbD-inspired systems modeling, linking the metabolic network state with the desired phenotype. There are some successful demonstrations combining metabolomics with metabolic flux analysis (MFA) which can be useful in enhancing the desired cell state by modulating metabolic pathways⁸⁵⁻⁸⁷. In the last 7 years, the adoption of metabolomics in stem cell bioprocessing has been initiated. More specifically, Silva and colleagues⁸⁸ used genome-transcriptome profiling and metabolomics as critical evaluation tools for assessing the robustness of the expansion

process of human ESCs in stirred-tank bioreactor cultures. They claimed that this new information can guide bioprocess design and medium optimization. In the same context, Alves and co-workers⁸⁹ explored the use of metabolomics together with other omics tools for the characterization of the *in vitro* expansion of human cardiac progenitor cells (CPC). They used those omics tools as quality control for the developed bioprocess, and they underlined the importance of the methodology as a future potency assay of their stem cell population. A more applied study recently demonstrated the potential of metabolomics together with other metrics to establish potency indicators. More specifically, the authors used MSCs metabolites and cytokines measurements as MSC an immunomodulatory potency assay during cell manufacturing^{90,91}.

The use of metabolomics represents a unique opportunity to develop improved methods to characterize and understand cell identity, purity, and potency (CQAs) of cartilaginous microtissues production, in the same manner as illustrated by the abovementioned studies. This PhD thesis is an effort to understand in depth the metabolic signatures of the cartilaginous microtissues, as a first step towards establishing novel critical quality attributes predicting the *in vivo* output. Open questions include, among others, the investigation of the mechanistic link between metabolic profile and specific functional properties, such as chondrogenic hypertrophy and angiogenesis *in vitro* and bone formation *in vivo*. This is crucial information that could help in the standardization of metabolic profiles as a potency indicator in the context of critical quality attributes. Furthermore, another challenge ahead is how we can maintain a metabolic potency indicator during expansion, harvesting, and cryopreservation for large scale production of cartilaginous microtissues.

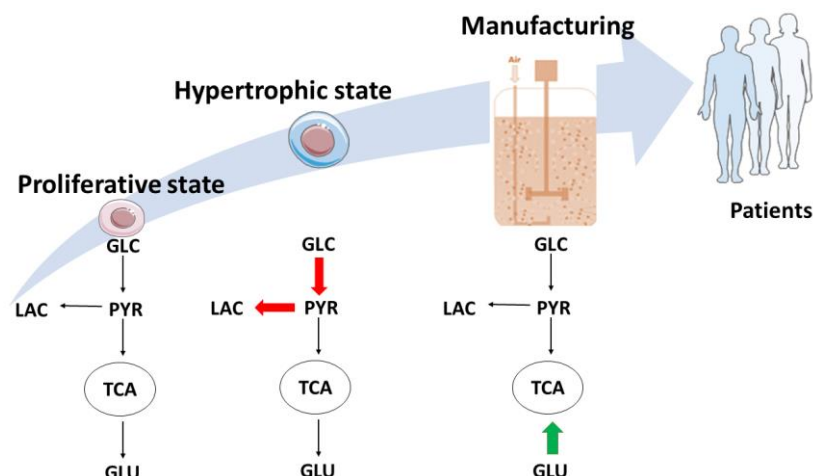


Figure 7. Metabolic network states following the cascade of developmental processes events during endochondral ossification: The missing link between biomanufacturing and predictable outcome in clinical translation. Adapted from Papantoniou *et al*⁹².

1.3 References

1. Long, F. Building strong bones: Molecular regulation of the osteoblast lineage. *Nat. Rev. Mol. Cell Biol.* **13**, 27–38 (2012).
2. Harada S. and Rodan, G.A. Control of osteoblast function and regulation of bone mass. *Nature* **423**, 1–7 (2003).
3. Calvi, L. M. *et al.* Osteoblastic cells regulate the hematopoietic stem cell niche. *Nature* **425**, 841–846 (2003).
4. Gómez-Barrena, E. *et al.* Bone fracture healing: Cell therapy in delayed unions and nonunions. *Bone* **70**, 93–101 (2015).
5. Schmidt, A. H. Autologous bone graft: Is it still the gold standard? *Injury* **52**, S18–S22 (2021).
6. Baldwin, P. *et al.* Autograft, Allograft, and Bone Graft Substitutes: Clinical Evidence and Indications for Use in the Setting of Orthopaedic Trauma Surgery. *J. Orthop. Trauma* **33**, 203–213 (2019).
7. Zara, J. N. *et al.* High doses of bone morphogenetic protein 2 induce structurally abnormal bone and inflammation in vivo. *Tissue Eng. - Part A* **17**, 1389–1399 (2011).
8. Lenas, P., Moos, M. & Luyten, F. P. *Developmental Engineering: A New Paradigm for the Design and Manufacturing of Cell-Based Products. Part I: From Three-Dimensional Cell Growth to Biomimetics of In Vivo Development.* www.liebertpub.com.
9. Henry M. Kronenberg. Developmental regulation of the growth plate. *Nature* **423**, 332–336 (2003).
10. Vortkamp, A. *et al.* Recapitulation of signals regulating embryonic bone formation during postnatal growth and in fracture repair. *Mech. Dev.* **71**, 65–76 (1998).
11. Lenas, P. & Luyten, F. P. An emerging paradigm in tissue engineering: From chemical engineering to developmental engineering for bioartificial tissue formation through a series of unit operations that simulate the in vivo successive developmental stages. *Ind. Eng. Chem. Res.* **50**, 482–522 (2011).
12. Hall, G. N. *et al.* Developmentally Engineered Callus Organoid Bioassemblies Exhibit Predictive In Vivo Long Bone Healing. **1902295**, 1–16 (2020).
13. McDermott, A. M. *et al.* Recapitulating bone development through engineered mesenchymal condensations and mechanical cues for tissue regeneration. *Sci. Transl. Med.* **11**, (2019).
14. Herberg, S. *et al.* Combinatorial morphogenetic and mechanical cues to mimic bone development for defect repair. *Sci. Adv.* **5**, 1–12 (2019)
15. Longoni, A. *et al.* Acceleration of Bone Regeneration Induced by a Soft-Callus Mimetic Material. *Adv. Sci.* **9**, 1–14 (2022).

16. Schmidt, T., Xiang, Y., Bao, X. & Sun, T. A paradigm shift in tissue engineering: From a top–down to a bottom–up strategy. *Processes* **9**, 1–17 (2021).
17. Hall, G. N. *et al.* Patterned, organoid-based cartilaginous implants exhibit zone specific functionality forming osteochondral-like tissues in vivo. *Biomaterials* **273**, 120820 (2021).
18. Decoene, I., Herpelinck, T., Geris, L., Luyten, F. P. & Papantoniou, I. Engineering bone-forming callus organoid implants in a xenogeneic-free differentiation medium. *Front. Chem. Eng.* **4**, 1–13 (2022).
19. Loverdou, N. *et al.* Stirred culture of cartilaginous microtissues promotes chondrogenic hypertrophy through exposure to intermittent shear stress. *Bioeng. Transl. Med.* 1–14 (2022) doi:10.1002/btm2.10468.
20. Mendes, L. F. *et al.* Advancing osteochondral tissue engineering: Bone morphogenetic protein, transforming growth factor, and fibroblast growth factor signaling drive ordered differentiation of periosteal cells resulting in stable cartilage and bone formation in vivo. *Stem Cell Res. Ther.* **9**, 1–13 (2018).
21. Knuth, C. A., Witte-Bouma, J., Ridwan, Y., Wolvius, E. B. & Farrell, E. Mesenchymal stem cell-mediated endochondral ossification utilising micropellets and brief chondrogenic priming. *Eur. Cells Mater.* **34**, 142–161 (2017).
22. Yanes, O. *et al.* Metabolic oxidation regulates embryonic stem cell differentiation. *Nat. Chem. Biol.* **6**, 411–417 (2010).
23. Panopoulos, A. D. *et al.* The metabolome of induced pluripotent stem cells reveals metabolic changes occurring in somatic cell reprogramming. *Cell Res.* **22**, 168–177 (2012).
24. Shapira, S. N. & Christofk, H. R. Metabolic Regulation of Tissue Stem Cells. 1–11 (2020).
25. C.M. Child, The physiological significance of the cephalocaudal differential in vertebrate development, *Anat. Rec.* **31** (1925) 369–383.
26. P.Polleselo, B. de Bernard, *et al*, Energy State of chondrocytes assessed by ³¹P-NMR studies of preosseous cartilage, *Biochem. Biophys. Res. Commun.* **180**, 216–222 (1991).
27. Loef, J., Duda, G. N., Sass, F. A. & Dienelt, A. The Metabolic Microenvironment Steers Bone Tissue Regeneration. **xx**, 1–12 (2017).
28. van Gastel, N. & Carmeliet, G. Metabolic regulation of skeletal cell fate and function in physiology and disease. *Nat. Metab.* **3**, 11–20 (2021).
29. Bouché, C., Serdy, S., Kahn, C. R. & Goldfine, A. B. The cellular fate of glucose and its relevance in type 2 diabetes. *Endocr. Rev.* **25**, 807–830 (2004).
30. Matthew G. Vander Heiden *et al.* ,Understanding the Warburg Effect: The Metabolic

- Requirements of Cell Proliferation. *Science* **324**,1029-1033(2009).
31. Stein, W. H. & Moore, S. The free amino acids of human blood plasma. *J. Biol. Chem.* **211**, 915–926 (1954).
 32. Zhang, J., Pavlova, N. N. & Thompson, C. B. Cancer cell metabolism: the essential role of the nonessential amino acid, glutamine. *EMBO J.* **36**, 1302–1315 (2017).
 33. Ambrosi, T. H., Longaker, M. T. & Chan, C. K. F. A Revised Perspective of Skeletal Stem Cell Biology. *Front. Cell Dev. Biol.* **7**, (2019).
 34. Salazar-Noratto, G. E. *et al.* Understanding and leveraging cell metabolism to enhance mesenchymal stem cell transplantation survival in tissue engineering and regenerative medicine applications. *Stem Cells* **38**, 22–33 (2020).
 35. Lunt, S. Y. & Vander Heiden, M. G. Aerobic glycolysis: Meeting the metabolic requirements of cell proliferation. *Annu. Rev. Cell Dev. Biol.* **27**, 441–464 (2011).
 36. Shum, L. C., White, N. S., Mills, B. N., De Mesy Bentley, K. L. & Eliseev, R. A. Energy Metabolism in Mesenchymal Stem Cells during Osteogenic Differentiation. *Stem Cells Dev.* **25**, 114–122 (2016).
 37. Stegen, S. *et al.* Adequate hypoxia inducible factor 1 α signaling is indispensable for bone regeneration. *Bone* **87**, 176–186 (2016).
 38. Fillmore, N. *et al.* Effect of fatty acids on human bone marrow mesenchymal stem cell energy metabolism and survival. *PLoS One* **10**, 1–17 (2015).
 39. Gastel, N. Van *et al.* Lipid availability determines fate of skeletal progenitor cells via SOX9. **579**, (2020).
 40. Kurmi, K. & Haigis, M. C. Nitrogen Metabolism in Cancer and Immunity. *Trends Cell Biol.* **30**, 408–424 (2020).
 41. Stegen, S. *et al.* Glutamine Metabolism Controls Chondrocyte Identity and Function. *Dev. Cell* **53**, 530-544.e8 (2020).
 42. Yu, Y. *et al.* Glutamine Metabolism Regulates Proliferation and Lineage Allocation in Skeletal Stem Cells. *Cell Metab.* **29**, 966-978.e4 (2019).
 43. Silverton, S. F., Matsumoto, H., DeBolt, K., Reginato, A. & Shapiro, I. M. Pentose phosphate shunt metabolism by cells of the chick growth cartilage. *Bone* **10**, 45–51 (1989).
 44. Lee, S. Y., Abel, E. D. & Long, F. Glucose metabolism induced by Bmp signaling is essential for murine skeletal development. *Nat. Commun.* **9**, 1–11 (2018).
 45. Stegen, S. *et al.* HIF-1 α metabolically controls collagen synthesis and modification in chondrocytes. *Nature* **565**, 511-515, (2019) doi:10.1038/s41586-019-0874-3.
 46. Handley, C. J., Speight, G., Leyden, K. M. & Lowther, D. A. Extracellular matrix metabolism by chondrocytes 7. Evidence that L-glutamine is an essential amino acid for chondrocytes and other connective tissue cells. *BBA - Gen. Subj.* **627**, 324–331 (1980).

47. Dunham, J. *et al.* Aerobic glycolysis of bone and cartilage: The possible involvement of fatty acid oxidation. *Cell Biochem. Funct.* **1**, 168–172 (1983).
48. Daniëls, V. W. *et al.* Cancer cells differentially activate and thrive on de novo lipid synthesis pathways in a low-lipid environment. *PLoS One* **9**, 13–19 (2014).
49. Kikuchi, M. *et al.* Crucial role of Elovl6 in chondrocyte growth and differentiation during growth plate development in mice. *PLoS One* **11**, 1–18 (2016).
50. Devignes, C. S., Carmeliet, G. & Stegen, S. Amino acid metabolism in skeletal cells. *Bone Reports* **17**, 101620 (2022).
51. Hollander, J. M. *et al.* A critical bioenergetic switch is regulated by IGF2 during murine cartilage development. *Commun. Biol.* **5**, 1–13 (2022).
52. Standke, S. J., Colby, D. H., Bensen, R. C., Burgett, A. W. G. & Yang, Z. Mass Spectrometry Measurement of Single Suspended Cells Using a Combined Cell Manipulation System and a Single-Probe Device. (2019) doi:10.1021/acs.analchem.8b05774.
53. Duncan, K. D. Advances in mass spectrometry based single-cell metabolomics. 782–793 (2019) doi:10.1039/c8an01581c.
54. Hansen, R. L. & Jin, Y. High-Spatial Resolution Mass Spectrometry Imaging : Toward Single Cell Metabolomics in Plant Tissues. 1–14 (2017) doi:10.1002/tcr.201700027.
55. Guillermier, C. *et al.* Imaging mass spectrometry reveals heterogeneity of proliferation and metabolism in atherosclerosis. **4**, 1–10 (2019).
56. Alexandrov, T. the Age of Artificial Intelligence. 61–87 (2020).
57. Kropp, C., Massai, D. & Zweigerdt, R. Progress and challenges in large-scale expansion of human pluripotent stem cells. *Process Biochem.* **59**, 244–254 (2017).
58. Lipsitz, Y. Y., Timmins, N. E. & Zandstra, P. W. Quality cell therapy manufacturing by design. **34**, 393–400 (2016).
59. Lambrechts, T. *et al.* Evaluation of a monitored multiplate bioreactor for large-scale expansion of human periosteum derived stem cells for bone tissue engineering applications. *Biochem. Eng. J.* (2015) doi:10.1016/j.bej.2015.07.015.
60. Mizukami, A. *et al.* A Fully-Closed and Automated Hollow Fiber Bioreactor for Clinical-Grade Manufacturing of Human Mesenchymal Stem/Stromal Cells. *Stem Cell Rev. Reports* **14**, 141–143 (2018).
61. Lambrechts, T. *et al.* Large-scale progenitor cell expansion for multiple donors in a monitored hollow fibre bioreactor. *Cytotherapy* **18**, 1219–1233 (2016).
62. Gupta, P., Geris, L., Luyten, F. P. & Papantoniou, I. An Integrated Bioprocess for the Expansion and Chondrogenic Priming of Human Periosteum-Derived Progenitor Cells in Suspension Bioreactors. *Biotechnol. J.* **13**, (2018).
63. Heathman, T. R. J. *et al.* Scalability and process transfer of mesenchymal stromal cell

- production from monolayer to microcarrier culture using human platelet lysate. *Cytotherapy* **18**, 523–535 (2016).
64. Lembong, J. *et al.* Bioreactor parameters for microcarrier-based human msc expansion under xeno-free conditions in a vertical-wheel system. *Bioengineering* **7**, 1–16 (2020).
 65. de Sousa Pinto, D. *et al.* Scalable Manufacturing of Human Mesenchymal Stromal Cells in the Vertical-Wheel Bioreactor System: An Experimental and Economic Approach. *Biotechnol. J.* **14**, 1–9 (2019).
 66. Timmins, N. E. *et al.* Closed system isolation and scalable expansion of human placental mesenchymal stem cells. *Biotechnol. Bioeng.* **109**, 1817–1826 (2012).
 67. Rafiq, Q. A., Coopman, K., Nienow, A. W. & Hewitt, C. J. Systematic microcarrier screening and agitated culture conditions improves human mesenchymal stem cell yield in bioreactors. *Biotechnol. J.* **11**, 473–486 (2016).
 68. Heathman, T. R. J. *et al.* Expansion, harvest and cryopreservation of human mesenchymal stem cells in a serum-free microcarrier process. *Biotechnol. Bioeng.* **112**, 1696–1707 (2015).
 69. Rafiq, Q. A., Brosnan, K. M., Coopman, K., Nienow, A. W. & Hewitt, C. J. Culture of human mesenchymal stem cells on microcarriers in a 5 l stirred-tank bioreactor. *Biotechnol. Lett.* **35**, 1233–1245 (2013).
 70. Tsai, A. C., Liu, Y., Yuan, X., Chella, R. & Ma, T. Aggregation kinetics of human mesenchymal stem cells under wave motion. *Biotechnol. J.* **12**, 1–13 (2017).
 71. Alimperti, S. *et al.* Serum-free spheroid suspension culture maintains mesenchymal stem cell proliferation and differentiation potential. *Biotechnol. Prog.* **30**, 974–983 (2014).
 72. Egger, D., Schwedhelm, I., Hansmann, J. & Kasper, C. Hypoxic three-dimensional scaffold-free aggregate cultivation of mesenchymal stem cells in a stirred tank reactor. *Bioengineering* **4**, (2017).
 73. Allen, L. M., Matyas, J., Ungrin, M., Hart, D. A. & Sen, A. Serum-Free Culture of Human Mesenchymal Stem Cell Aggregates in Suspension Bioreactors for Tissue Engineering Applications. *Stem Cells Int.* **2019**, (2019).
 74. Zweigerdt, R., Olmer, R., Singh, H., Haverich, A. & Martin, U. Scalable expansion of human pluripotent stem cells in suspension culture. *Nat. Protoc.* **6**, 689–700 (2011).
 75. Nath, S. C., Harper, L. & Rancourt, D. E. Cell-Based Therapy Manufacturing in Stirred Suspension Bioreactor: Thoughts for cGMP Compliance. *Front. Bioeng. Biotechnol.* **8**, 1–16 (2020).
 76. Grayson, W. & Stephenson, M. Recent advances in bioreactors for cell-based therapies. *F1000Research* **7**, 1–9 (2018).
 77. Kempf, H. *et al.* Controlling Expansion and Cardiomyogenic Differentiation of Human

- Pluripotent Stem Cells in Scalable Suspension Culture. *Stem Cell Reports* **3**, 1132–1146 (2014).
78. Kempf, H., Kropp, C., Olmer, R., Martin, U. & Zweigerdt, R. Cardiac differentiation of human pluripotent stem cells in scalable suspension culture. *Nat. Protoc.* **10**, 1345–1361 (2015).
 79. Qian, X. *et al.* Brain-Region-Specific Organoids Using Mini-bioreactors for Modeling ZIKV Exposure. *Cell* **165**, 1238–1254 (2016).
 80. Przepiorski, A. *et al.* A Simple Bioreactor-Based Method to Generate Kidney Organoids from Pluripotent Stem Cells. *Stem Cell Reports* **11**, 470–484 (2018).
 81. Crispim, J. F. & Ito, K. De novo neo-hyaline-cartilage from bovine organoids in viscoelastic hydrogels. *Acta Biomater.* **128**, 236–249 (2021).
 82. Asnaghi, M. A. *et al.* Biomarker Signatures of Quality for Engineering Nasal Chondrocyte-Derived Cartilage. *Front. Bioeng. Biotechnol.* **8**, 1–13 (2020).
 83. Tohyama, S. *et al.* Distinct metabolic flow enables large-scale purification of mouse and human pluripotent stem cell-derived cardiomyocytes. *Cell Stem Cell* **12**, 127–137 (2013).
 84. Kuppusamy, K. T. *et al.* Let-7 family of microRNA is required for maturation and adult-like metabolism in stem cell-derived cardiomyocytes. *Proc. Natl. Acad. Sci. U. S. A.* **112**, E2785–E2794 (2015).
 85. Huynh, T. Y. L., Zareba, I., Baszanowska, W., Lewoniewska, S. & Palka, J. Understanding the role of key amino acids in regulation of proline dehydrogenase/proline oxidase (prodh/pox)-dependent apoptosis/autophagy as an approach to targeted cancer therapy. *Molecular and Cellular Biochemistry* vol. 466 35–44 (2020).
 86. Oburoglu, L. *et al.* Glucose and glutamine metabolism regulate human hematopoietic stem cell lineage specification. *Cell Stem Cell* **15**, 169–184 (2014).
 87. Badur, M. G., Zhang, H. & Metallo, C. M. Enzymatic passaging of human embryonic stem cells alters central carbon metabolism and glycan abundance. *Biotechnol. J.* **10**, 1600–1611 (2015).
 88. Silva, M. M. *et al.* Robust Expansion of Human Pluripotent Stem Cells: Integration of Bioprocess Design With Transcriptomic and Metabolomic Characterization. *Stem Cells Transl. Med.* **4**, 731–42 (2015).
 89. Serra, M. *et al.* In vitro expansion of human cardiac progenitor cells: exploring ' omics tools for characterization of cell-based allogeneic products. *Transl. Res.* **171**, 96-110.e3 (2016).
 90. Maughon, T. S. *et al.* Metabolomics and cytokine profiling of mesenchymal stromal cells identify markers predictive of T-cell suppression. *Cytotherapy* **24**, 137–148 (2022).

91. Odeh-Couvertier, V. Y. *et al.* Predicting T-cell quality during manufacturing through an artificial intelligence-based integrative multiomics analytical platform. *Bioeng. Transl. Med.* **7**, 1–13 (2022).
92. Papantoniou, I. *et al.* Turning Nature’s own processes into design strategies for living bone implant biomanufacturing: a decade of Developmental Engineering. *Adv. Drug Deliv. Rev.* **169**, 22–39 (2021).

Chapter 2.

Objectives of the research

2.1 General aim

The field of Regenerative Medicine and Tissue Engineering seeks to build functional tissues able to regenerate defects and restore function of damaged organs. In recent years there is increasing research activity on the engineering of microtissue and organoid structures able to recapitulate robust biological events encountered in embryonic development. In the skeletal tissue engineering context, these strategies have shown great promise, by enabling the formation of microtissue-based cartilaginous implants able to regenerate critical size tibial defects in mice, as shown in a previous study in our lab. Although this is a very promising approach, there are several challenges regarding future clinical translation. We currently do not possess a set of critical quality attributes for the microtissue-based implant which can predict its bone forming potential. Additionally, microtissue production is based on manual planar microwell setups requiring extensive manual operation and hence limiting further bioprocess scale-up and automation.

The goal of this thesis is to gain novel insights into the processes related to these challenges, which may contribute to the translation of the lab-based proof of concept to an ATMP ready for clinical translation. More specifically, a major aim of this study is to explore metabolomics as a tool for identifying molecular signatures of the *in vitro* differentiation of cartilaginous microtissues which form bone upon implantation. A second aim of this PhD is the investigation of suspension culture in a novel in-house developed microbioreactor system as a model for large-scale stirred tank processes, and a first effort to integrate metabolomics (exometabolomics) as read-out of the dynamic process.

2.2 Specific objectives

The abovementioned general aims were translated into the several specific objectives, discussed in the different chapters of this thesis.

Objective 1: Given the importance of metabolism for cell fate commitment, we hypothesized that every stage of the consecutive events of chondrogenic differentiation *in vitro* is characterized by a specific metabolic profile. We carried out exometabolomics and endometabolomic analyses and we were able to characterize the metabolic alterations encountered in initial proliferative phases and subsequent events encountered in more mature stages of chondrogenic differentiation of hPDC-based microtissues. Additionally, building up to the data of metabolic profiling, we aimed investigating the impact of pathways of interest, as

revealed from our study, in the chondrogenic differentiation *in vitro* and the bone formation capacity of cartilaginous microtissues *in vivo*. This study is reported in chapter 3.

Objective 2: Next we aimed to investigate the impact of dynamic culture conditions during cartilaginous differentiation in microtissues using a novel microreactor system. This will enable the culture of microtissues in a suspension format which can then easily be scaled-up. We characterized the mechanical environment to which cartilaginous microtissues were exposed during mixing, using a center-based model (CBM) coupled with a computational fluid dynamics (CFD) solver. We identified operating conditions where suspension of the microtissue dispersion could be obtained while avoiding shear damage. We investigated the impact of dynamic culture in gene markers associated with chondrogenic differentiation and hypertrophy. Finally, we performed exometabolomics analysis to assess the impact of dynamic culture on the secretome of microtissues, with the intent to use such readouts as critical quality attributes of the scaled-up process. This study is discussed in Chapter 4.

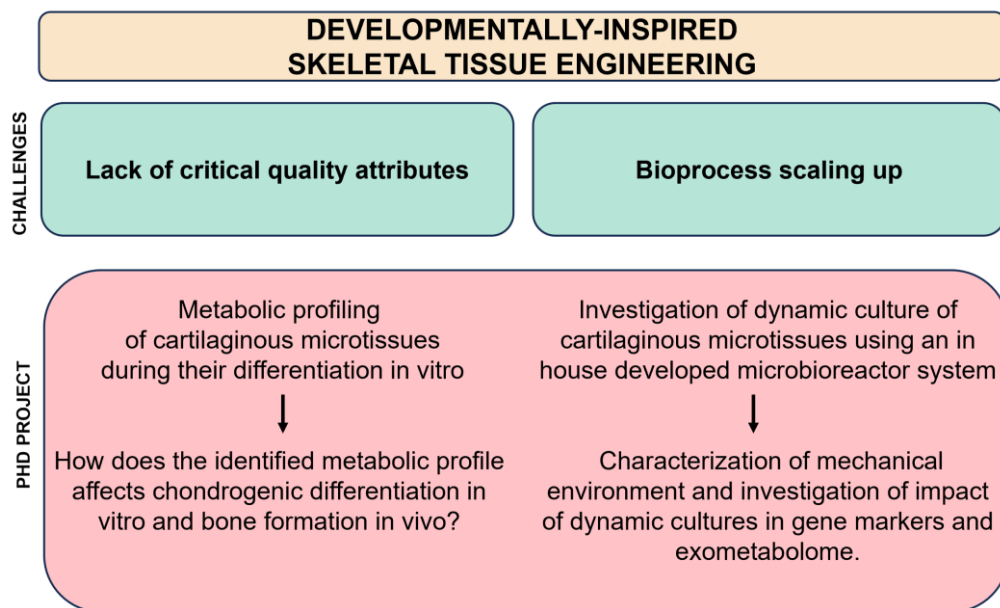


Figure 1. Overview of the PhD project

Chapter 3. The use of metabolomics to identify quality attributes and drivers for tissue engineered cartilage to bone transition

3

Loverdou N^{1,2,3,4,.}, Nilsson Hall, G^{1,2,.}, Stegen S^{1,5,.}, Caballero Garcia M^{6,.}, Staumont B^{3,.}, Ghesquiere B^{7,.}, Bernaerts K^{8,.}, Carmeliet, P^{6,.}, Carmeliet G^{1,5,.}, Papantoniou, I^{1,2,*.}, Geris, L^{1,2,3,4,.*}

*these authors share senior authorship

¹Prometheus, Division of Skeletal Tissue Engineering, KU Leuven, Leuven, Herestraat, Belgium,

²Skeletal Biology & Engineering Research Centre, Department of Development & Regeneration, KU Leuven, Leuven, Herestraat, Belgium

³Biomechanics Research Unit, GIGA-R In Silico Medicine, Université de Liege, Avenue de l'Hôpital 11—BAT 34, Liège 1, Belgium

⁴Biomechanics Section, KU Leuven, Celestijnenlaan, Leuven, Belgium

⁵Laboratory of Clinical and Experimental Endocrinology, Department of Chronic Diseases and Metabolism. KULeuven, Leuven, Belgium

⁶Laboratory of Angiogenesis and Vascular Metabolism, VIB-KULeuven Center for Cancer Biology, Leuven, Belgium

⁷Metabolomics Expertise Center, VIB-KULeuven, Leuven, Belgium

⁸Department of Chemical Engineering, KU Leuven, Celestijnenlaan, Leuven, Belgium

Manuscript in preparation

3.1 Abstract

In order to translate cell-based products such as tissue engineered implants to the clinic a thorough characterization of their critical quality attributes is required. Metabolomics holds great potential, due to its accuracy in reflecting the cellular function, for the characterization of the abovementioned products but is still largely unexplored in the context of tissue engineering. In this study, we identified the metabolic signature of consecutive stages of chondrogenic differentiation of cartilaginous microtissues formed from human periosteal derived cells (hPDCs). These microtissues were differentiated towards hypertrophy and were able to undergo endochondral ossification after *in vivo* implantation. We showed time-dependent increase in labeled glutamine tracing resulting in the generation of proline and hydroxyproline, linked to extracellular matrix (ECM) synthesis observed in the early phases of the chondrogenic differentiation process, followed by ECM turnover in the later stages. Furthermore, we identified glucose-dependent *de novo* fatty acid synthesis in the undifferentiated state of the microtissues that increased during chondrogenic differentiation. Intriguingly, pharmacological inhibition of fatty acid synthesis resulted in a significant downregulation of well-known genetic markers of endochondral bone development. In addition, fatty acid inhibition resulted in cartilaginous microtissues that were unable to form bone upon implantation, in contrast with the control groups where full ossicles containing cortical, trabecular bone as well as bone marrow were observed. Taken together, this study highlights the importance of cellular metabolism and *de novo* fatty acid synthesis for chondrogenic differentiation and cartilage microtissue maturation, as well as their functionality observed via endochondral ossification upon implantation. This functional link to *in vivo* outcomes renders metabolic markers involved in fatty acid synthesis as excellent biomarkers for future skeletal tissue engineering products.

3.2 Introduction

Over the last decade major advances in bone tissue engineering have been achieved due to the development of *in vitro* engineered cartilaginous templates that are able to robustly undergo cartilage-to-bone transitions upon implantation^{1,2,3,4}. These cartilaginous templates have been shown to recapitulate developmental events encountered during embryonic limb development, rendering them as a robust model for *in vivo* implantation and regeneration. Recently, a developmental engineering strategy based on self-assembly of human periosteum derived cells has been introduced⁴. This strategy has shown promising results for the healing of critical size bone defects in mice with restoration of the bone morphology including a well-developed bone marrow compartment within 6 weeks of implantation of a cartilaginous microtissue-based construct. Further translation of these laboratory-scale promising studies towards an industrial setting will require the identification of a panel of Critical Quality Attributes, e.g., molecular measurable characteristics that are linked with the final product functionality⁵.

Metabolism is the cellular level function that most accurately reflects cellular phenotype. In the era of omics technologies, metabolomics has been used as a sensitive tool for evaluating mammalian cell physiology^{6,7} and thus holds great potential for cell culture engineering. It has been demonstrated that metabolism is crucially connected with the cellular programs of development^{8,9}. Additionally, several studies have shown that metabolomics can be used to evaluate osteogenic differentiation of progenitor cells in 2D cultures¹⁰ or to investigate the metabolic responses in skeletal stem cells when exposed to nanotopographical cues¹¹. These demonstrate that although in its infancy, this is an area of research gaining strong attention paving the way for exploitation of metabolomics as potency marker for tissue engineering constructs.

Advances in metabolic profiling and analysis (i.e., metabolomics, stable isotope tracing) as well as mouse models with specific deletion of metabolic enzymes facilitated the progressive increase of metabolic knowledge for skeletal cell metabolism including chondrocyte metabolism. More specifically, we know that chondrocytes mainly depend on glycolysis¹², but also need some levels of glucose oxidation to avoid energy stress¹³. Chondrocyte proliferation has been found to be linked with serine synthesis pathway¹⁴. Moreover, mechanistic studies have shown that chondrocyte metabolism controls collagen synthesis and modification¹³. Nutrient availability and, more specifically, extracellular lipid availability is an important determinant of chondrogenic commitment¹⁵. Although these studies, both *in vitro* and *in vivo*, add significant information to our current knowledge of chondrocyte metabolism, there are still important questions regarding the metabolic profile of articular chondrocytes and growth plate

chondrocytes to be addressed. Additionally, it is of high importance to conduct studies with human cells, needed for clinical translation of the metabolic findings. The holistic characterization of metabolic pathways in our 3D cell culture model of cartilaginous microtissues, consisting of human periosteum-derived cells can contribute to our knowledge of human chondrocyte metabolism and chondrogenic differentiation. Cartilaginous microtissues formed from human progenitor cells can serve as a robust and clinically relevant model for exploring metabolism given their capacity to undergo bone formation upon implantation as previously shown⁴.

In this work, we provide novel insights into the dynamic evolution of cellular metabolism during chondrogenic differentiation/maturation of microtissues built with human periosteal derived cells (hPDC). Stable isotope tracer analysis revealed progressive fatty acid synthesis as a metabolic alteration connected to the last time points of the long-term culture of the cartilaginous microtissues. Exploring the chemical inhibition of the abovementioned metabolic pathway, bulk RNA sequencing revealed the downregulation of several key genes of the chondrogenic differentiation process. Additionally, *in vivo* experiments revealed that fatty acid synthesis inhibition resulted in implants showing poor survival in contrast to the non-treated controls where robust bone formation occurred after implantation. Overall, the findings of this study contribute to connecting *in vitro* chondrogenic differentiation towards hypertrophy and cellular metabolism, suggesting a functional role of metabolic reprogramming during chondrogenic differentiation in bone tissue engineering processes. These results demonstrate the potential of metabolomics as an accurate cell physiology specific quality control tool for the production of cartilaginous microtissues and pave the way for the implementation of metabolic strategies for the optimization of callus microtissues production in developmental engineering applications.

3.3 Materials and methods

3.3.1 Cell expansion

Cells were isolated from periosteal biopsies as previously described¹⁶. Briefly, the periosteal biopsies were washed and digested in type IV collagenase (440 units/mg; Invitrogen, BE) in growth medium (high-glucose Dulbecco's modified Eagle's medium (DMEM; Invitrogen, BE) supplemented with 10% fetal bovine serum (FBS; BioWhittaker, BE), and an antibiotic–antimycotic solution (100 units/ml penicillin, 100 µg/ml streptomycin, and 0.25 µg/ml amphotericin B; Invitrogen, BE). Cells were grouped into cell pools to avoid individual patient characteristics dominating obtained results. Three cell pools were used in this study. The main cell pool consisted of five female donors of age 11-17 years old (Pool 1 in Appendix A). For the *in vitro* metabolic analysis, cells of 2 other cell pools were used additionally. Specifically, one cell pool (Pool 2 in Appendix A) consisted of 2 male donors of age 20-29 and 2 female donors of age 25-47. The other one (Pool 3 in Appendix A) consisted of seven male of age 17-29 years old and two female donors of age 21-28 years old. The hPDC pools were expanded (5700 cells cm⁻²) until passage 7 (*in vivo*, RNA - seq) and 10 (*in vitro*) at 37 °C, 5% CO₂, and 95% humidity in Dulbecco's modified Eagle medium (DMEM, Life Technologies, UK) with 10% fetal bovine serum (HyClone FBS, Thermo Scientific, USA), 1% antibiotic–antimycotic (100 units mL⁻¹ penicillin, 100 mg mL⁻¹ streptomycin, and 0.25 mg mL⁻¹ amphotericin B), and 1 × 10⁻³ m sodium pyruvate (Life Technologies, UK). Medium was changed every 2–3 days, and cells were harvested with TrypLE Express (Life Technologies, UK) at a confluence of 80–90%. TrypLE Express was used for all passaging and harvesting steps during cell handling. The ethical committee for Human Medical Research (KU Leuven/UZ Leuven) approved all procedures, and patients' informed consent forms were obtained (ML7861).

3.3.2 Micro-tissue formation

Negative microwell molds were fabricated with polydimethylsiloxane (PDMS, Dow Corning Sylgard 184 elastomer, MAVOM Chemical Solutions) as described elsewhere¹⁷. To create microwells (150 µm depth, 200 µm diameter), 3% agarose (Thermo Fisher) was poured over the PDMS mold and let to cool down. The agarose layer with microwells was punched into dimensions fitting tightly a 24 well plate (area ~ 1.8 cm²), placed in a 24-well plate, and sterilized under UV. One 24 well plate well contained approximately 2000 microwells. Subsequently, 500.000 hPDCs were seeded per well resulting in microtissues with approximately 250 cells/microtissue. Microtissues were differentiated in a largely xeno-free chemically defined chondrogenic medium composed of LG-DMEM (Gibco) supplemented with 1% antibiotic-antimycotic (100units/mL penicillin, 100mg/mL streptomycin and 0.25mg/mL

amphotericin B), 1 mM ascorbate-2 phosphate, 100 nM dexamethasone, 40 µg/mL proline, 20 µM of Rho-kinase inhibitor Y27632 (Axon Medchem), ITS+ Premix Universal Culture Supplement (Corning) (including 6.25 µg/mL insulin, 6.25 µg/mL transferrin, 6.25 µg/mL selenious acid, 1.25 µg/mL bovine serum albumin (BSA), and 5.35 µg/mL linoleic acid), 100 ng/mL BMP-2 (INDUCTOS®), 100 ng/mL GDF5 (PeproTech), 10 ng/mL TGFβ1 (PeproTech), 1 ng/mL BMP-6 (PeproTech) and 0.2 ng/mL FGF-2 (R&D systems)¹⁸. Microtissues were cultured for 21 days, and half of the media (1 mL) was exchanged 2 times per week.

3.3.3 *In vitro* treatment (Chemical Inhibition of FAS)

Tetrahydro-4-methylene-2R-octyl-5-oxo-3S-furancarboxylic acid (C75, Sigma Aldrich) (20µM) was added to the medium on Day 14 of the microtissue differentiation protocol and was supplemented during following media changes (twice till Day 21). Dimethylsulfoxide (DMSO) was used as the vehicle control.

3.3.4 DNA quantification and gene expression analysis

Microtissues from one well were pooled together to represent one sample and lysed in 350 µl RLT buffer (Qiagen) and 3.5 µl β-mercaptoethanol (VWR). DNA was quantified using the Qubit dsDNA HS Assay Kit (Invitrogen). Briefly, 10 µl lysed sample was diluted in 90 µl milliQ water. Next, 5 µl was added to 195 µl of working solution, vortexed, and incubated for 5 minutes at room temperature. The DNA content was measured using a Qubit R Fluorometer. Next, RNA was isolated using RNeasy Mini Kit (Qiagen) whereafter RNA concentration and quality were assessed with NanoDrop 2000 (Thermo Scientific). Complementary DNA (cDNA) was synthesized with PrimeScript reagent kit (TaKaRa) followed by quantitative real-time polymerase chain reaction (qRT-PCR) using SYBR® Green (Life Technologies) and StepOnePlus R Real-Time PCR System (Applied Biosystems). The heating cycle was as follows: hold at 45 °C for 2min, at 95 °C for 30 s, followed by 40 cycles of 95 °C for 3 s and 60 °C for 20 s. Relative differences in expression were calculated using the $2^{-\Delta\Delta Ct}$ method normalized to the housekeeping gene Hypoxanthine-guanine phosphoribosyltransferase 1 (HPRT1)¹⁹.

3.3.5 Cell Viability Assay

Cell viability was qualitatively evaluated using LIVE/DEAD Viability/Cytotoxicity Kit (Invitrogen) following the manufacturer's description. Briefly, microtissues were rinsed in PBS and incubated for 45 min with 2 µM calcein AM and 4 µM ethidium homodimer in PBS. After removal of the staining solution, the samples were imaged in their media using a fluorescence microscope (Olympus IX83).

3.3.6 Cell Proliferation Assay

Cell proliferation was assessed using the Click-iT EdU (5-ethynyl-20-deoxyuridine) Imaging Kit (Life Technologies, USA) according to the manufacturer's protocol. Briefly, microtissues were incubated with 10 μM EdU for 48 h. Next, samples were fixed in 4% paraformaldehyde (PFA) and EdU was detected with Alexa Fluor azide and Hoechst 33342 (5 $\mu\text{g ml}^{-1}$) for nuclei staining followed by visualization with fluorescence microscope (Olympus IX83).

3.3.7 Exometabolomics

In order to avoid bias due to sampling, we used all the media for the exometabolomic analysis. Also, samples were taken each time (Day 0, Day 7, Day 14, Day 21) 2 days after the media changes. In that way, we had consistency for changes related to the refreshing of the medium. For every sample, 990 μl of 80% methanol with 2 μM d27 myristic acid was added to 10 μl of sample. Extracts were stored overnight at 80°C and were centrifuged prior to LC-MS analysis.

3.3.8 Metabolic analysis

In order to trace the contribution of glucose and glutamine to other metabolites, microtissues were cultured from the time of assembly till Day 23 in glucose free or glutamine free DMEM (custom media, ThermoFisher) supplemented with 5,5 mM [U- ^{13}C]-glucose or 2 mM [U- ^{13}C]-glutamine (Cambridge Isotope Laboratories, Tewksbury, MA, USA) respectively. Metabolite extractions were performed as previously described⁹⁷, 48h after culture for Day 0 and after every medium change for Day 7, Day 14, and Day 21. For microtissue samples, wells were washed with ice cold 0.9 % saline solution. All samples were stored at -80°C until metabolite extraction. 800 μl of -20°C cold 65% methanol was added to the wells and cells were mechanically extracted from microtissues with a pipette tip and suspensions were transferred to Eppendorf tubes. Next, 500 μl of -20°C cold chloroform was added, and samples were vortexed at 4 $^\circ\text{C}$ for 10 minutes to extract metabolites. Phase separation was achieved by centrifugation at 4 $^\circ\text{C}$ for 10 minutes, after which the chloroform phase (containing the total fatty acid content) was separated and dried by vacuum centrifugation.

3.3.9 Metabolite measurement via GC-MS

Total fatty acid samples were esterified with 500 μl 2% sulfuric acid in methanol overnight at 50 $^\circ\text{C}$ and extracted by the addition of 600 μl hexane and 100 μl saturated aqueous NaCl. Samples were centrifuged for 5 min and the hexane phase was separated and dried by vacuum centrifugation. Samples were resuspended in hexane, after which total fatty acids were measured with a 7890A GC system (Agilent Technologies) combined with a 5975C or a 7000

inert MSD system (AgilentTechnologies). 1ml of each sample was injected in split-less or 3:1 split (7000) mode with an inlet temperature of 270 °C onto a DB35MS column (Agilent Technologies). Helium was used as a carrier gas with a flowrate of 1 ml per min. The oven was held at 80 °C for 1 min and ramped with 5 °C per min to 300 °C. The mass spectrometry system was operated under electron impact ionization at 70 eV and a mass range of 100–650 amu was scanned. Mass distribution vectors were extracted from the raw ion chromatograms using a custom Matlab M-file, which applies consistent integration bounds and baseline correction to each ion. Moreover, we corrected for naturally occurring isotopes. Total contribution of carbon was calculated using the following equation:

$$\text{Total contribution of carbon} = \frac{\sum_{i=0}^n i m_i}{n \sum_{i=0}^n m_i}$$

where n is the number of C atoms in the metabolite, i represents the different mass isotopomers and m refers to the abundance of a certain mass. For metabolite levels, arbitrary units of the metabolites of interest were normalized to an internal standard and DNA content.

3.3.10 Metabolite measurement via LC-MS

Polar metabolites were measured as described before²¹. Polar metabolites were resuspended in 60% acetonitrile. Targeted measurements of polar metabolites were performed with a 1290 Infinity II HPLC (Agilent) coupled to a 6470 triple-quadrupole mass spectrometer (Agilent). Samples were injected onto an iHILIC-Fusion(P) column. The solvent, composed of acetonitrile and ammonium acetate (10 mM, pH 9.3), was used at a flow rate of 0.100 ml/min. Data analysis was performed with the Agilent Mass Hunter software. Metabolite levels were normalized to DNA content.

3.3.11 Total synthesis of collagen and protein

Total collagen and protein synthesis was quantified by incubating cells with 20 µCi ml⁻¹ L-2,3,4,5-³H-proline (PerkinElmer), as described previously²². Briefly, after overnight labeling, cells were lysed in extraction buffer (11% acetic acid in H₂O with 0.25% BSA), and collagenous proteins were precipitated by the addition of 20% trichloroacetic acid. Radioactivity was determined by liquid scintillation counting and normalized for DNA content.

3.3.12 Fatty Acid Synthesis

Cells were incubated in full growth medium supplemented with [U-¹⁴C]-Acetate for 24 hours followed by snap freezing and methanol-water-chloroform extraction. Phase separation was

achieved by centrifugation at 4 degrees and the methanol-water phase containing polar metabolites was used as negative control. Radioactivity in the chloroform phase containing fatty acids was quantified by liquid scintillation counting and values were normalized to protein concentration determined in the dried protein interphase.

3.3.13 Transcriptomics analysis

The Genomics Core Leuven performed the sequencing and the RNA-seq expression analysis as follows. Library preparation was performed with the Illumina TruSeq Stranded mRNA Sample Preparation Kit, according to the manufacturer's protocol. Denaturation of RNA was performed at 65 °C in a thermocycler and cooled down to 4 °C. Samples were indexed to allow for multiplexing. Sequencing libraries were quantified using the Qubit fluorometer (ThermoFisher Scientific, MA, USA). Library quality and size range were assessed using the Bioanalyzer (Agilent Technologies) with the DNA 1000 kit (Agilent Technologies, CA, USA) according to the manufacturer's recommendations. Each library was diluted to a final concentration of 2×10^{-9} M and sequenced on Illumina HiSeq4000 according to the manufacturer's recommendations generating 50 bp single-end reads. A minimum of 14M reads per sample were produced. Quality of the sequencing data was successfully controlled using FastQC (<http://www.bioinformatics.babraham.ac.uk/projects/fastqc/>) and Picard tools (<http://broadinstitute.github.io/picard/>) along with MultiQC²⁶. For the differential expression analysis at the gene level, raw gene counts were generated using STAR for all annotated transcripts. After filtering out lowly expressed transcripts, the data were normalized (Trimmed Mean of Medians) to account for library size differences across samples and differential gene expression analysis was performed using the edgeR package (v3.28.1)²⁷. The significance threshold for differential expression was defined as a log₂ fold change > 1 or < -1 and an adjusted p-value < 0.05 (false discovery rate (FDR)), after correction for multiple testing using the Benjamini-Hochberg method²⁸. Volcano plots, heatmaps (pheatmap package v1.0.12) and dotcharts were generated in R (v3.6.2). Gene Set Enrichment Analysis (GSEA) was performed in R using fgsea package (v1.12.0) and using collections from the Molecular Signatures Database (MSigDB: <https://www.gsea-msigdb.org>). Over-representation analysis was also performed in R using the enrichKEGG function in clusterProfiler package (v3.14.3).

3.3.14 Formation of microtissue-based implants

Cylindrical non-adherent macrowells to be used as a mold for microtissue assembly with a diameter and a depth of 2 mm were created with 3% w/v agarose (Invitrogen, Belgium) and sterilized under UV. Microtissues were recuperated from their microwells by gently pipetting up and down several times. The microtissue suspension was concentrated with centrifugation

to a volume corresponding to the macrowells. Next, approx. 3000 microtissues were added into the macrowells and incubated for 1 h to sediment. Microtissues were allowed to self-assemble over 24 hours resulting in a structurally stable mesotissue construct. For the fatty acid inhibition experiments chondrogenic medium with C75 and vehicle solution (control) respectively were added and mesotissue constructs were incubated in this formulation for 24 h.

3.3.15 *In vivo* implantation and analysis

A subcutaneous mouse model was used to assess the microtissues' capacity to form bone after assembly. The fused constructs were implanted subcutaneously in immune compromised mice (Rj:NMRInu/nu) and explants were retrieved after 4 weeks and fixed in 4% PFA. All procedures on animal experiments were approved by the local ethical committee for Animal Research, KU Leuven (P036-2016). The animals were housed according to the regulations of the Animalium Leuven, KU Leuven. Fixated explants were scanned with nanofocus Computed Tomography (nano CT) (Phoenix Nanotom M®, GE Measurement and Control Solutions) for 3D visualization of mineralized tissue. Scans were performed at 60 kV, 140 μ A and with diamond target, mode 0, 1 frame average, 0 image skip, 500 ms exposure time, 2400 images, and a 0.1 mm aluminum filter resulting in a voxel size of 2 μ m. CTAn (Bruker micro-CT, BE) was used for image processing of mineralized tissue based on automatic Otsu segmentation and 3D visualizations of the mineralized tissue were created in CTvox (Bruker micro-CT, BE).

3.3.16 Histology and immunohistochemistry

Microtissues were flushed out, fixed in 2% PFA overnight, mixed in 3% agarose, dehydrated, and embedded in paraffin overnight. Ectopic explants were fixed in 4% PFA for 4 h, decalcified in ethylenediaminetetraacetic acid in PBS (pH 7.5) for 10 solution changes at 4°C, dehydrated, embedded in paraffin overnight, and sectioned at 5 μ m thickness. Histology was performed according to previously reported methods of H&E, and Safranin O staining⁴.

3.3.17 Statistical analysis

Data are presented as mean or individual values \pm SD., and n values represent the number of independent experiments performed. For each independent in vitro experiment, at least three technical replicates were used. For the in vivo experiment four technical replicates were used. Data were compared with one-way or two-way ANOVA and Tukey's Multiple Comparison test or Student's t-test. Results were considered statistically different for p-values lower than 0.05 (*p < 0.05, **p < 0.01, ***p < 0.001). Statistical analysis was performed with GraphPad Prism 8 (GraphPad Software, Inc., USA) unless otherwise stated.

3.4 Results

3.4.1 Long term culture of bone forming hPDC microtissues led to significant changes in metabolic pathways.

Microtissues were generated through spontaneous aggregation in microwell culture plates and subsequently cultured in chondrogenic medium for 21 days (Figure 1a). In this study, time points of Day 0, Day 7, Day 14, and Day 21 of in vitro culture were used, as these time points had previously been shown to capture the transition from the proliferating to the pre/hypertrophic state (Figure 1b,c). Transcriptomic analysis of genes related to metabolism revealed distinct profiles of the different time points (Figure 1d) motivating further investigation of possible metabolic alterations during the chondrogenic differentiation cascade. As a first step, an exometabolomic analysis was performed, showing higher glucose consumption and lactate production during the chondrogenic differentiation of hPDCs microtissues (Figure 1e). This is in line with studies highlighting the glycolytic metabolism of growth plate chondrocytes^{12,23}.

Subsequently, we performed Stable Isotope Tracer Analysis and used labeled glucose (Figure 2) and glutamine (Figure 3), as the major energy sources of the cells²³. The cellular level of glucose and glutamine derived metabolites was determined after 48h of incubation with the tracers. ¹³C₆-glucose incorporation into lactate, intracellular level of lactate, and lactate production from the medium analysis all point towards increased glycolysis over the course of differentiation. Additionally, we observed glucose oxidation in the TCA cycle, as 22-26 % of glucose tracer led to citrate and 12-18% to other TCA metabolites (Figure 2d). This is aligned with mechanistic studies showing that glucose oxidation is needed for ATP production in chondrocytes²². Glucose-dependent fueling of the TCA cycle was mainly via pyruvate dehydrogenase (m+2, m+4 mass distribution vectors (MDVs)) and less via pyruvate carboxylase (m+3 MDV). Interestingly, glucose dependent fueling of the TCA cycle via pyruvate carboxylase increased significantly during differentiation, while m+2 was decreased significantly. The significant increase of glucose enrichment in serine at Day 7 (Figure 2e) where we notice a significant increase in proliferation, confirms the important role of glucose-mediated de novo serine biosynthesis for chondrocyte proliferation, as showed by Stegen et al¹⁴. Finally, the tracer analysis using labeled glucose revealed high enrichment in the hexosamine biosynthesis pathway with a high percentage of enrichment in uridine diphosphate N-acetylglucosamine (UDP-GlcNAc), which is at 50 % on Day 0 and significantly increases in enrichment at Day 7 (~70%) (Figure 2f). UDP-GlcNAc is an important metabolite for N- and O-linked glycosylation and building block for glycosaminoglycans, thus crucial for cartilage anabolism²⁴.

THE USE OF METABOLOMICS TO IDENTIFY QUALITY ATTRIBUTES AND DRIVERS FOR TISSUE ENGINEERED CARTILAGE TO BONE TRANSITION

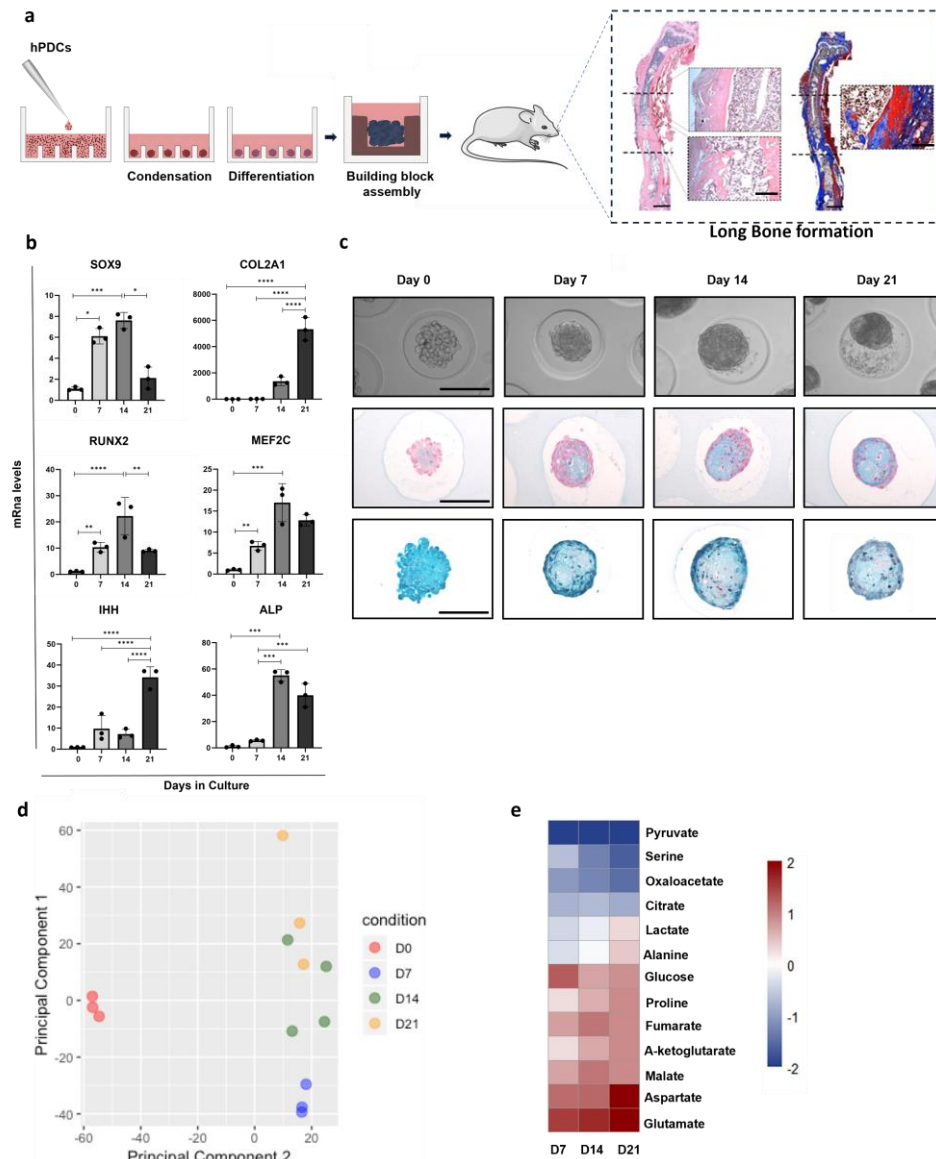


Figure 1. Microtissues assembled by hPDCs undergo chondrogenic differentiation, towards prehypertrophic cartilaginous microtissues able to form bone *in vivo*. Distinct metabolic gene profiles were observed during culture time and exometabolomics confirmed the metabolic alterations during the cascade of chondrogenic differentiation events.

a) Schematic overview of the bioengineering process starting with cellular aggregation, condensation, and differentiation (3 weeks) followed by cartilaginous microtissues assembly and implantation in ectopic and orthotopic environments. Hematoxylin and Eosin (H&E) and Masson's Trichrome histology validated the healing of murine critical-sized long bone defect. Scale bars: overview 1mm and zoom in 100 μ m. Figure is adapted from Nilsson Hall *et al*⁴ b) Quantification of mRNA transcript of chondrogenic and prehypertrophic gene markers was performed and normalized to D0 (n=3). The data are represented as individual values \pm SEM *p< 0.05, **p< 0.01, ***p< 0.001, one way ANOVA followed by Tukey's multiple comparison test. c) Representative brightfield images of microtissues over time, Alcian Blue, and Safranin O staining over time. Scale bar: 50 μ m. d) Principal component analysis of metabolic genes over time, n=4*. e) Heatmap of logfold change of metabolites of central carbon metabolism in the medium of D7, D14, and D21 *in vitro* culture of microtissues in comparison to D0.

Interestingly, $^{13}\text{C}_6$ -glucose labeling to palmitate (Figure 4a,4b) was observed with a significant increase at Day 7 (from 5 to 20%) which remained constant towards Day 21 of the *in vitro* culture (Figure 4c). For the increase seen on Day 7, we can speculate that *de novo* fatty acid synthesis can be explained by the increased proliferation of the cells in the early time points of the differentiation process. For later time points such as Day 14 and Day 21 which are associated more with chondrogenic differentiation and ECM maturation rather than proliferation, the glucose carbon contribution to palmitate required further investigation, which is discussed in section 3.4.2. The transcriptomics analysis comparing Day7 to Day14, and Day7 to Day21 revealed significant upregulation of the stearoyl-CoA Desaturase SCD gene (1.45 and 2.45 log fold change respectively) which is crucial for the synthesis of monounsaturated fatty acids, components of triglycerides and membranes phospholipids. The genes ATP citrate lyase (ACLY) and Acyl-CoA Thioesterase 4 (ACOT4), involved in lipid biosynthesis also showed significant upregulation in Day21 vs Day14 and Day7 respectively (Figure 4e).

We next sought to understand the use of glutamine during microtissue chondrogenic differentiation. Stable isotope labeled glutamine revealed that glutamine carbon contributed to the TCA cycle (e.g., citrate 42-48 %) and was used for amino acid (aspartate, proline, alanine) biosynthesis (Figure 3b). Glutamine contributed to citrate from both oxidation (M+4) and reductive carboxylation (M+5) for all the time points of interest. However, it is of note that microtissues of D21 in comparison to microtissues of D0 were characterized by an increase in contribution to M+5 and a decrease in M+4, suggesting a switch from oxidation to reductive carboxylation towards the D21-prehypertrophic state of microtissues (Figure 3c). Reductive carboxylation is an indication for a hypoxic environment, as it is a known feature in hypoxic cells²⁵, but this needs further investigation. We observed the highest glutamine contribution to aKG (80 %) (Figure 3b), which, according to mechanistic studies is specific for chondrocytes, differentiating them from other cell types¹³. Furthermore, there was a high and constant percentage of glutamine derived carbons to aspartate, an important amino acid for protein and nucleotide synthesis²⁶, needed for the proliferation of microtissues (Figure 3b). A significant increase (~20 to 40 %) in enrichment of proline was observed in Day 7 microtissues versus Day 0 with no further changes for Day 14 or Day 21 (Figure 3d, left panel). A similar pattern was shown for the contribution of glutamine carbon in hydroxyproline (Figure 3d, right panel). As evidenced by Safranin O staining (Figure 1c), Day 7 microtissues confirmed an increased presence of ECM within the microtissues. To further investigate whether this increase in metabolic flux in proline and hydroxyproline was linked to extracellular matrix production, we used radio labeled proline (l-2,3,4,5- ^3H -proline) in the culture medium and confirmed that collagen synthesis was significantly decreased after 1 week of culture (Figure 3e). Together

with the previously shown upregulation of extracellular matrix degradation pathway in the transcriptome level⁴, glutamine enrichment to proline and hydroxyproline can be linked to extracellular matrix production till Day 7, whereas for Day 14 and Day 21 the labeled proline and hydroxyproline presumably rather is a product of extracellular matrix remodeling.

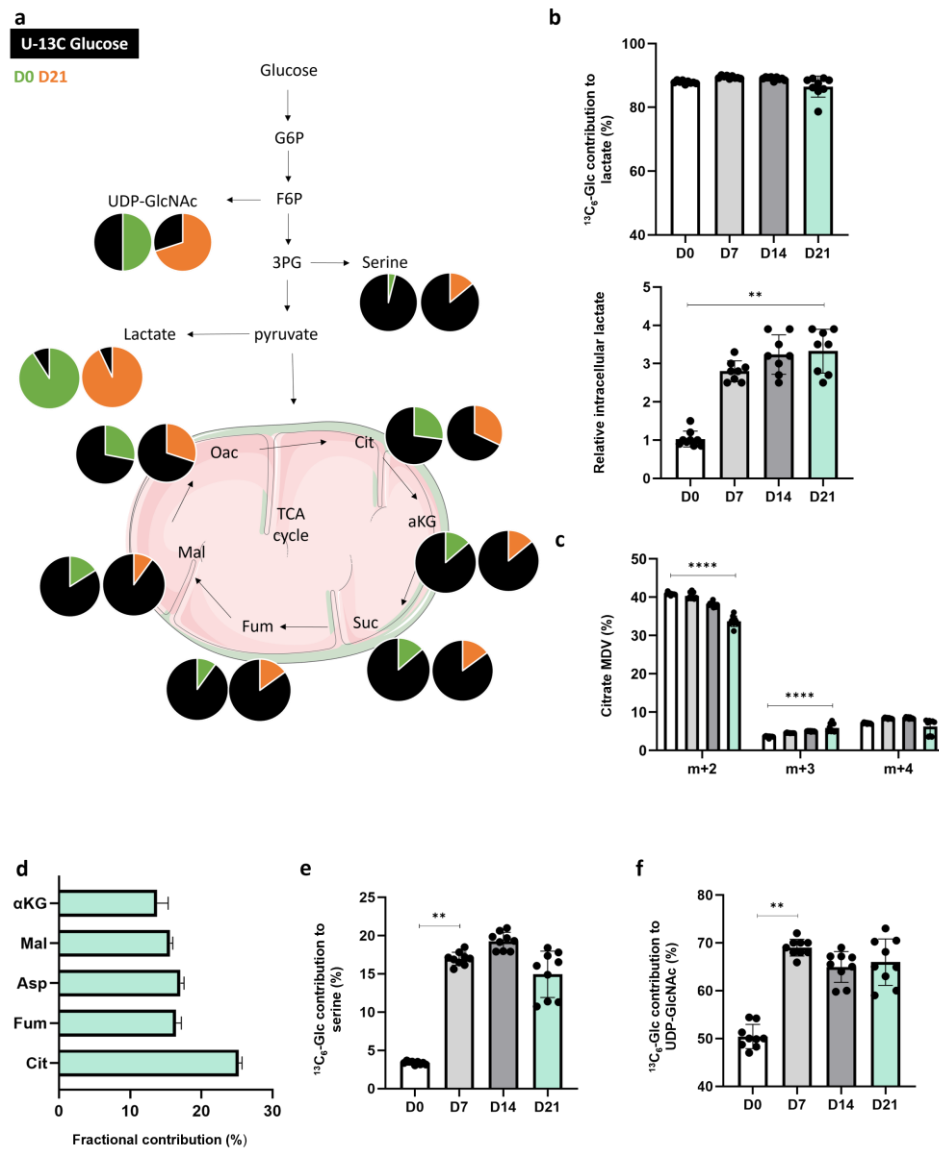


Figure 2. Use of glucose carbon in cartilaginous microtissues over time

a) Global overview of glycolysis pathway in D0 vs D21 chondrogenic microtissues. The fractional contribution of $^{13}\text{C}_6\text{Glc}$ to intracellular metabolites of microtissues of D21 and D0 are indicated with orange and green color respectively. b) Fractional contribution of $^{13}\text{C}_6\text{Glc}$ to lactate over culture time, (n=9). c) Relative intracellular abundance of lactate over culture time, (n=9). d) $^{13}\text{C}_6\text{Glc}$ incorporation to TCA cycle metabolites at D21 of the in vitro culture indicates the importance of glucose oxidation for the in vitro chondrogenic differentiation, n=9. e) $^{13}\text{C}_6\text{Glc}$ incorporation to serine over in vitro culture time. D7 microtissues showed a statistically significant increase in enrichment of glucose tracer in serine, (n=9). f) $^{13}\text{C}_6\text{Glc}$ incorporation to UDP-GlcNAc over in vitro culture time. D7 microtissues showed a statistically significant

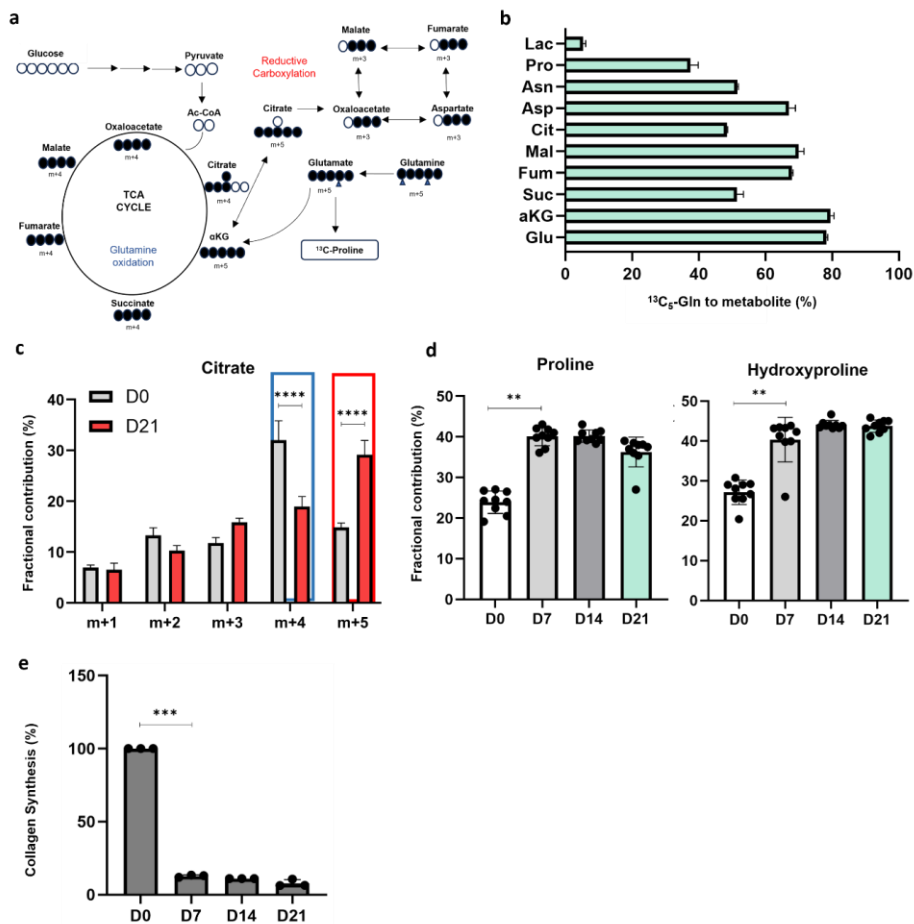


Figure 3. Glutamine metabolism and collagen synthesis during chondrogenic differentiation of cartilaginous microtissues.

a) Schematic overview of $^{13}\text{C}_5$ Gln contribution to TCA cycle and reductive carboxylation of chondrogenic microtissues in vitro culture. Blue filled circles represent ^{13}C , whereas white circles represent ^{12}C . b) Fractional contribution of $^{13}\text{C}_5$ Gln to TCA cycle metabolites and amino acids of D21 chondrogenic microtissues, (n=9). c) Glutamine derived citrate mass distribution vector (MDV) after 48h $^{13}\text{C}_5$ Gln incorporation. The blue box represents the significant increase in glutamine oxidation at Day 0 of in vitro culture microtissues, whereas the red box represents the significant increase in reductive carboxylation respectively, (n=9). d) $^{13}\text{C}_5$ Gln incorporation to proline and hydroxyproline showed a significant increase at Day 7 of in vitro culture of chondrogenic microtissues, (n=9). e) Collagen synthesis assay using radio-labeled proline, (n=4). The data are represented as individual values \pm SEM *p< 0.05, **p< 0.01, ***p< 0.001, one way ANOVA followed by Tukey's multiple comparison test.

To assess robustness of the above-mentioned metabolic signatures in samples coming from other groups of patients, we repeated experiments with other cell pools (see Materials and Methods section). More specifically, we performed $^{13}\text{C}_6$ -glucose tracing (Appendix A, Figure 1a) in microtissues assembled from two additional cell pools of different ages. In addition, we performed $^{13}\text{C}_5$ -glutamine tracer analysis, (Appendix A, Figure 2a) of microtissues assembled from one of these two. Regarding $^{13}\text{C}_6$ -glucose tracing results, we observed enhanced

glycolysis in all three pools as evidenced by high percentage glucose labeling to lactate and lactate production at Day 21 compared to Day 0. (Appendix A, Figure 1b-c). Relative lactate production to D0 was significantly higher in pool 1 relative to the other two at Day 21, indicating possibly an even more enhanced glycolytic metabolic phenotype (extended data, Figure 1c). Furthermore, in pool 1 and pool 2 glucose-dependent fueling of the TCA cycle was mainly via pyruvate dehydrogenase (m+2, m+4 mass distribution vectors (MDVs)) and less via pyruvate carboxylase (m+3 MDV). Notably, in cell pool 3 we observed a significantly higher percentage of m+6 MDV compared to the other cell pools, indicating that glucose has been efficiently metabolized through glycolysis and then fully incorporated into the TCA cycle (Appendix A, Figure 1d). Additionally, we noticed differences in other glucose-derived metabolic pathways and more specifically serine biosynthesis (Appendix A, Figure 1e). In all three pools, relatively high percentages of labeled serine were observed from Day 7 to Day 21. For cell pools 1 and 3, we noticed a similar behavior in terms of significant increase of labelling in Day 7 compared to Day 0. In contrast, for cell pool 2, the percentage of labeling was similar between Day 0 and Day 7. This is an interesting finding that raises the question if cell pools 1 and 3 at Day 7 are characterized by higher proliferation given the fact that *de novo* serine synthesis generates nucleotides that are necessary for proliferation. Interestingly, high percentages of glucose-derived palmitate and a significant increase of Day 21 versus Day 0 has been observed in all of the three cell pools, indicating that *de novo* glucose dependent fatty acid synthesis is donor independent (Appendix A, Figure 1f). However, we could observe a significantly higher percentage of labeled palmitate in cell pool 1 and cell pool 3 compared to cell pool 2 at Day 0 and Day 14 (Appendix A, Figure 1f). The glutamine tracer analysis showed the shift from glutamine oxidation to reductive carboxylation at Day 21 in cell pools 1 and 2 (Appendix A, Figure 2a,b). Furthermore, the fractional contribution of glutamine to the TCA cycle metabolites was similar in both pools 1 and 2 (Appendix A, Figure 2c). Finally, glutamine enrichment in proline and hydroxyproline showed a similar pattern during the differentiation of the microtissues with no statistically significant differences in the percentages of labeling (Appendix A, Figure 2d). This suggests that glutamine-derived metabolic features are donor independent.

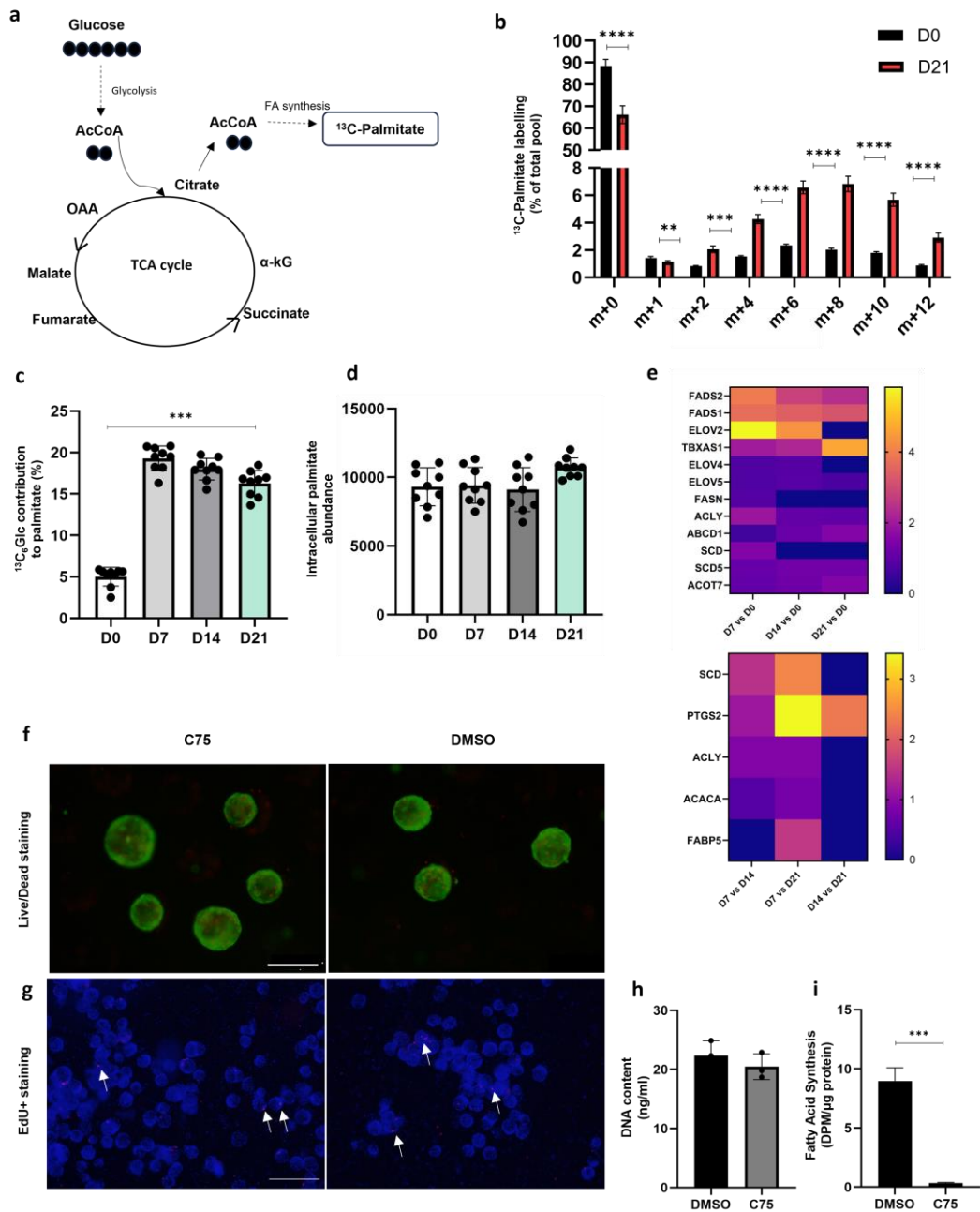


Figure 4. *De novo* glucose dependent fatty acid synthesis during differentiation of cartilaginous microtissues.

a) Schematic of carbon atoms (circles) transitions of labeled glucose used to detect label incorporation into palmitate. b) Glucose derived palmitate mass distribution vector (MDV) after 48h ¹³C₁₃ Glc incorporation. c) Palmitate labeling from ¹³C₁₃ Glc at different time points during cartilaginous microtissues differentiation. d) Relative abundance of palmitate during cartilaginous microtissues differentiation. e) Transcriptomics revealed significant upregulation of genes related to fatty acid synthesis, as shown by the heatmaps. The scale refers to log₂ fold change. f) Representative images of LIVE (green)/ DEAD (red) staining for Day 21 microtissues treated with 20 μM of C75 for 1 week and 20 μM of DMSO (vehicle) respectively. Scale bar: 200 μm, h) Representative images of EdU staining (EdU, red) of Day 21 microtissues treated with 20 μM of C75 for 1 week and 20 μM of DMSO (vehicle) respectively, blue represents the nucleus. Scale bar: 500 μm. h) DNA quantification of Day 21 microtissues treated with 20 μM of C75 for 1 week and DMSO (vehicle) respectively i) [U-¹⁴C]-Acetate assay confirmed the pharmacological inhibition of FAS in the C75-treated microtissues as opposed to the vehicle (DMSO) treated ones.

3.4.2 Chemical inhibition of Fatty Acid Synthase led to downregulation of genes related to endochondral ossification

To further investigate the functional role of glucose-dependent *de novo* fatty acid synthesis in chondrocytes, a largely unexplored pathway in the context of endochondral ossification, we performed chemical inhibition of Fatty Acid Synthase (FASN). We selected *tetrahydro-4-methylene-2R-octyl-5-oxo-3S-furancarboxylic acid* (C75), an inhibitor widely used in cancer metabolism studies^{27,28}. As already reported in other cell types²⁹, treatment of the microtissues during 1 week with 20 μ M of C75, resulted in the inhibition of fatty acid synthesis, as assessed by the ¹⁴C acetate assay (Figure 4i). Live/Dead staining and the DNA content measurements indicated no significant differences in the viability of microtissues treated with C75 compared to the control ones, and EdU staining did not show impairment of proliferation in the treated microtissues (Figure 4f,4g,4h).

To identify alterations in gene expression induced by the inhibitor, we carried out transcriptomic profiling of microtissues cultured in the presence of DMSO (vehicle control) and C75. We identified 574 significant ($p < 0.05$ and $\log_2\text{-fold} > 1$) differentially expressed genes, 324 downregulated and 250 upregulated (Fig 5a). We used pathway analysis (Enrichr)^{30,31} with GO Biological Process, WikiPathway, KEGG, and REACTOME, revealing significant downregulation of endochondral ossification (WP474), calcium signaling (KEGG) and upregulation of osteoblast proliferation (REACTOME). Moreover, significant downregulation was observed in other relevant pathways, including FGFR3 and c GMP-PKG signaling (Fig. 5b). There is evidence that the latter plays an important role in bone regeneration by regulating the BMP and VEGF production in osteoblasts³². Regarding the upregulated pathways, FASN inhibition led to ferroptosis at the transcriptome level (Figure 5b). Heme oxygenase 1 (HMOX1), which is one of the 30 most significantly upregulated genes (\log_2 fold change 2.88), has been suggested as an important (pro) ferroptotic marker implicated in osteoporosis³³. The upregulation of matrix metalloproteinases activation (Figure 5b), possibly connected with the phenomenon of ferroptosis is another pathway of interest for the *in vitro* process studied here. In the context of endochondral ossification, the significant downregulation of the MAPK pathway (Figure 5b) is of particular interest, given its crucial role in the regulation of cartilage development³⁴. At the metabolic level, we also noticed upregulation of genes related to glutathione metabolism, oxidative stress, fatty acid biosynthesis and arachidonic metabolism, (Appendix A, Figure 3). Glutathione metabolism is a key regulator for cell viability in oxidative stress conditions and, together with the increase in the folate biosynthesis pathway (Figure 5b), suggests metabolic flexibility of the Day 21 microtissues possibly due to ferroptosis as explained in the discussion.

Additionally, we analyzed the influence of FASN inhibition on well-known regulators of endochondral ossification. Notably, we observed significant downregulation of chondrocyte hypertrophy activators such as IHH, MEF2C, FOXA2, and RUNX3³⁴ (Figure 5c). C75 treated samples showed significant downregulation in the gene expression of collagens (COL91, COL11A1) and in signaling factors related to pre-hypertrophic /hypertrophic chondrocytes and osteoblasts such as SP7 (OSX), ALPL, and IBSP^{35,36} , (Figure 5c) linked to matrix mineralization and osteogenic differentiation³⁴. Among the most significantly downregulated genes were the IFITM5 (-6.16 logfoldchange), a marker of osteogenic differentiation also expressed in hypertrophic chondrocytes as revealed from previously published single cell RNAseq studies^{37,38,39} , and SMPD3 (-4.86 logfoldchange), a lipid-metabolizing enzyme present in bone and cartilage has been identified as key regulator for endochondral bone development⁴⁰ (Figure 5c).

Interestingly the fatty acid synthesis inhibition led to downregulation of the SCIN gene⁴¹, crucial for bone resorption (Figure 5c). Moreover, when we looked for angiogenesis related gene markers, as a critical regulator for cartilage to bone transition, we noticed significant downregulation of IRF6 and SCUBE1 (Figure 5c). Notably, THBS1, an endogenous inhibitor of angiogenesis⁴² showed significant upregulation in the C75 treated microtissues (Figure 5c). Moreover, we observed significant downregulation of the genes REEP1, F13A1, CAPN6, S100A, and FOXA2 related to the prehypertrophic/hypertrophic state of chondrocytes (Figure 5c). Importantly, these genes were among the endochondral ossification related genes, that were significantly upregulated in the comparison of D21 vs D14 microtissues in our previous study⁴. Additionally, these genes correlated to further maturation as evidenced by the formation of a bone ossicle with the presence of a bone marrow compartment in the D21 microtissues-based constructs as opposed to the D14 microtissues-based constructs.

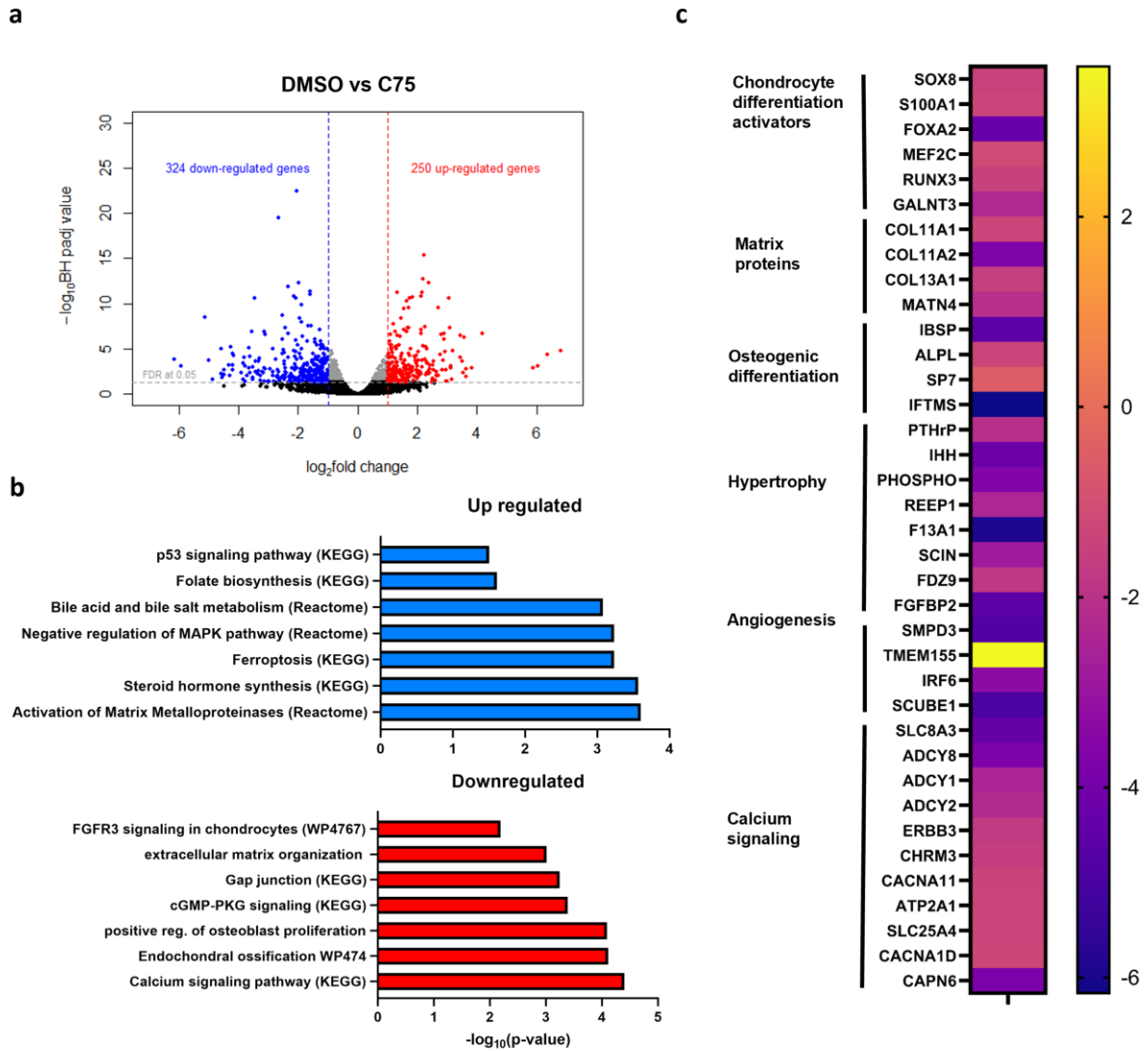


Figure 5. Transcriptomics analysis of C75 treated microtissues vs vehicle control ones of Day 21.

a) Volcano plot of differentially expressed genes from RNA-seq data between the C75 treated microtissues and the vehicle. X- and Y- axis represent \log_2 fold change and \log_{10} -pvalue, respectively. Blue dots and red dots represent downregulated and upregulated genes respectively with \log_2 fold change > 1 and padj < 0.05. b) Gene enrichment analysis in microtissues upon treatment with C75 versus the vehicle control ones of Day 21. Top up-/downregulated pathways from KEGG, Wiki, Reactome, and GO Biological processes. The scale refers to \log_{10} pvalue. c) Heatmap of differentially expressed genes related to chondrogenic hypertrophy, matrix proteins and endochondral ossification regulators, osteoblasts, angiogenesis, and calcium signaling pathway. The scale refers to \log_2 fold change.

3.4.3 Chemical inhibition of FASN led to poor survival of the TE constructs after implantation.

Since fatty acid synthesis inhibition led to significant downregulation of critical genes/regulators of the *in vitro* chondrogenic differentiation, we aimed to investigate whether the C75 inhibition had an effect on the bone forming potential of the microtissues after *in vivo* implantation. Day 21 microtissue constructs were exposed to C75 while a control group of constructs was cultured in the vehicle solution. All constructs were implanted ectopically (subcutaneously) for 4 weeks in immunodeficient mice to investigate bone forming capacity of the microtissues. For the first group (C75-treated constructs), only 1 out of 4 was retrieved. In contrast, 4 out of 4 of the vehicle controls were harvested.

Nanofocus Computed Tomography (nanoCT) as well as Safranin O staining on histological sections confirmed the presence of cortical-like bone, trabecular structure, and well-developed bone marrow compartments. These were similar to the constructs cultured in chondrogenic medium without DMSO (Figure 6). In contrast, in the C75-treated explant, we observed only a very small portion of the tissue that was mineralized (d~500µm) which was associated with a minimal formation of bone marrow compartment (Figure 6). These histology results might be explained through our transcriptomics data, which showed significant downregulation of not only hypertrophic related genes but also angiogenic factors, both of crucial importance for endochondral ossification.

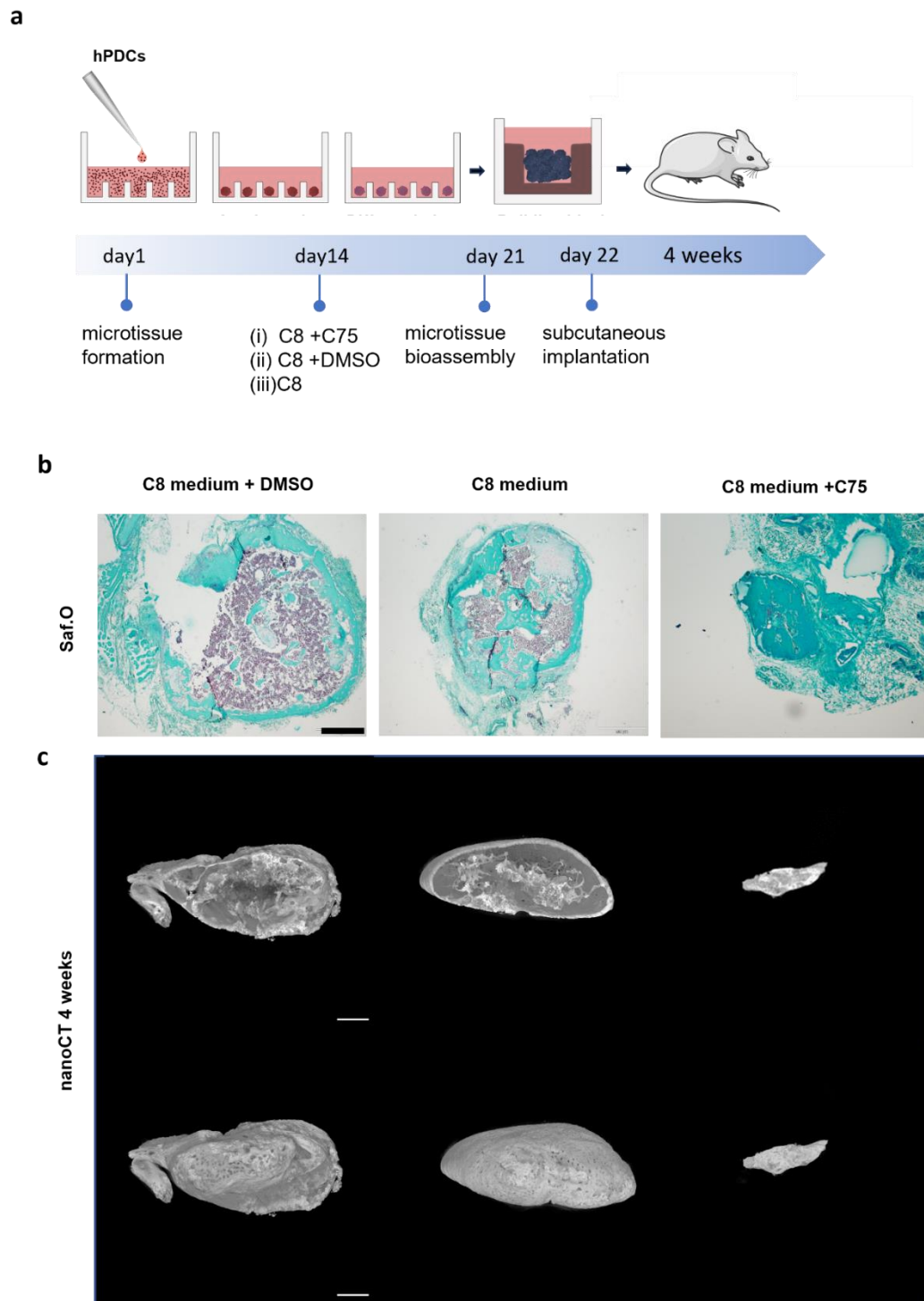


Figure 6. Chemical inhibition of fatty acid synthesis led to poor survival of the in vivo constructs explanted after 4 weeks as opposed to the vehicle ones.

a) Schematic representation of culture, assembly of microtissues and implantation in mice models b) Safranin O staining of vehicle treated (DMSO) Day 21 construct (left) versus chondrogenic differentiation medium treated (middle) and C75 treated (right). C) 3D rendering of nanoCT images of Day 21 construct treated with vehicle (DMSO) (left) versus chondrogenic differentiation medium (middle) and C75 (right) explanted after 4 weeks in vivo. Scale bar 500 μ m.

3.5 Discussion

In this study, we characterized the metabolic profiles of hPDC-derived cartilaginous microtissues. More specifically, stable isotope tracer analysis revealed metabolic alterations during the consecutive stages of chondrogenic differentiation of these microtissues. Interestingly, we observed recapitulation of known metabolic signatures as reported for growth plate chondrocytes as well as alterations in metabolic pathways largely unexplored for the *in vitro* chondrogenic differentiation process. We showed that upregulation of the glutamine carbons in proline and hydroxyproline was linked to ECM production in the early phases of the *in vitro* culture process, followed by matrix turnover in the later stages. Furthermore, we identified a progressive increase in glucose-dependent *de novo* fatty acid synthesis towards the (pre)hypertrophic stage of the microtissues differentiation process, making it a potential critical quality attribute for functionality of microtissue-based constructs for transplantation *in vivo*. Chemical inhibition of FASN using the small molecule C75 led to significant downregulation of important regulators of endochondral bone formation and poor survival of the *in vivo* constructs in comparison to the vehicle controls.

Lipids play a wide variety of roles in cell physiology, as energy sources, signaling molecules, protein modification, and cellular components, although these roles vary between cell types⁴³. In the context of chondrogenesis, there are some studies highlighting the role of lipids. Ceramidase acid seems to improve chondrogenic differentiation of BMSCs⁴⁴ while there is an early study showing that lipid content is higher in cultured growth plate chondrocytes than articular chondrocytes⁴⁵. Another class of lipids with importance for chondrocytes is the class of phospholipids. More specifically, a recent study revealed that LPLAT4, a key enzyme in the metabolism of glycerophospholipids, is involved in chondrogenic hypertrophy and bone mineralization⁴⁶. Moreover, in the context of endochondral ossification it has been shown that intracellular biosynthesis of cholesterol and lipids in gene level is necessary for normal bone growth⁶⁸. Interestingly the role of FAs in the fracture healing process can include the one of “tissue messengers”⁴⁷ for neighboring cells, the macrophages. There is increasing evidence that macrophages are needed for endochondral ossification during fracture repair. In a recent study it was shown that apoptotic chondrocytes modulate the pro-osteogenic differentiation properties of macrophages by releasing FAs⁴⁸. Fatty acids are important energy sources for osteoblasts as shown by van Gestel et al, who demonstrated that FAO occurs in skeletal progenitor cells and osteoblasts, and that loss of CPT1, a key enzyme of FAO, led to decreased osteogenic differentiation^{15,49} but did not affect the chondrogenic differentiation of skeletal progenitors¹⁵.

In the context of endochondral bone formation for long-bone fracture healing, to the best of our knowledge, the role of *de novo* lipogenesis has not been thoroughly investigated. Initially, the fracture callus is an avascular fibrocartilaginous tissue where diffusion mechanisms will dictate nutrient availability. More specifically, while glucose and amino acids can be available to cells via diffusion mechanisms, larger molecules like lipids cannot access the matrix-embedded chondrocytes^{15,50}. Thus, it has been suggested that, as seen in cancer cells⁵¹, it is possible that chondrocytes depend on *de novo* fatty acid synthesis for their energy needs, cell membrane function, signaling, and post translational modifications. To date, there is one study by Kikuchi *et al*⁶² that revealed that genetic deletion of ELOV6, an enzyme that regulates the elongation of very long chain fatty acids, led to decreased chondrogenic proliferation, increased chondrogenic hypertrophy, and decreased trabecular bone in mice, thus indicating an important role for fatty acid synthesis in cartilage to bone transition during bone development.

Blocking FASN was shown to promote ferroptosis, a reactive oxygen species and iron-dependent cell death caused by excessive lipid peroxidation^{53,54}, in cancer cells^{55,60} and was in line with our transcriptomics analysis (Figure 5b). These are interesting results that require further investigation including validation of ferroptosis occurring as a process. Recently, ferroptosis has been shown to be implicated in osteoarthritis and osteoporosis but not in the context of endochondral ossification in the growth plate^{56,57}. It is of note to mention that in our study, bulk RNAseq analysis revealed significant upregulation of MMP13 and MMP7, important ECM degrading enzymes. Interestingly, in the context of osteoarthritis, a recent study showed that ferroptotic chondrocytes promoted the expression of MMP13⁵⁶. Moreover, chemical inhibition of FASN led to the significant upregulation of the KEGG pathways for steroid hormone biosynthesis and folate synthesis (Figure 5b). On the metabolic level, we also noticed upregulation of genes related to glutathione metabolism, HIF signaling, fatty acid biosynthesis, and arachidonic metabolism (Appendix A, Figure 3). Glutathione metabolism is a key regulator for cell viability in oxidative stress conditions and, together with the increase in the folate biosynthesis pathway (Figure 5b), suggests possible compensation mechanisms of the microtissues against ferroptosis, as has been reported in cancer cells⁵⁷. The upregulation of genes related to the HIF signaling pathway could be also an indication that the cells try to compensate for the induced ferroptosis^{58,59}. The phenomenon of ferroptosis along with the downregulation of angiogenesis related markers could further explain the poor survival and marginal mineralization potential of the implanted constructs upon treatment with C75 as opposed to the vehicle controls. It is of note that a recent study⁶⁰ showed that FASN inhibition induced ferroptosis in mutant KRAS (KM) lung cancer cells, which are associated with resistance to therapy, highlighting the importance of *de novo* fatty acid synthesis and revealing

a protective role of this pathway against ferroptosis. There is need for further investigation on whether *de novo* lipogenesis in chondrocytes undergoing hypertrophy, especially in a microenvironment poor in lipids, plays a significant role in escaping ferroptosis and thus cell survival, as it is described in the abovementioned study.

This study provides valuable insights related to the characterization of the identity and potency of cartilaginous microtissues. Recent studies in other biological systems have demonstrated that metabolic pathways play a critical role in regulating cell differentiation⁶¹⁻⁶⁷. Future studies will be necessary to investigate the mechanistic link between their metabolic profile and specific functional properties, such as chondrogenic hypertrophy *in vitro* and bone formation *in vivo*. We envisage that these research efforts will lead to the uptake of metabolic profiles as critical quality attributes.

3.6 Conclusion

In this work, we characterized the metabolic profiles of cartilaginous microtissues during their chondrogenic differentiation process *in vitro*. Our study reveals the importance of metabolism as a critical regulator of the *in vitro* process and suggests an important role for *de novo* fatty acid synthesis in the *in vivo* bone forming capacity of cartilaginous microtissues via cartilage to bone transition. Chemical inhibition of fatty acid synthesis using the small molecule C75 resulted in significant downregulation of gene markers typically associated with endochondral ossification and inhibition of bone formation *in vivo*. Furthermore, it paves the way for establishing metabolic profiles as critical quality attributes for the production of functional chondrogenic microtissues.

3.7 References

1. Alsberg, E., Anderson, K. W., Albeiruti, A., Rowley, J. A. & Mooney, D. J. Engineering growing tissues. *Proc. Natl. Acad. Sci. U. S. A.* **99**, 12025–12030 (2002).
2. McDermott, A. M. *et al.* Recapitulating bone development through engineered mesenchymal condensations and mechanical cues for tissue regeneration. *Sci. Transl. Med.* **11**, (2019).
3. Herberg, S. *et al.* Combinatorial morphogenetic and mechanical cues to mimic bone development for defect repair. *Sci. Adv.* **5**, 1–12 (2019).
4. Hall, G. N. *et al.* Developmentally Engineered Callus Organoid Bioassemblies Exhibit Predictive In Vivo Long Bone Healing. **1902295**, 1–16 (2020).
5. Lipsitz, Y. Y., Timmins, N. E. & Zandstra, P. W. Quality cell therapy manufacturing by design. **34**, 393–400 (2016).
6. Vernardis, S. I., Goudar, C. T. & Klapa, M. I. Metabolic profiling reveals that time related physiological changes in mammalian cell perfusion cultures are bioreactor scale independent. *Metab. Eng.* **19**, 1–9 (2013).
7. Lewis, A. M., Abu-Absi, N. R., Borys, M. C. & Li, Z. J. The use of 'Omics technology to rationally improve industrial mammalian cell line performance. *Biotechnol. Bioeng.* **113**, 26–38 (2016).
8. P. Polleselo, B. de Bernard, *et al.* Energy State of chondrocytes assessed by ³¹P-NMR studies of preosseous cartilage, *Biochem. Biophys. Res. Commun.* **180**, 216–222 (1991)..
9. Miyazawa, H. & Aulehla, A. Revisiting the role of metabolism during development. *Dev.* **145**, (2018).
10. Klontzas, M. E., Vernardis, S. I., Heliotis, M., Tsiroidis, E. & Mantalaris, A. Metabolomics Analysis of the Osteogenic Differentiation of Umbilical Cord Blood Mesenchymal Stem Cells Reveals Differential Sensitivity to Osteogenic Agents. *Stem Cells Dev.* **26**, 723–733 (2017).
11. McNamara, L. E. *et al.* Nanotopographical control of stem cell differentiation. *J. Tissue Eng.* **1**, 1–13 (2010).
12. Lee, S. Y., Abel, E. D. & Long, F. Glucose metabolism induced by Bmp signaling is essential for murine skeletal development. *Nat. Commun.* **9**, 1–11 (2018).
13. Stegen, S. *et al.* HIF-1 α metabolically controls collagen synthesis and modification in chondrocytes. *Nature* **565**, 511–515 (2019).
14. Stegen, S. *et al.* De novo serine synthesis regulates chondrocyte proliferation during bone development and repair. *Bone Res.* **10**, (2022).
15. Gastel, N. Van *et al.* Lipid availability determines fate of skeletal progenitor cells via

- SOX9. **579**, (2020).
16. Eyckmans, J., Roberts, S. J., Schrooten, J. & Luyten, F. P. A clinically relevant model of osteoinduction: a process requiring calcium phosphate and BMP/Wnt signalling. *J. Cell. Mol. Med.* **14**, 1845–1856 (2010).
 17. Leijten, J., Teixeira, L. S. M., Bolander, J., Ji, W. & Vanspauwen, B. Bioinspired seeding of biomaterials using three dimensional microtissues induces chondrogenic stem cell differentiation and cartilage formation under growth factor free conditions. 1–12 (2016) doi:10.1038/srep36011.
 18. Mendes, L. F. *et al.* Combinatorial Analysis of Growth Factors Reveals the Contribution of Bone Morphogenetic Proteins to Chondrogenic Differentiation of Human Periosteal Cells. *Tissue Eng. - Part C Methods* **22**, 473–486 (2016).
 19. Livak, K. J. & Schmittgen, T. D. Analysis of relative gene expression data using real-time quantitative PCR and the 2- $\Delta\Delta$ CT method. *Methods* **25**, 402–408 (2001).
 20. Lorendeau, D. *et al.* Dual loss of succinate dehydrogenase (SDH) and complex I activity is necessary to recapitulate the metabolic phenotype of SDH mutant tumors. *Metab. Eng.* **43**, 187–197 (2017)..
 21. Elia, I. *et al.* Proline metabolism supports metastasis formation and could be inhibited to selectively target metastasizing cancer cells. *Nat. Commun.* **8**, 1–11 (2017).
 22. Stegen, S. *et al.* *HHS Public Access*. vol. 565 (2020).
 23. van Gastel, N. & Carmeliet, G. Metabolic regulation of skeletal cell fate and function in physiology and disease. *Nat. Metab.* **3**, 11–20 (2021).
 24. Riegger, J., Baumert, J., Zaucke, F. & Brenner, R. E. The hexosamine biosynthetic pathway as a therapeutic target after cartilage trauma: Modification of chondrocyte survival and metabolism by glucosamine derivatives and pugnac in an ex vivo model. *Int. J. Mol. Sci.* **22**, (2021).
 25. Wang, Y. *et al.* Coordinative metabolism of glutamine carbon and nitrogen in proliferating cancer cells under hypoxia. *Nat. Commun.* **10**, (2019).
 26. Ling, Z. N. *et al.* Amino acid metabolism in health and disease. *Signal Transduct. Target. Ther.* **8**, (2023).
 27. Kuhajda, F. P. *et al.* Synthesis and antitumor activity of an inhibitor of fatty acid synthase. *Proc. Natl. Acad. Sci. U. S. A.* **97**, 3450–3454 (2000).
 28. Koundouros, N. & Poulogiannis, G. Reprogramming of fatty acid metabolism in cancer. *Br. J. Cancer* **122**, 4–22 (2020).
 29. Gao, Y. *et al.* Growth arrest induced by C75, a fatty acid synthase inhibitor, was partially modulated by p38 MAPK but not by p53 in human hepatocellular carcinoma. *Cancer Biol. Ther.* **5**, 978–985 (2006).
 30. Kuleshov, M. V. *et al.* Enrichr: a comprehensive gene set enrichment analysis web

- server 2016 update. *Nucleic Acids Res.* **44**, W90–W97 (2016).
31. Chen, E. Y. *et al.* Enrichr: Interactive and collaborative HTML5 gene list enrichment analysis tool. *BMC Bioinformatics* **14**, (2013).
 32. Schall, N. The role of cGMP / PKG1 signaling in osteogenic differentiation. (2021).
 33. Xia, Y. *et al.* Identification and validation of ferroptosis key genes in bone mesenchymal stromal cells of primary osteoporosis based on bioinformatics analysis. *Front. Endocrinol. (Lausanne)*. **13**, 1–15 (2022).
 34. Henry M. Kronenberg. Developmental regulation of the growth plate. *Nature* **423**, 332–336 (2003).
 35. Park, J. *et al.* Dual pathways to endochondral osteoblasts: A novel chondrocyte-derived osteoprogenitor cell identified in hypertrophic cartilage. *Biol. Open* **4**, 608–621 (2015).
 36. Marinovich, R. *et al.* The role of bone sialoprotein in the tendon-bone insertion. *Matrix Biol.* **52–54**, 325–338 (2016).
 37. Hanagata, N. *et al.* Characterization of the osteoblast-specific transmembrane protein IFITM5 and analysis of IFITM5-deficient mice. *J. Bone Miner. Metab.* **29**, 279–290 (2011).
 38. Maranda, V., Gaumond, M. H. & Moffatt, P. The Osteogenesis Imperfecta Type V Mutant BRIL/IFITM5 Promotes Transcriptional Activation of MEF2, NFATc, and NR4A in Osteoblasts. *Int. J. Mol. Sci.* **23**, (2022).
 39. Bell. 2018_Pnas_Si_Spe. *Proc. Natl. Acad. Sci.* **120**, 2017 (2017).
 40. Li, J. *et al.* Smpd3 Expression in both Chondrocytes and Osteoblasts Is Required for Normal Endochondral Bone Development. *Mol. Cell. Biol.* **36**, 2282–2299 (2016).
 41. D. Nurminsky *et al.* Regulation of chondrocyte differentiation by actin-severing protein adseverin. *Dev. Biol.* **302**, 427–437 (2007).
 42. Liao, F. *et al.* ECFC-derived exosomal THBS1 mediates angiogenesis and osteogenesis in distraction osteogenesis via the PI3K/AKT/ERK pathway. *J. Orthop. Transl.* **37**, 12–22 (2022).
 43. Boskey, A. L. & Reddi, A. H. Changes in lipids during matrix: Induced endochondral bone formation. *Calcif. Tissue Int.* **35**, 549–554 (1983).
 44. Simonaro, C. M. *et al.* Acid Ceramidase Maintains the Chondrogenic Phenotype of Expanded Primary Chondrocytes and Improves the Chondrogenic Differentiation of Bone Marrow-Derived Mesenchymal Stem Cells. *PLoS One* **8**, (2013).
 45. Le Lous, M., Corvol, M. T. & Maroteaux, P. Lipid composition of two types of chondrocytes in primary culture. *Calcif. Tissue Int.* **33**, 403–407 (1981).
 46. Tabe, S. *et al.* Lysophosphatidylcholine acyltransferase 4 is involved in chondrogenic differentiation of ATDC5 cells. *Sci. Rep.* **7**, 1–11 (2017).
 47. Titus, S. Li, F., Stobezki, R., Akula, K., Unsal, E. , Jeong, K., Dickler, M., Mar Robson,

- M., Moy, F. , Goswami, S., Oktay, K. Impairment of BRCA1-related DNA Double Strand Break Repair Leads to Ovarian Aging in Mice and Humans, 2013, *Sci Transl Med.*, 5(172):1-25 HHS Public Access. *Physiol. Behav.* **176**, 139–148 (2016).
48. Zheng, Z. Y. *et al.* Fatty acids derived from apoptotic chondrocytes fuel macrophages FAO through MSR1 for facilitating BMSCs osteogenic differentiation. *Redox Biol.* **53**, 102326 (2022).
 49. Kim, S. P. *et al.* Fatty acid oxidation by the osteoblast is required for normal bone acquisition in a sex- And diet-dependent manner. *JCI Insight* **2**, 1–16 (2017).
 50. Torzilli, P. A., Grande, D. A. & Arduino, J. M. Diffusive properties of immature articular cartilage. *J. Biomed. Mater. Res.* **40**, 132–138 (1998).
 51. Daniëls, V. W. *et al.* Cancer cells differentially activate and thrive on de novo lipid synthesis pathways in a low-lipid environment. *PLoS One* **9**, 13–19 (2014).
 52. Kikuchi, M. *et al.* Crucial role of Elovl6 in chondrocyte growth and differentiation during growth plate development in mice. *PLoS One* **11**, 1–18 (2016).
 53. Zhang, C., Liu, X., Jin, S., Chen, Y. & Guo, R. Ferroptosis in cancer therapy: a novel approach to reversing drug resistance. *Mol. Cancer* **21**, 1–12 (2022).
 54. Li, J. *et al.* Ferroptosis: past, present and future. *Cell Death Dis.* **11**, (2020).
 55. Li, Y. *et al.* Targeting fatty acid synthase modulates sensitivity of hepatocellular carcinoma to sorafenib via ferroptosis. *J. Exp. Clin. Cancer Res.* **42**, 1–19 (2023).
 56. Xiong, Y. *et al.* The Regulatory Role of Ferroptosis in Bone Homeostasis. *Stem Cells Int.* **2022**, (2022).
 57. Lv, Z. *et al.* Single cell RNA-seq analysis identifies ferroptotic chondrocyte cluster and reveals TRPV1 as an anti-ferroptotic target in osteoarthritis. *eBioMedicine* **84**, 104258 (2022).
 58. Chen, Y. *et al.* CRISPR screens uncover protective effect of PSTK as a regulator of chemotherapy-induced ferroptosis in hepatocellular carcinoma. *Mol. Cancer* **21**, 1–17 (2022).
 59. Su, J. *et al.* Prospective Application of Ferroptosis in Hypoxic Cells for Tumor Radiotherapy. *Antioxidants* **11**, 1–17 (2022).
 60. Bartolacci, C. *et al.* Targeting de novo lipogenesis and the Lands cycle induces ferroptosis in KRAS-mutant lung cancer. *Nat. Commun.* **13**, (2022).
 61. Kuppusamy, K. T. *et al.* Let-7 family of microRNA is required for maturation and adult-like metabolism in stem cell-derived cardiomyocytes. *Proc. Natl. Acad. Sci. U. S. A.* **112**, E2785–E2794 (2015).
 62. Panopoulos, A. D. *et al.* The metabolome of induced pluripotent stem cells reveals metabolic changes occurring in somatic cell reprogramming. *Cell Res.* **22**, 168–177 (2012).

63. Bhute, V. J. *et al.* Metabolomics identifies metabolic markers of maturation in human pluripotent stem cell-derived cardiomyocytes. *Theranostics* **7**, 2078–2091 (2017).
64. Callaghan, N. I. *et al.* Harnessing conserved signaling and metabolic pathways to enhance the maturation of functional engineered tissues. *npj Regen. Med.* **7**, (2022).
65. Oburoglu, L. *et al.* Glucose and glutamine metabolism regulate human hematopoietic stem cell lineage specification. *Cell Stem Cell* **15**, 169–184 (2014).
66. Tohyama, S. *et al.* Distinct metabolic flow enables large-scale purification of mouse and human pluripotent stem cell-derived cardiomyocytes. *Cell Stem Cell* **12**, 127–137 (2013).
67. Zhang, H. *et al.* Distinct Metabolic States Can Support Self-Renewal and Lipogenesis in Human Pluripotent Stem Cells under Different Culture Conditions. *Cell Rep.* **16**, 1536–1547 (2016).
68. Tsushima, H. *et al.* Intracellular biosynthesis of lipids and cholesterol by Scap and insig in mesenchymal cells regulates long bone growth and chondrocyte homeostasis. *Dev.* **145**, (2018).

Chapter 4.

Stirred culture of cartilaginous microtissues promotes chondrogenic hypertrophy through exposure to intermittent shear stress

4

Loverdou N.^{1,2,3,4}, Cuvelier M.^{1,5}, Nilsson Hall, G.^{1,2}, Christiaens A.S.⁶, Decoene, I.^{1,2}, Bernaerts K.⁶, Smeets B.^{1,5}, Ramon, H.⁵, Luyten, F.P.^{1,2}, Geris, L.^{1,2,3,4}, Papantoniou, I.^{1,2,8*}.

- ¹Prometheus, Division of Skeletal Tissue Engineering, KU Leuven, Leuven, Herestraat, Belgium,
²Skeletal Biology & Engineering Research Centre, Department of Development & Regeneration, KU Leuven, Leuven, Herestraat, Belgium
³Biomechanics Research Unit, GIGA-R In Silico Medicine, Université de Liege, Avenue de l'Hôpital 11—BAT 34, Liège 1, Belgium
⁴Biomechanics Section, KU Leuven, Celestijnenlaan, Leuven, Belgium
⁵Biosystems Department, MeBioS, KU Leuven, Kasteelpark Arenberg, Leuven, Belgium
⁶Department of Chemical Engineering, KU Leuven, Celestijnenlaan, Leuven, Belgium
⁷Leuven Chem&Tech, Celestijnenlaan, Leuven, Belgium
⁸Institute of Chemical Engineering Sciences, Foundation for Research and Technology-Hellas (FORTH), Stadiou St, Platani, Patras, Greece

Manuscript adapted from *Bioengineering and Translational Medicine* (2022), doi.org/10.1002/btm2.10468

4.1 Abstract

Cartilage microtissues are promising tissue modules for bottom up biofabrication of implants leading to bone defect regeneration. Hitherto, most of the protocols for the development of these cartilaginous microtissues have been carried out in static setups, however, for achieving higher scales, dynamic process needs to be investigated. In the present study, we explored the impact of suspension culture on the cartilage microtissues in a novel stirred microbioreactor system. To study the effect of the process shear stress, experiments with three different impeller velocities were carried out. Moreover, we used mathematical modeling to estimate the magnitude of shear stress on the individual microtissues during dynamic culture. Identification of appropriate mixing intensity allowed dynamic bioreactor culture of the microtissues for up to 14 days maintaining microtissue suspension. Dynamic culture did not affect microtissue viability, although lower proliferation was observed as opposed to the statically cultured ones. However, when assessing cell differentiation, gene expression values showed significant upregulation of both Indian Hedgehog (*IHH*) and collagen type X (*COLX*), well known markers of chondrogenic hypertrophy, for the dynamically cultured microtissues. Exometabolomics analysis revealed similarly distinct metabolic profiles between static and dynamic conditions. Dynamic cultured microtissues showed a higher glycolytic profile compared with the statically cultured ones while several amino acids such as proline and aspartate exhibited significant differences. Furthermore, *in vivo* implantations proved that microtissues cultured in dynamic conditions are functional and able to undergo endochondral ossification. Our work demonstrated a suspension differentiation process for the production of cartilaginous microtissues, revealing that shear stress resulted to an acceleration of differentiation towards hypertrophic cartilage.

4.2 Introduction

Patients with failing intrinsic tissue regeneration, such as those with complex and large bone defects in compromised biological conditions, need solutions coming from the field of tissue engineering¹. There is growing evidence that the implantation of engineered cartilage-intermediate tissues results in efficient bone formation and bone defect regeneration^{2,3} via endochondral ossification, a regenerative process mimicking embryonic limb development⁴. Cartilage-intermediate tissue implants have been engineered through the use of adult human progenitor cells from various sources such as bone marrow^{5,6} and periosteum (hPDCs)⁷. This strategy has been explored in multiple tissue formats such as chondrogenically primed microaggregates⁸, hypertrophic microtissues⁴, hollow tubes⁹, and cell sheets¹⁰ which resulted in regeneration of critical size long bone defects.

In a recent study⁴, the use of planar culture technologies through the use of non-adherent microwells resulted in the formation of cartilaginous microtissue modules, able to self-assemble in larger implants and regenerate large tibial defects in murine animal models. However, suspension culture of the abovementioned functional microtissues, needs to be further explored, as this will further pave the way towards the development of scaled up bioprocesses able to produce clinically relevant amounts of microtissue populations. Bioreactors allow for scalability while providing capacity for real-time monitoring and control of the culture and differentiation process of stem cells¹¹. Stirred tank reactors represent a universal, well-established vessel type for the production of adult progenitor cells on microcarriers¹² and human pluripotent stem cells¹³. These systems have also been used to culture articular chondrocytes seeded on microcarriers¹⁴. Several differentiation protocols for the production of differentiated induced pluripotent stem (iPS) cells in stirred tank bioreactors have been reported for different tissues including cardiac^{15,16}, neural^{17,18}, and kidney¹⁹ cell types. Few studies have focused on the static suspension culture of cartilage microtissues from iPS cells²⁰ or chondrocyte microtissues from bovine source in a stirred culture environment²¹ with limited process characterization. We have previously explored a microcarrier-based stirred tank suspension process for expansion and differentiation of human adult periosteal-derived progenitors with incomplete chondrogenic differentiation and maturation due to limited cell condensation on the microcarrier surface²², hence there is still room to explore the potential for culture microtissues in stirred bioreactor systems.

An inherent component in dynamic suspension culture is the effect of fluid-generated shear stresses on the culture progenitor cells or microtissues. Currently there is lack of knowledge on the impact of process-generated shear stresses on chondrogenic maturation towards hypertrophy in suspension cultures of cartilaginous microtissues. Furthermore, to date, in vitro

studies have reported mixed results related to the impact of mechanical stress on chondrogenic differentiation with diverse mechanical regimes enhancing primary chondrocyte hypertrophy³ or inhibiting it during adult MSC culture⁵. For a thorough characterization of the process environment to be made, CFD models have been developed²³. However, a limitation of these approaches is that they rely on bulk estimates without considering the discrete nature of these microtissue suspensions²⁴ and the active (adhesive) properties of cell aggregates/microtissue structures.

In this study, we aimed at investigating the suspension culture of cartilaginous microtissues and the role of fluid-generated shear stresses on the process of chondrogenic differentiation towards hypertrophy. To carry out these experiments, we produced a microbioreactor system that provided the same volume and microtissue density as that of the static-planar setup. Mechanical stimulation during culture on single microtissues was characterized and quantified through simulations with advanced mathematical models representing individual microparticles instead of only the fluid component. Additionally, exometabolomics analysis was conducted to further characterize the cellular state due to the mechanical stimulation. Our work suggests that culture in suspension bioreactors is possible and that shear stress alters the phenotypic and metabolic state of the microtissue with a rapid commitment to hypertrophy.

4.3 Materials and Methods

4.3.1 Cell expansion

Cells of five female donors of age 14 ± 3 years old were isolated from periosteal biopsies as previously described.²⁵ Briefly, the periosteal biopsies were washed and digested in type IV collagenase (440 units/ mg; Invitrogen, BE) in growth medium (high-glucose Dulbecco's modified Eagle's medium DMEM; Invitrogen, BE) supplemented with 10% fetal bovine serum (FBS; BioWhittaker, BE), and an antibiotic– antimycotic solution (100 units/ml penicillin, 100 µg/ml streptomycin, and 0.25 µg/ml amphotericin B; Invitrogen, BE). After digestion, all the donor cells were pooled together to create a cell pool. The cell pool was further expanded with a cell density of 5700 cells/cm² (80% confluency per passage) in growth medium at 37 °C, 5% CO₂ and 95% humidity. Growth medium was changed three times per week until 80% confluency when the cells were harvested with TrypLE™ Express (Life Technologies, UK) for 10 min at 37°C. All procedures were approved by the ethical committee for Human Medical Research (KU Leuven) and patients' informed consent forms were obtained (ML7861).

4.3.2 Microtissue formation

Negative microwell molds were fabricated with polydimethylsiloxane (PDMS, Dow Corning Sylgard 184 elastomer, MAVOM Chemical Solutions) as described elsewhere²⁶. To create microwells (150 μm depth, 200 μm diameter), 3% agarose (Thermo Fisher) was poured over the PDMS mold and let to cool down. The agarose layer with microwells was punched into dimensions fitting tightly a 24 well plate (area $\sim 1.8\text{ cm}^2$) and placed in a 24-well plate and sterilized under UV. One 24 well plate well contained approximately 2000 microwells. Subsequently, 500,000 hPDCs were seeded per well resulting in microtissues with approximately 250 cells/microtissue. Microtissues were differentiated in a xeno-free chemically defined chondrogenic medium composed of LG-DMEM (Gibco) supplemented with 1% antibiotic- antimycotic (100 units/ml penicillin, 100 mg/ml streptomycin and 0.25 mg/ml amphotericin B), 1 mM ascorbate-2 phosphate, 100 nM dexamethasone, 40 $\mu\text{g/ml}$ proline, 20 μM of Rho-kinase inhibitor Y27632 (Axon Medchem), ITS+ Premix Universal Culture Supplement (Corning) (including 6.25 $\mu\text{g/ml}$ insulin, 6.25 $\mu\text{g/ml}$ transferrin, 6.25 $\mu\text{g/ml}$ selenious acid, 1.25 $\mu\text{g/ml}$ bovine serum albumin (BSA), and 5.35 $\mu\text{g/ml}$ linoleic acid), 100 ng/ml BMP-2 (INDUCTOS), 100 ng/ml GDF5 (PeproTech), 10 ng/ml TGF β 1 (PeproTech), 1 ng/ml BMP-6 (PeproTech) and 0.2 ng/ml FGF-2 (R&D systems)²⁷. Static controls were cultured for 16 days, and half of the media (1 ml) was exchanged 2 times per week. For the dynamic condition, cells were seeded as described earlier in order to aggregate and after 2 days microtissues were transferred to the mini-bioreactor and cultured for an additional 14 days with 1 ml fresh medium added 2 times per week.

The small microtissues were assembled in an Aggrewell800 well culture plate to create a second static control with larger assembled microtissues (referred to the manuscript as “static large microtissues”). One well of the Aggrewell800 well plate contains an array of 300 μ - wells with 800 μm in size. The well plate was pre-treated using the Anti-Adherence Rinsing Solution (STEMCELL Technologies) to reduce surface tension and prevent adhesion. Microtissues from the agarose μ -wells (2000 microtissues) were flushed out and transferred to the AggrewellTM800 (300 microwells) 2 days after seeding. This would result in approximately seven small microtissues that fuse into a larger microtissue (Figure 2).

4.3.3 Bioreactor design and culture

The mini-bioreactor (miniBR) setup consisted of four impeller rows, each with six impellers adapted to fit onto a 24 well plate (Corning). The impeller rows and exchangeable impellers were printed using polyamide 12, Nylon (PA12) and selective laser sintering (Formando, BE). The impeller row and impellers were connected with bevel brass gears (Reely) and metal

bearings (W 604-2RS1, SKF) to allow smooth stirring. Each row of six impellers was driven by a ST3518 stepper motor (Nanotec) driven by SMCI-12 motor controllers (Nanotec). In this way, 24 mini-stirred tank reactors with a volume of 2 ml were created using four impeller rows. An in-house developed software (Windows Forms application, NET) written in Visual Basic was used to control the four impeller rows individually. Before use, the 24 well plate was coated with Sigmacote (Sigma Aldrich) to prevent adherence of the microtissues and all components were gas sterilized (Ethylene Oxide). The bioreactor was placed in an incubator at 37 °C, 5% CO₂ and 95% humidity to achieve appropriate cell culture conditions. Microtissues cultured for 2 days were carefully flushed out from their microwells and 2000 microtissues were added to one well of the coated 24 well plate which corresponds to the microtissue density in the static control. The impellers were inserted and started as fast as possible to avoid microtissue fusion and the mini-BR were run at 7, 13, and 20 rad/s corresponding to low, medium, and high speed for 14 days. Chondrogenic media was changed 2 times per week.

4.3.4 Microtissue characterization

Microtissues were characterized microscopically during the differentiation process to assess microtissue size, proliferation, and viability. Cell proliferation was assessed using the Click-iT EdU (5-ethynyl-20-deoxyuridine) Imaging Kit (Life Technologies, USA) according to the manufacturer's protocol. Briefly, microtissues were incubated with 10 µM EdU for 48 h. Next, samples were fixed in 4% paraformaldehyde (PFA) and EdU was detected with Alexa Fluor azide and Hoechst 33342 (5 µg ml⁻¹) for nuclei staining followed by visualization with fluorescence microscope (Olympus IX83) and a confocal microscope (ZEISS LSM 880, Cell Imaging Core (CIC) KU Leuven) with 1 µm step size along the z-axis. Cell viability was qualitatively evaluated using LIVE/DEAD Viability/Cytotoxicity Kit (Invitrogen) following the manufacturer's description. Briefly, microtissues were rinsed in PBS and incubated for 45 min with 2 µM calcein AM and 4 µM ethidium homodimer in PBS. After removal of the staining solution, the samples were imaged in their media using a fluorescence microscope (Olympus IX83).

4.3.5 DNA quantification and gene expression analysis

Microtissues from one well were pooled together to represent one sample and lysed in 350 µl RLT buffer (Qiagen) and 3.5 µl β-mercaptoethanol (VWR). DNA was quantified using the Qubit dsDNA HS Assay Kit (Invitrogen). Briefly, 10 µl lysed sample was diluted in 90 µl milliQ water. Next, 5 µl was added to 195 µl of working solution, vortexed, and incubated for 5 minutes at room temperature. The DNA content was measured using a Qubit R Fluorometer. Next, RNA

was isolated using RNeasy Mini Kit (Qiagen) whereafter RNA concentration and quality was assessed with NanoDrop 2000 (Thermo Scientific). Complementary DNA (cDNA) was synthesized with PrimeScript reagent kit (TaKaRa) followed by quantitative real-time polymerase chain reaction (qRT-PCR) using SYBR® Green (Life Technologies) and StepOnePlus R Real-Time PCR System (Applied Biosystems). The heating cycle was as follows: hold at 45 °C for 2 min, at 95 °C for 30 s, followed by 40 cycles of 95 °C for 3s and 60 °C for 20 s. Relative differences in expression were calculated using the $2^{-\Delta\Delta C_t}$ method normalized to the housekeeping gene Hypoxanthine-guanine phosphoribosyltransferase 1 (HPRT1)²⁸.

4.3.6 Formation of microtissue-based implants

Microtissues from two wells of a 24-well plate (containing approximately ~2400 microtissues) cultured statically we collected on day 14. In addition, from the miniBR after 14 days microtissues were assembled from two wells of 24-well plates. In both cases microtissue suspensions were dispensed in fresh wells containing in their bottom, a layer of agarose with an inverted conical 3 mm diameter well (3 mm in diameter) developed in-house. Microtissues were allowed to sediment for 60 min at 37 °C, 5% CO₂, and 95% humidity leading to the entrapment of the entire population of suspended microtissues in the agarose well. Subsequently, chondrogenic media was added and the microtissue assemblies were let to fuse for 24 h leading to the formation of a mechanically stable mesotissue.

4.3.7 *In vivo* implantation analysis

A subcutaneous mouse model was used to assess the microtissues' capacity to form bone after assembly. The fused mesotissues were implanted subcutaneously in immune compromised mice (Rj:NMRInu/nu) and explants were retrieved after 4 weeks and fixed in 4% PFA. Fixated explants were scanned with nano-computed tomography (nano-CT) (Phoenix Nanotom M, GE Measurement and Control Solutions) for 3D visualization of mineralized tissue. Scans were performed at 60 kV, 140 µA and with diamond target, mode 0, 1 frame average, 0 image skip, 500 ms exposure time, 2400 images, and a 0.1 mm aluminum filter resulting in a voxel size of 2 µm. CTAn (Bruker micro-CT, BE) was used for image processing of mineralized tissue based on automatic Otsu segmentation and 3D visualizations of the mineralized tissue were created in CTvox (Bruker micro-CT, BE). All procedures on animal experiments were approved by the local ethical committee for Animal Research, KU Leuven. The animals were housed according to the regulations of the Animalium Leuven, KU Leuven.

4.3.8 Sampling and metabolite extraction

In order to avoid bias due to sampling, we used all the media for the exometabolomic analysis. Also, samples were taken each time (D0, D7, D14). 2 days after the media changes. In that way, we had consistency for changes related to the refreshing of the medium. For every sample, 990µl of 80% methanol with 2 µM d27 myristic acid was added to 10 µl of sample. Extracts were stored overnight at -80 °C and were centrifuged.

4.3.9 Liquid chromatography-mass spectrometry (LC–MS) analysis

HPLC analysis was carried out on a reversed phase ACQUITY UPLC HSS T3 C18 (1.8 µm, 2.1 x 100mm) column from WATERS on a Q Exactive Hybrid Quadrupole-Orbitrap (Thermo Scientific) system. The mobile phase was delivered at a flow rate of 0.250 ml/min.

The mobile phase consisted of two eluents (A and B). Eluent A was composed of 10 mM TBA and 15 mM acetic acid, and eluent B was 100% Methanol. After injection of 10 µl of sample, gradient elution was performed at 37–41–100% B with linear decreases at 0–7–14–31 min. Finally, 9 min of initial conditions was applied to re-equilibrate the column for further analyses.

4.3.10 Statistical analysis

All experiments were performed with at least three replicates per condition. Data were represented as individual values or box plots, if otherwise not stated. Data were compared with one-way or two-way ANOVA and Tukey's multiple comparisons test. Results were considered statistically different for p values lower than 0.05 (*p < 0.05, **p < 0.01, ***p < 0.001). Statistical analysis was performed with GraphPad Prism 9 (GraphPad Software, Inc., USA), unless otherwise stated.

4.3.11 Computational model of cartilaginous microtissues in the miniBR

To quantify the mechanical environment of the cartilaginous microtissues we used a lattice-free center-based model (CBM) coupled with a computational fluid dynamics (CFD) solver. The full model details are provided in the Supplementary Information (SI) and are briefly summarized here. The CBM was used to simulate cartilaginous microtissues inside of the miniBR while the CFD solver was used to resolve the fluid flow in the reactor. In contrast to bulk estimates, this approach considers the path history of each individual tissue, providing more accurate estimates for relevant mechanical output measures when compared to bulk average estimates.

In a stirred tank with impeller radius R_i and rotational velocity ω , the fluid Reynold number is expressed as $Re_f = \frac{4 \rho_f \omega R_i^2}{\mu_f}$, with fluid density ρ_f and viscosity μ_f . We assume laminar flow for $Re_f < 2000$. Given the dimensions of the vessel, see Figure 2, this holds for ω up to 20 rad/s. Under these conditions, incompressible Stokes equations can be used to model fluid dynamics in the miniBR.

In the CBM, individual microtissues are represented by deformable spherical particles with a size distribution based on microscopy measurements. Using a discrete element-like approach, we solved the equation of motion for each particle to simulate how the micro-tissues moved and interacted. For this, we explicitly determined the forces acting on individual particles at each time step, see SI (ref 2,3m). Furthermore, based on the forces acting on the particles and local fluid velocities we estimated e.g., the magnitude of shear stress acting on the microtissues. We estimate drag and lift forces acting on the particles due to the local fluid flow by probing the local fluid velocity, pressure, and shear gradients, see SI. Given the low Stokes number, $Stk = \frac{t_0 v_t}{2R_p} < 1$, where $t_0 = \frac{\rho_p (2R_p)^2}{18 \mu_f}$ with v_t , R_p , ρ_p the particle terminal velocity, radius, and density, micro-tissues are expected to follow the streamlines closely and behave as stream tracers, allowing for a one-way CFD-CBM coupling. Furthermore, due to $Re_p = \frac{2 \rho_p v_t R_p}{\mu_f} < 1$, Stokes drag can be assumed, providing an analytical expression for drag force. The reported shear stress was estimated by calculating the von Mises stress of each simulated microtissue, averaged over its trajectory in the miniBR, see Figure 2a.

4.4 Results

4.4.1 In-silico characterization of the dynamic process environment in mini-bioreactors

To allow high-throughput screening of culture in stirrer-based bioreactor culture, a mini-bioreactor (miniBR) system was developed. Centimeter-sized impellers were 3D printed and attached in parallel to a motor to fit commercially available 24-well plates (Figure 1a). Four rows were produced and placed into a 24-well plate to generate 24 stirred tank mini-bioreactors (Figure 1b). To investigate the effect of mechanical stimulation on culture outcome, miniBR experiments with three different impeller velocities (7-13-20 rad/s), corresponding to low, medium, and high shear conditions were performed.

To estimate the magnitude of shear stress acting on the individual microtissues during dynamic culturing simulations with a coupled CBM-CFD model were performed, see Figure 1c-d. In the computational model, we initialized particles that represent microtissues based on the observed size distribution of the dynamic culture conditions and simulated the three miniBR

setups. As expected, the relative magnitude of the experienced shear stress increases with the angular velocity of the impeller. In the low shear setup, we estimated the clusters to experience shear stress in the range of 1-3 mPa, while for the high shear setup, we found a range of 6-10 mPa. The medium shear setup exhibited a broader distribution where the estimated shear stress ranged between 1-6 mPa.

A low shear zone exists beneath the impeller while a higher shear zone was observed above the impeller. This low shear zone may cause issues for the low rpm setups, as the probability for progressive microtissue agglomeration increases in this stagnant region. For the low rpm setup, the typical shear stress in the stagnant and recirculating populations almost coincide, see Figure 2a. In the medium shear regime, the stagnant and recirculating region are associated with distinct levels of shear stress, resulting in a broader overall distribution of shear stress, see Figure 1d. We found that the stagnant region persists in a range of relative spheroid mass density $(\rho_p - \rho_f)/\rho_f$ between 0 and 0.06.

4.4.2 Cartilaginous differentiation in dynamic and static culture environments

In order to generate cartilaginous microtissues, we first allowed cells to aggregate for 2 days, forming stable microtissues, before inoculating the bioreactor. This provided a population of microtissues that possessed an almost monomodal size distribution with an average diameter of $d = 120 \mu\text{m}$, providing a homogeneous in size starting population. Preliminary experiments with the miniBR setup illustrated that we could culture cells dynamically to form microaggregates for up to 14 days in culture media containing chondrogenic induction factors. Furthermore, we observed that microtissues were able to fuse into larger structures during the first 3 days of culture, after which this process stopped, resulting in a steady state size distribution for the remainder of culture. This size ranged between 0.01 and 0.04 mm² (projected area) as observed. To account for the phenomenon of fusion, we used two static controls; one where spheroids cultured with the same dimensions as the initial inoculation population (200–250 μm) and a second control where multiple microtissues were seeded in larger size microwells, allowing them to fuse into larger sized microtissues (400–450 μm) at the same time point as we inoculated the bioreactor (Figure 3). We quantified certain morphological attributes (Figures 3c and Appendix B, Figure S1) for each microtissue population. Starting with the microtissue perimeter we noticed variation in the dynamic condition in comparison to the static references with clear difference already at Day 7 but even more distinct at Day 14. As confirmed by our observations in bright field images, bioreactor cultured microtissues were able to assemble in larger microtissues (fusion phenomenon). Some variation in the perimeter size was observed also in the static large microtissues in comparison to the small static reference as indeed in the larger microtissues

there was a variation in sizes, as a result of fusion (limited in comparison to the bioreactor). Microtissue roundness in static and dynamic cultured microtissues seem to display similar results between them and across time (Appendix B, Figure S1). However, at Day 14 there is a bigger variation for bioreactor cultured microtissues following the large static ones, something that can be explained also by the different degree of fusion that we noticed in bioreactor cultured microtissues. Regarding microtissue circularity, we observed a bigger variation in bioreactor and large static microtissues at Days 7 and 14, aligned with microtissue perimeter and microtissue roundness results. We estimated approximately the cell density in different conditions as the cell number of the microtissue divided by the microtissue volume (Appendix B, Figure S2). Cell density is significantly lower in dynamic and big static microtissues in comparison to the small static ones at Day 7 and the difference is even bigger at Day 14. Regarding the culture time dependent differences at Days 7 and 14 we observed a significant decrease in comparison to the starting point, Day 0 for all the conditions. There is a clear decrease in cell number also for the static condition (extrapolated by DNA quantification, Figure 4a). However, in the case of big static and bioreactor conditions apart from the significantly higher decrease we have in parallel an increase in diameter which results in significantly lower cell density. We observed that viability was not affected either by the fusion event on Day 2 or the size of the microtissues in the static controls, while the same applied for the microtissues cultured in the bioreactor which were observed to consist of a largely viable population (Figure 4 live/dead staining). In order to provide quantitative data related to cell viability and proliferation, we conducted DNA quantification ($n = 4$) for the microtissues of different conditions (small static, big static, and dynamic conditions) over time. At Day 7, we observed a statistically significant decrease ($p = 0.0499$) in DNA content between small static and bioreactor condition while there was a decrease but not statistically significant for DNA content between big static reference and bioreactor condition. At Day 14 there is an even larger statistically significant difference in DNA content between small static and bioreactor conditions ($p < 0.0001$). Between big static reference and bioreactor cultured microtissues, we noticed a statistically significant decrease in DNA content ($p = 0.0135$) (Figure 4a). When investigating the presence of proliferating cells, we did see a distinct difference between the static and dynamic conditions, with a lower fraction of EDU+ cells present in the bioreactor condition (Figure 5). In order to provide quantitative data related to cell proliferation, we conducted quantification of EdU positivity from fluorescent images for the different conditions and different time points. For each condition and time point, we focused on 50–200 microtissues. There is a clear decrease in EdU positive cells in the bioreactor condition for both Days 7 and Day 14 with the Day 14 showing the lowest fraction

STIRRED CULTURE OF CARTILAGINOUS MICROTISSUES PROMOTES CHONDROGENIC HYPERTROPHY THROUGH EXPOSURE TO INTERMITTENT SHEAR STRESS

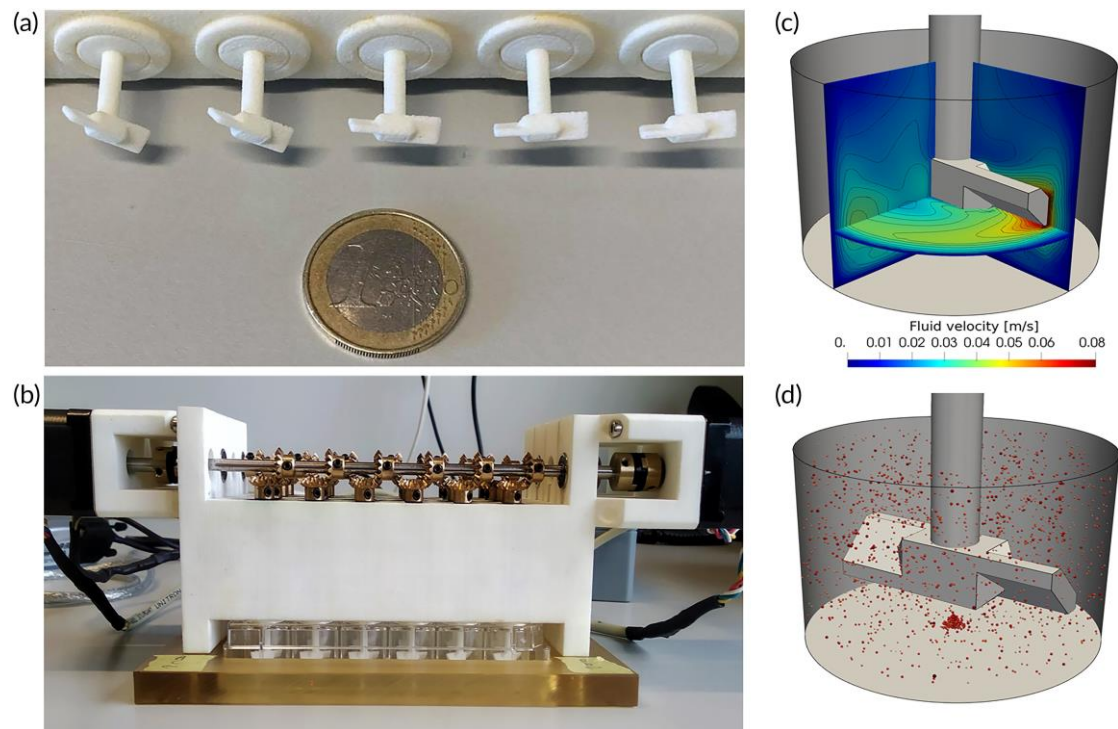


Figure 1. Experimental setup of the mini bioreactor and Computational Fluid Dynamics (CFD) modeling.

(a, b) Mini bioreactor system with 3D printed marine impeller. (c) Cross section of CFD simulated magnitude of the fluid velocity for an impeller speed of 13 rad/s. (d) Visualization of spheroid position during stirred culture. The size of the shown spheroids has been magnified for visual clarity.

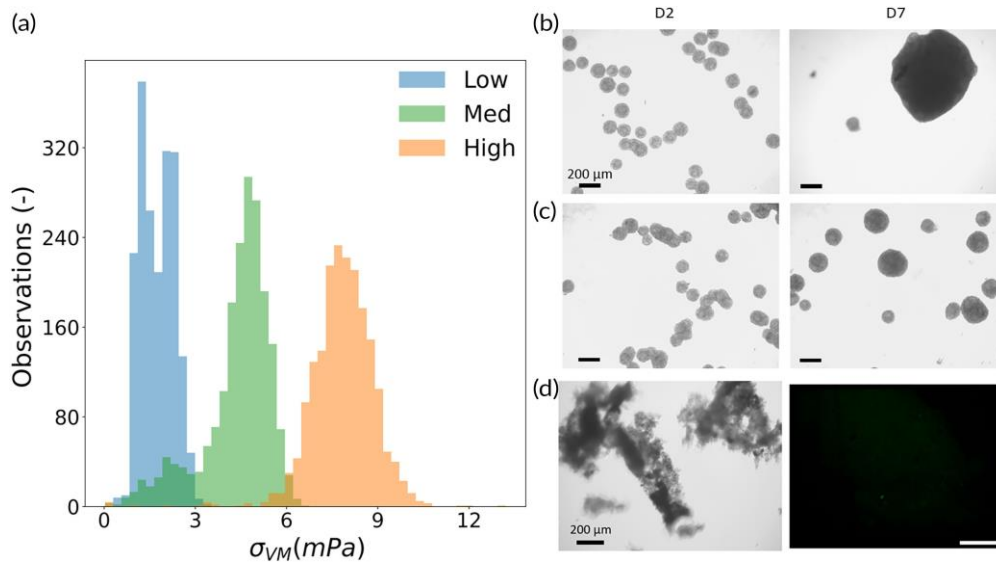


Figure 2. Microtissue growth after 1 week stirred culture exposed to different shear stresses

(a) Distribution of shear stress experienced by individual spheroids in low, medium, and high shear stress condition (caused by impeller speeds resp. 7, 13, and 20 rad/s). (b–d) Brightfield images of stirred cultures spheroids for Days 2 and 7 in low, medium, and high shear stress conditions. (b) The lowest rotational speed after 7 days resulted in dead zones where the microtissues were no longer suspended and merged into bigger aggregates. (c) The aggregation phenomenon also occurred in the medium speed, but smaller aggregates could also be observed. (d) At the highest rotational speed, highest hydrodynamic forces caused cell lysis or apoptosis (cell debris present already at Day 2, almost no microtissues at Day 7). Scale bar: 200 μm .

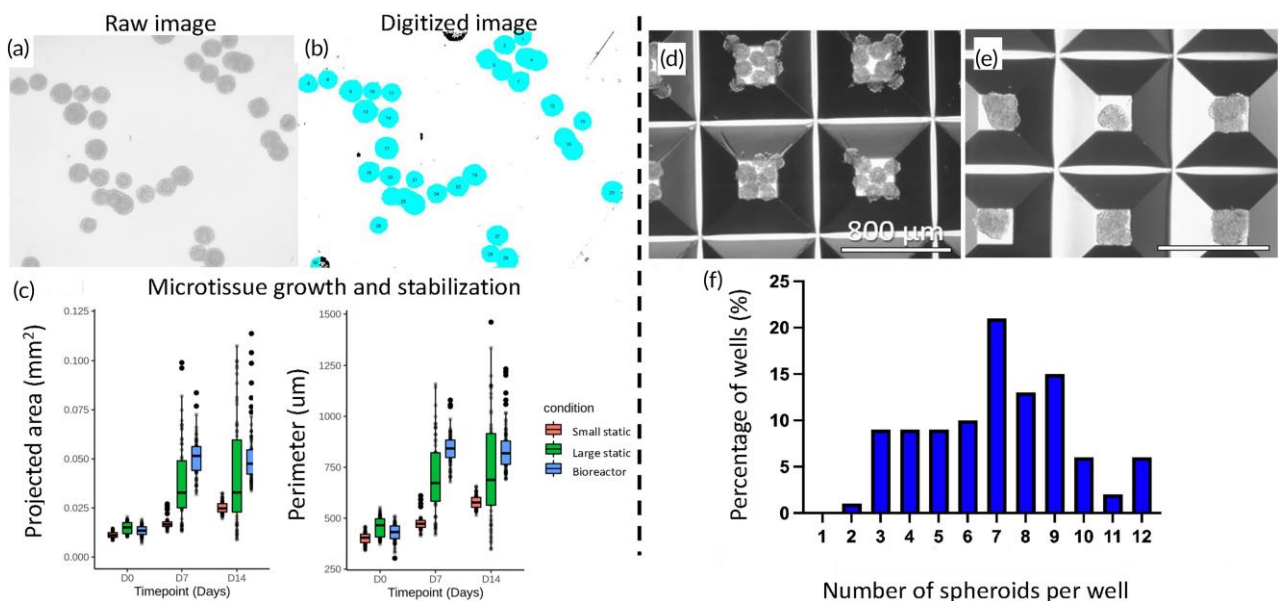


Figure 3. Size distribution of the stirred cultured microtissues and their static references.

(a, b) Representative brightfield microscopy image of microtissues cultured in suspension were analyzed using ImageJ software through digitized images. (c) Microtissue growth results as measured by projected area and perimeter were visualized using box plots. In these box plots, the middle line indicates the median value, the box indicates the interquartile range (50% of the data), the end of the whiskers represents one and a half times the interquartile range and the dots represent outliers. (d) As a static control capturing microtissue fusion Aggrewwells were used for the seeding of small microtissues. (e, f) As a second static control, multiple spheroids were seeded in larger size microwells, allowing them to fuse into larger sized microtissues. Impeller speed used is 13 rad/s. Scale bar: 800 μm

STIRRED CULTURE OF CARTILAGINOUS MICROTISSUES PROMOTES CHONDROGENIC HYPERTROPHY THROUGH EXPOSURE TO INTERMITTENT SHEAR STRESS

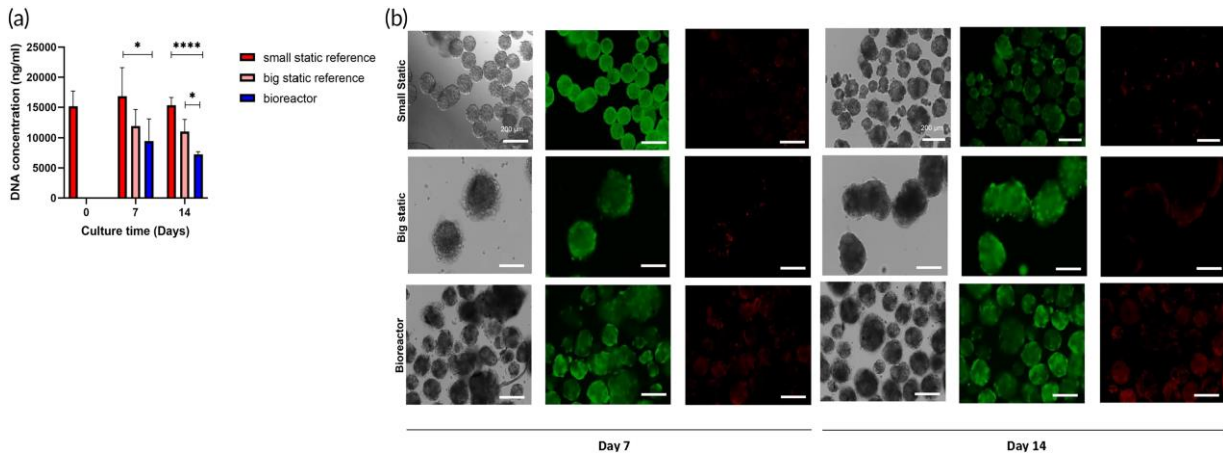


Figure 4. Cell viability for Days 7 and 14 by means of brightfield images

(a, d), (a) DNA quantification of static and dynamic cultured microtissues over time ($n = 4$, mean values \pm SEM). (b) Live staining and Dead staining. The rows respectively show results for microtissues from the small static condition (up row), large static condition (middle row) and dynamic conditions (down row). Impeller speed used is 13 rad/s. Scale bar: 200 μm

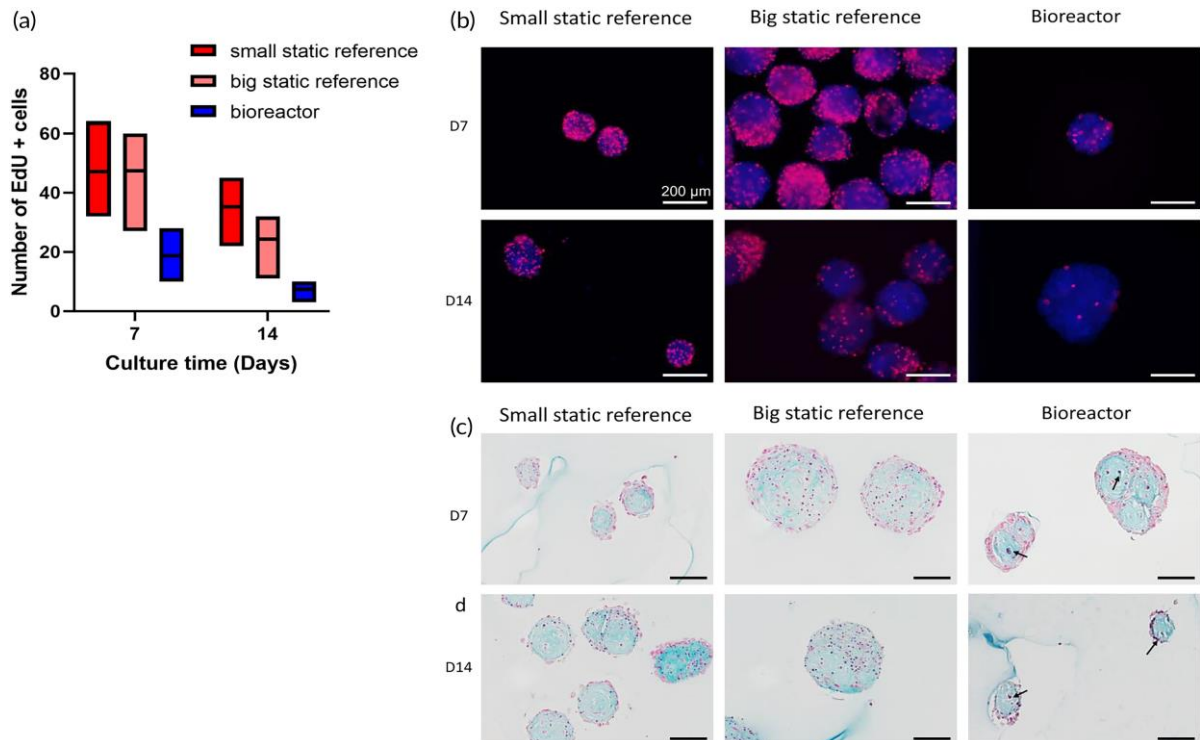


Figure 5. Histological assessment of microtissues in static and bioreactor conditions.

(a) Semi quantification of cell proliferation of static and dynamic microtissues over time (minimum of 50 microtissues per condition). (b) Representative fluorescence images of proliferating cells (EdU positive, red) of small, bigger static and bioreactor cultured microtissues at Day 7. (c) EdU positive staining of small, bigger static and bioreactor cultured microtissues at Day 14. (d) Alcian blue staining of small, bigger static and bioreactor cultured microtissues at Day 7. In dynamic conditions, we observed fewer EdU positive cells at both Days 7 and 14. In all conditions abundant ECM compartments were present. Impeller speed used is 13 rad/s. Scale bar: 200 μm.

of EdU positive cells (Figure 5). Small and large static microtissues display similar proliferation for Day 7, whereas there is a difference in proliferating cells at Day 14 with large static microtissues having fewer proliferative cells. These data are aligned with the DNA content quantification (Figure 4a) and suggest lower proliferation in dynamic cultured microtissues compared with the static ones. Alcian Blue staining at low pH, specific for glycosaminoglycan (GAG) confirmed the presence of cartilage-like extracellular matrix compartments within the microtissues across conditions. We noticed an increase at Day 14 compared with Day 7 for both static and dynamic conditions. Pre-hypertrophic like cells were visible after 2 weeks of culture (Figure 5c,d, black arrows). Gene expression values (Figure 6) showed a significant upregulation of both Indian hedgehog (*IHH*, 30-fold) and Collagen type X (*COLX*, 23-fold), a well-known marker of chondrogenic hypertrophy, for the day 7 and day 14 time points for the dynamically cultured microtissues. Moreover, the chondrogenic marker Chondromodulin showed a large upregulation (16-fold) for the last time point (day 14). For the transcription factor *RUNX2*, linked with chondrocyte hypertrophy and early osteoblast differentiation, no statistically significant differences were seen on day 14 between the static large microtissues and the dynamically cultured ones although a clear upregulation for the dynamically cultured spheroids was observed at the early timepoint (day 7). The transcription factor Osterix (*OSX*) which is directly regulated by *RUNX2* and expressed in prehypertrophic chondrocytes and osteoblasts showed a significant downregulation (0.06-fold) for Day 14 and (0.04-fold) for Day 7 in dynamic cultured microtissues compared with the static ones. Finally, we did not observe any statistically significant difference in the expression of VEGF between static and dynamic cultured microtissues. The VEGF expression for both static references (small and large static microtissues) follows a similar trend. At Day 7, we have a significant upregulation in comparison to Day 0 microtissues whereas at Day 14 we observed downregulation. In contrast, dynamic cultured microtissues showed an upregulation in Day 14 in comparison to Day 7. Since genes related to chondrocyte hypertrophy and the presence of prehypertrophic cells (Figure 5c,d) were detected, subcutaneous *in vivo* implantations were performed after 14-days differentiation to assess the microtissues' capacity to mineralize upon implantation and execute cartilage to bone transition (i.e endochondral ossification). Approximately 2400 microtissues were assembled in an agarose macro-well with a diameter of 3 mm, to create millimeter sized constructs as previously described⁴ (Figure 7). Constructs assembled from day 14 microtissues from both static and dynamically cultured microtissues resulted in the formation of mineralized constructs with $26 \pm 14\%$ (4/4) and $24 \pm 6\%$ (2/3) mineralized tissue (MV/TV), respectively (Figure 7) with cortical-like bone structures.

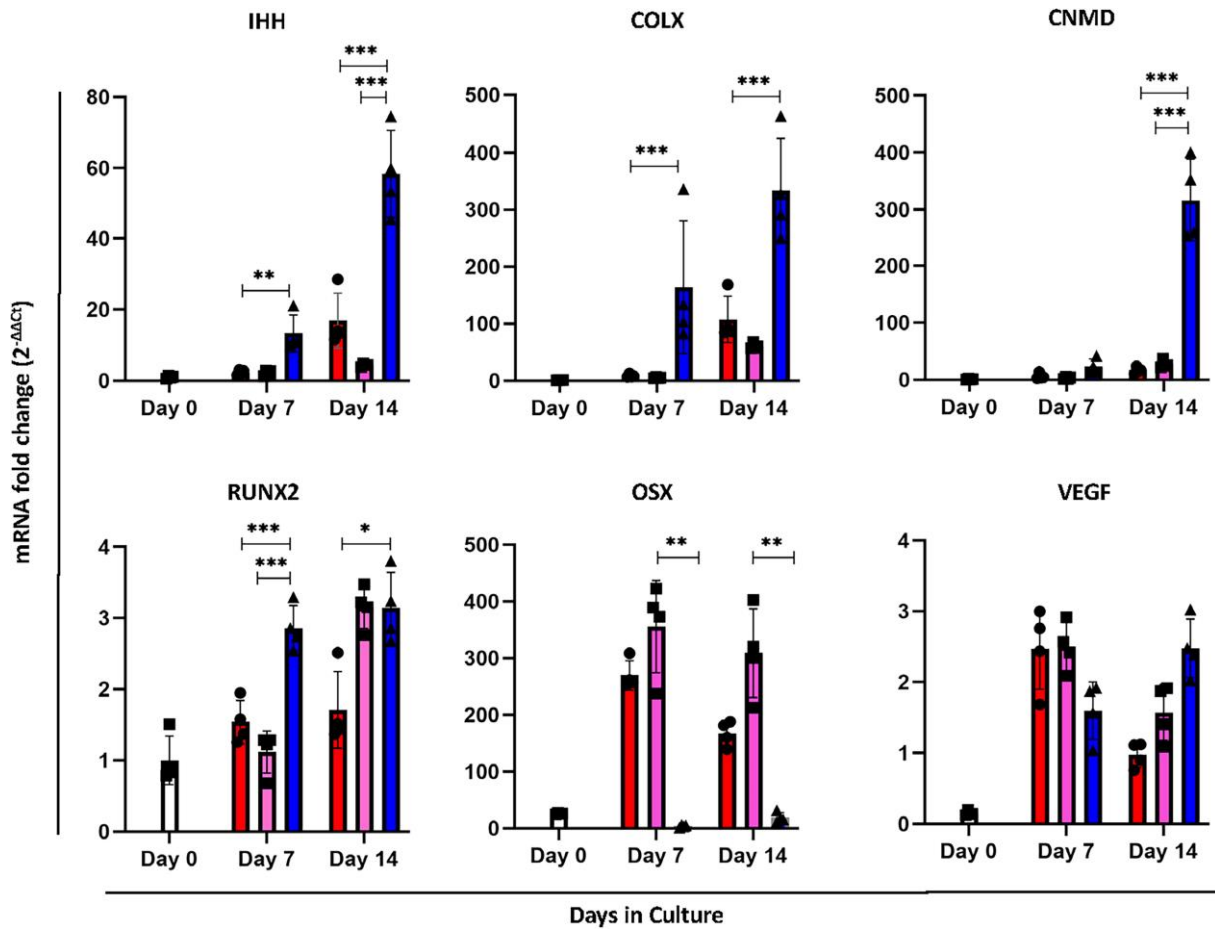


Figure 6. Gene expression of static and stirred cultures showed enhanced hypertrophy.

Quantification of mRNA transcripts of gene markers normalized to Day 0 ($n = 4$ individual values \pm SEM), * $p < 0.05$, ** $p < 0.01$, *** $p < 0.001$, one way ANOVA followed by Tukey's multiple comparison test. Blue color represents the dynamic condition, pink the static big microtissues and red the static small microtissues. Impeller speed used is 13 rad/s.

4.4.3 Exometabolomics of chondrogenic differentiation

We used LC–MS based metabolomics to measure extracellular metabolites in the media of bioreactor-cultured and in static culture spheroids (Figure 8). Time points of interest were Day 0 (starting of the bioreactor culture), Days 7, and 14. Like the transcriptome level, we saw different metabolic profiles between static and dynamic conditions. More specifically, whereas both conditions were characterized by high glucose consumption and lactate production on Days 7 and 14, in the bioreactor condition there was a significant increase in glucose consumption and lactate production for Day 14. On Day 7 no statistical difference in glucose consumption was observed whereas there was significant difference in lactate production between static and dynamically cultured microtissues. Moreover, the amino acids glutamate, aspartate, and citrate showed a significant increase in the dynamic condition compared with

the static references on Day 7, whereas no significant difference was observed for Day 14. For both Days 7 and 14 we observed a significant increase in alanine production, which can be linked to the high glycolytic profile of the cartilaginous microtissues as mentioned above. Notably, proline, an important amino acid in the context of extracellular matrix function, showed upregulation in dynamic conditions for both Days 7 and 14 whereas on Day 0 it was consumed. The serine secretome profile was distinct in dynamic conditions and the bigger aggregates than the static condition. In the static condition serine was constantly consumed whereas in the dynamic condition and the bigger aggregates, serine was in excess in the spent medium. Additionally, serine showed a significant increase in dynamically cultured condition compared with the static large microtissues on both Days 7 and 14.

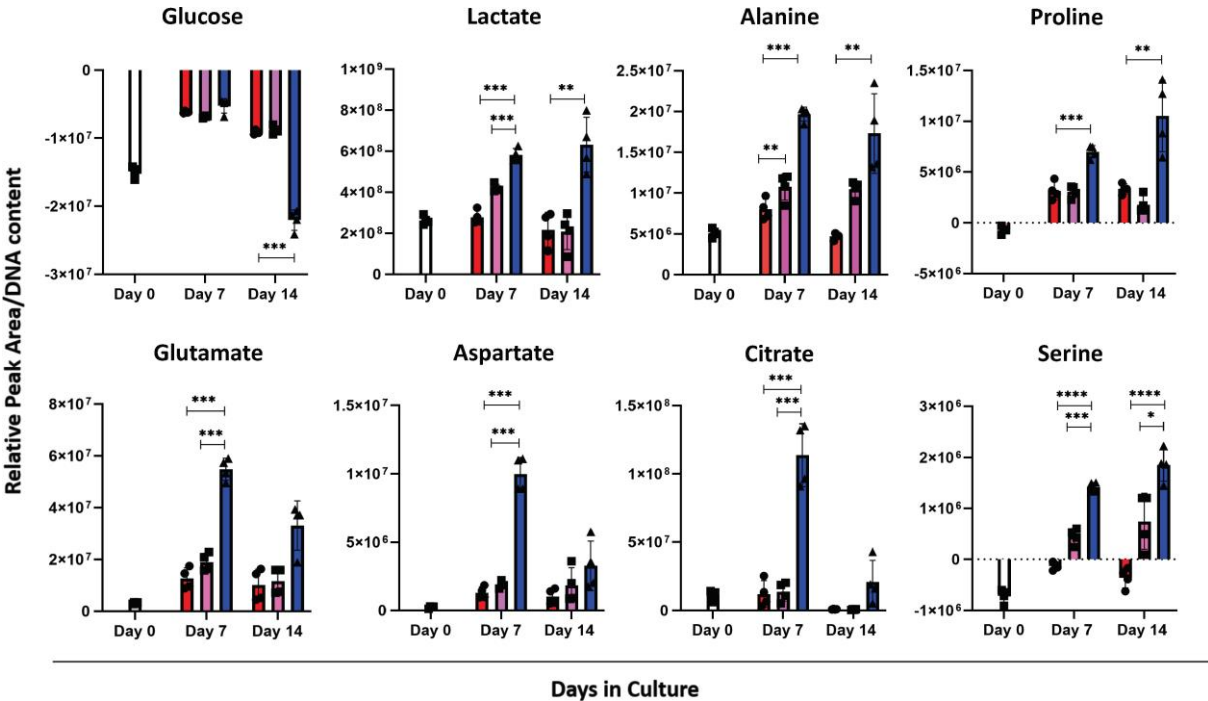


Figure 7 Exometabolomic analysis of medium from hPDCs microtissues cultured in static and in stirred culture analyzed by LC-MS based metabolomics.

Extracellular media were sampled at Day 0, Day 7, and Day 14. The results were normalized based on DNA content measurements ($n=4$ individual values \pm SEM), $*p<0.05$, $**p<0.01$, $***p<0.001$, one way ANOVA followed by Tukey's multiple comparison test. Blue color represents the dynamic condition, pink the static large aggregates, and red the static microtissues. Impeller speed is 13 rad/s.

STIRRED CULTURE OF CARTILAGINOUS MICROTISSUES PROMOTES CHONDROGENIC HYPERTROPHY THROUGH EXPOSURE TO INTERMITTENT SHEAR STRESS

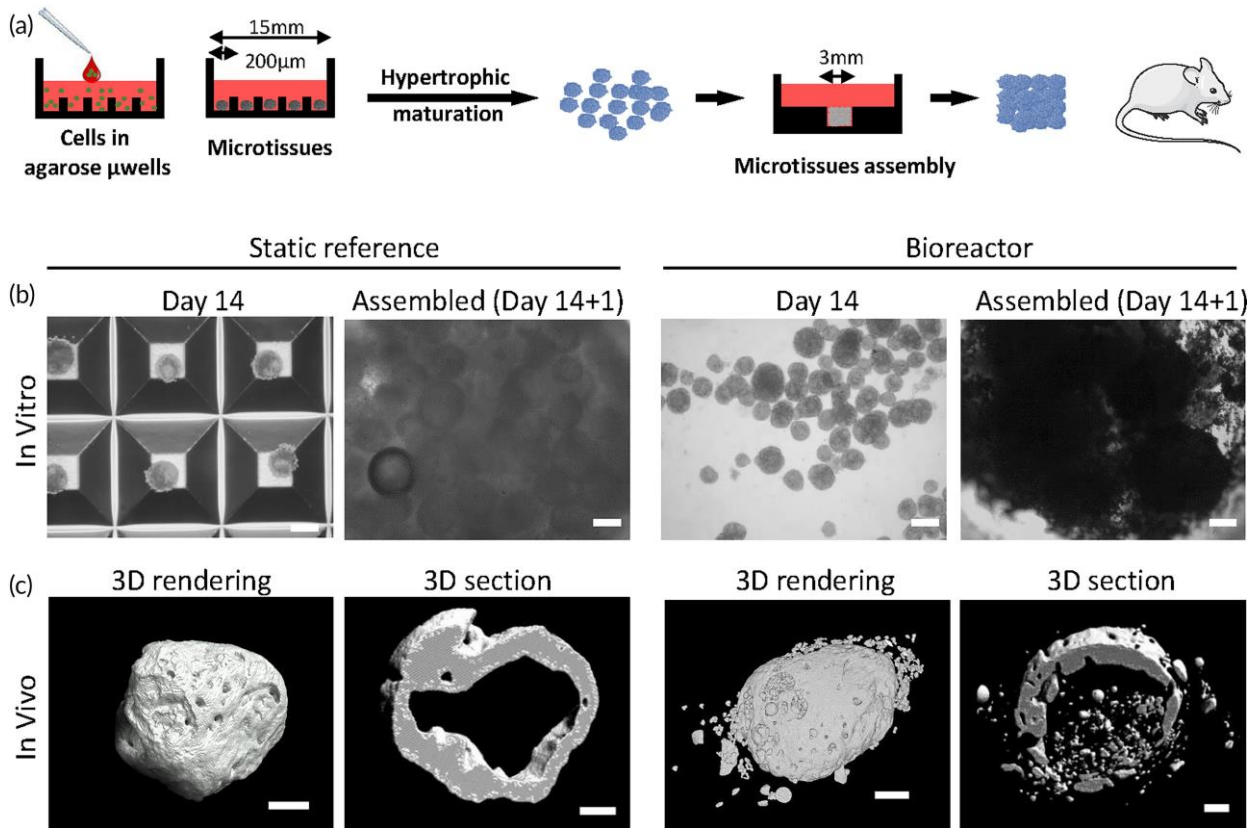


Figure 8 Assembly of cartilage microtissue intermediates into larger bone forming constructs for static and dynamic cultured microtissues.

a. Schematic representation of culture, assembly of microtissues, and implantation in mice models. b. Brightfield images of microtissues differentiated for 14 days either statically or dynamically in the miniBR (Day 14) and brightfield images of microtissues assembled into millimeter sized constructs (Assembled (Day14+1)). c. 4 weeks subcutaneous implantation of assembled microtissues differentiated in static or dynamic (miniBR) condition. Images show 3D representation of the entire mineralized tissue and a cross-section of the volume. Impeller speed of the bioreactor cultured microtissues is 13 rad/s. Scale bars represent 100 μ m.

4.5 Discussion

Cartilage microtissues are promising tissue modules for bottom up biofabrication of implants leading to bone defect regeneration²⁹. Cartilage microtissue differentiation in well-defined culture conditions recapitulates developmental events encountered in the developing embryonic limb bud, which serves as a robust biological paradigm, called developmental engineering^{4,8,29}. Most of the protocols for the development of these cartilaginous microtissues have been carried out in static setups so far, however, a bioreactor-based suspension process can provide the basis for further scale up as well as automation. In the present study, we explored the impact of dynamic culture in cartilaginous microtissues properties in a novel microbioreactor system generating a stirred environment. However, the dynamic bioprocess in a stirred environment can induce additional maturation cues through mechanical stimulation.

Due to the developmental engineering approach followed in this work, we strived to obtain information from the mechanobiology in embryonic systems. In a seminal study, Carter and Wong³⁰ indicated that high shear stresses (in relation to their distribution within the joint) were calculated at the ossific nucleus and at the location where the ossification groove (or zone of Ranvier) was formed. In addition, it was suggested that intermittently applied shear stresses promoted hypertrophic differentiation and endochondral ossification.³⁰ As observed by our mathematical modeling study, cartilaginous microtissues were intermittently exposed to regions of high shear stress and low shear stress regimes within the bioreactor system. The distinct difference in proliferation between static and bioreactor conditions could be linked to the commitment of cells towards ECM production rather than proliferation something that is known during chondrogenic differentiation³¹ but in this instance accentuated by the dynamic culture conditions. Additionally, the lower cell density in the bioreactor cultured microtissues (Appendix B, Figure S2) indicates also the commitment of cells towards ECM production in dynamic culture conditions. Studies performed in limb development during embryogenesis revealed that *COLX* and *IHH* expression patterns correlated with stage-matched patterns of biophysical stimuli,³² indicating the importance of these genes as downstream mechano-transducing genes regulating endochondral ossification. A significant upregulation of both these genes was also observed in our work for the dynamically cultured microtissues when compared with the two static controls, corroborating these basic biology observations in an *in vitro* context. CNMD is an endogenously anti-angiogenic protein³³ that is expressed in the prehypertrophic zone of the growth plate³⁴ and in this study was used as an “intermediate” maturity marker. This gene and its upregulation could indicate that microtissue differentiation has reached a level comparable to that of the prehypertrophic zone (given that hypertrophic markers such as *COLX* and *IHH* are also clearly upregulated). Furthermore, in a recent study, the response to dynamic loading showed enhanced chondrogenic differentiation through upregulation of *COL2A1* and *AGGRECAN* gene expression in engineered cartilage tissues

formed from human MSCs³⁵. Finally, it is interesting to note that in a recent study, cartilaginous implants in segmental bone defects resulted in quicker healing when they were mechanically stimulated indicating the crucial role of stresses in the progression of endochondral ossification². *In vitro* quality controls indicate that shear stress enhances chondrogenic differentiation of human progenitor cells cultured in *in vitro* engineered tissues towards a (pre)hypertrophic phenotype. More specifically distinct upregulation of the hypertrophic markers Indian Hedgehog signaling molecule (IHH) and collagen type X alpha 1 chain (COL10A1) together with the significant downregulation of Osterix (OSX) osteogenic marker suggests that the dynamic microtissues showed a later hypertrophic stage than the static ones and thus are more committed to hypertrophy rather than osteogenic differentiation. *In vivo* implantations demonstrate that microtissues cultured in dynamic conditions are functional and able to undergo endochondral ossification upon implantation. However, they do not show difference to the static condition for the period of implantation. Given that a cortex and a cavity was already present in the explants, in future studies an earlier time point should be examined to assess whether dynamically cultured microtissue could form bone faster than statically cultured ones.

A challenge when trying to study the impact of dynamic culture conditions on cultured cells and tissue modules is the quantification of cell or tissue related mechanical stimuli. In addition, microtissue fusion during culture is another factor that might influence the dispersion within the bioreactor. In order to provide a quantitative link between the cultured microtissues and the process environment, CFD studies only taking into account the development of mechanical stimulus in a continuous medium³⁶⁻³⁸ fail to match the actual tissue-relevant stimulus magnitudes or stimulus history. In this study, we provided a quantitative link between the cultured microtissue suspension and the process environment via coupled CFD-DEM approach, quantifying mechanical stress at the level of individual microtissues. There are several recent studies underlying the importance of studying metabolism as a critical regulator for bone regeneration process. Chondrocyte metabolism and more specifically glutamine metabolism controls the collagen synthesis and modification³⁹ and targeting skeletal metabolism has been shown as advantageous for the expansion and self-renewal of skeletal progenitors.⁴⁰ In this study, we aim for exometabolomic analysis, as a first effort to illustrate changes in the metabolome in the dynamic culture and due to the mechanical stimulation. From a metabolic perspective, cartilaginous microtissues showed increased glucose consumption and lactate production during culture time, indicative of a highly glycolytic metabolism which is a characteristic of growth plate chondrocytes^{41,42}. Higher glycolysis has been also reported in chondrocytes under compression⁴³. Additionally, lactate accumulation that is higher in the dynamic condition can be beneficial for bone regeneration. Lactate has been observed to stimulate collagen deposition in an autocrine and paracrine manner,

thereby contributing to soft callus progression,⁴⁴ although further *in vivo* studies will be required to corroborate this for the specific type of microtissue implants. Regarding the amino acid profiles, among the most interesting differences in the context of chondrogenic differentiation, between static and dynamic conditions was proline secretion, which can be linked with the process of extracellular matrix remodeling as seen for similar chondrogenic differentiation processes.⁴ Proline, as a product of ECM degradation can be used as a precursor of other amino acids and as an energy source^{45,46}. Moreover, mechanical stimulation in the bioreactor condition can stimulate the synthesis of matrix degrading enzymes⁴⁷ Interestingly, we observed aspartate and glutamate secretion significantly higher in the dynamic conditions, especially on Day 7. These secretome profiles can be linked with hypertrophic-like biology, as aspartate is shown to be elevated in synovial fluids from OA patients⁴⁸ whereas aspartate release significantly increases by 90% in IL-1 β stimulated chondrocytes.⁴⁹ The serine secretome profile also showed distinct differences between static and dynamic conditions. Taken together, these metabolites provide a panel of metrics that could be measured from the supernatant providing a target for non-destructive assessment of the progression of chondrogenic differentiation towards hypertrophy. These secreted metabolites could in the future provide markers that could be monitored during bioreactor culture for non-destructive assessment of phenotypic state of the cultured microtissues, however further validation also through *in vivo* studies, is required.

4.6 Conclusion

In this work, we investigated the impact of dynamic culture conditions during cartilaginous differentiation in microtissues using a novel microbioreactor system. Through the use of mathematical models, an *in-silico* representation and quantification of the dynamic system and microtissue shear history was conducted. We identified operating conditions where suspension conditions could be maintained and chondrogenic differentiation was possible. This dynamic process led to an accelerated differentiation of cartilaginous microtissues towards hypertrophy that also resulted in distinct metabolic readouts in the culture medium.

4.7 References

1. Einhorn TA, Gerstenfeld LC. Fracture healing: Mechanisms and interventions. *Nat Rev Rheumatol*. 2015;11(1):45-54. doi:10.1038/nrrheum.2014.164
2. Colnot C. Skeletal cell fate decisions within periosteum and bone marrow during bone regeneration. *J Bone Miner Res*. 2009;24(2):274-282. doi:10.1359/jbmr.081003
3. Bahney CS, Hu DP, Taylor AJ, et al. Stem cell-derived endochondral cartilage stimulates bone healing by tissue transformation. *J Bone Miner Res*. 2014;29(5):1269-1282. doi:10.1002/jbmr.2148
4. Hall GN, Mendes LF, Gklava C, Geris L, Luyten FP, Papantoniou I. Developmentally Engineered Callus Organoid Bioassemblies Exhibit Predictive In Vivo Long Bone Healing. 2020;1902295:1-16. doi:10.1002/adv.201902295
5. Scotti C, Piccinini E, Takizawa H, et al. Engineering of a functional bone organ through endochondral ossification. *Proc Natl Acad Sci U S A*. 2013;110(10):3997-4002. doi:10.1073/pnas.1220108110
6. Scotti C, Tonnarelli B, Papadimitropoulos A, et al. Recapitulation of endochondral bone formation using human adult mesenchymal stem cells as a paradigm for developmental engineering. *Proc Natl Acad Sci U S A*. 2010;107(16):7251-7256. doi:10.1073/pnas.1000302107
7. Hall GN, Tam WL, Andrikopoulos KS, et al. Patterned, organoid-based cartilaginous implants exhibit zone specific functionality forming osteochondral-like tissues in vivo. *Biomaterials*. 2021;273(April):120820. doi:10.1016/j.biomaterials.2021.120820
8. Bolander J, Ji W, Leijten J, et al. Healing of a Large Long-Bone Defect through Serum-Free In Vitro Priming of Human Periosteum-Derived Cells. *Stem cell reports*. 2017;8(3):758-772. doi:10.1016/j.stemcr.2017.01.005
9. Herberg S, Varghai D, Alt DS, et al. Scaffold-free human mesenchymal stem cell construct geometry regulates long bone regeneration. doi:10.1038/s42003-020-01576-y
10. McDermott AM, Herberg S, Mason DE, et al. Recapitulating bone development through engineered mesenchymal condensations and mechanical cues for tissue regeneration. *Sci Transl Med*. 2019;11(495). doi:10.1126/scitranslmed.aav7756
11. Kropp C, Massai D, Zweigerdt R. Progress, and challenges in large-scale expansion of human pluripotent stem cells. *Process Biochem*. 2017;59:244-254. doi:10.1016/J.PROCBIO.2016.09.032
12. Rafiq QA, Coopman K, Nienow AW, Hewitt CJ. Systematic microcarrier screening and agitated culture conditions improves human mesenchymal stem cell yield in bioreactors. *Biotechnol J*. 2016;11(4):473-486. doi:10.1002/biot.201400862

13. Zweigerdt R, Olmer R, Singh H, Haverich A, Martin U. Scalable expansion of human pluripotent stem cells in suspension culture. *Nat Protoc.* 2011;6(5):689-700. doi:10.1038/nprot.2011.318
14. Frondoza C, Sotiabi A, Hungerford D. *Human Chondrocytes Proliferate and Produce Matrix Components in Microcarrier Suspension Culture.* Vol 17.; 1996.
15. Kempf H, Kropp C, Olmer R, Martin U, Zweigerdt R. Cardiac differentiation of human pluripotent stem cells in scalable suspension culture. *Nat Protoc.* 2015;10(9):1345-1361. doi:10.1038/nprot.2015.089
16. Kempf H, Olmer R, Kropp C, et al. Controlling Expansion and Cardiomyogenic Differentiation of Human Pluripotent Stem Cells in Scalable Suspension Culture. *Stem Cell Reports.* 2014;3(6):1132-1146. doi:10.1016/J.STEMCR.2014.09.017
17. Qian X, Nguyen HN, Song MM, et al. Brain-Region-Specific Organoids Using Mini-bioreactors for Modeling ZIKV Exposure. *Cell.* 2016;165(5):1238-1254. doi:10.1016/j.cell.2016.04.032
18. Rigamonti A, Repetti GG, Sun C, et al. Large-scale production of mature neurons from human pluripotent stem cells in a three-dimensional suspension culture system. *Stem Cell Reports.* 2016;6(6):993-1008. doi:10.1016/j.stemcr.2016.05.010
19. Przepiorski A, Sander V, Tran T, et al. A Simple Bioreactor-Based Method to Generate Kidney Organoids from Pluripotent Stem Cells. *Stem Cell Reports.* 2018;11(2):470-484. doi:10.1016/j.stemcr.2018.06.018
20. Yamashita A, Morioka M, Yahara Y, et al. Generation of scaffoldless hyaline cartilaginous tissue from human iPSCs. *Stem Cell Reports.* 2015;4(3):404-418. doi:10.1016/j.stemcr.2015.01.016
21. Crispim JF, Ito K. De novo neo-hyaline-cartilage from bovine organoids in viscoelastic hydrogels. *Acta Biomater.* 2021;128:236-249. doi:10.1016/j.actbio.2021.04.008
22. Gupta P, Geris L, Luyten FP, Papantoniou I. An Integrated Bioprocess for the Expansion and Chondrogenic Priming of Human Periosteum-Derived Progenitor Cells in Suspension Bioreactors. *Biotechnol J.* 2018;13(2). doi:10.1002/biot.201700087
23. Dang T, Borys BS, Kanwar S, et al. Computational fluid dynamic characterization of vertical-wheel bioreactors used for effective scale-up of human induced pluripotent stem cell aggregate culture. *Can J Chem Eng.* 2021;99(11):2536-2553. doi:10.1002/cjce.24253
24. Borys BS, Le A, Roberts EL, et al. Using computational fluid dynamics (CFD) modeling to understand murine embryonic stem cell aggregate size and pluripotency distributions in stirred suspension bioreactors. *J Biotechnol.* 2019;304:16-27. doi:10.1016/j.jbiotec.2019.08.002
25. Eyckmans J, Roberts SJ, Schrooten J, Luyten FP. A clinically relevant model of

- osteoiduction: a process requiring calcium phosphate and BMP/Wnt signalling. *J Cell Mol Med.* 2010;14(6B):1845-1856. doi:10.1111/j.1582-4934.2009.00807
26. Leijten J, Teixeira LSM, Bolander J, Ji W, Vanspauwen B. Bioinspired seeding of biomaterials using three dimensional microtissues induces chondrogenic stem cell differentiation and cartilage formation under growth factor free conditions. 2016;(February):1-12. doi:10.1038/srep36011
 27. Mendes LF, Tam WL, Chai YC, Geris L, Luyten FP, Roberts SJ. Combinatorial Analysis of Growth Factors Reveals the Contribution of Bone Morphogenetic Proteins to Chondrogenic Differentiation of Human Periosteal Cells. *Tissue Eng - Part C Methods.* 2016;22(5):473-486. doi:10.1089/ten.tec.2015.0436
 28. Livak KJ, Schmittgen TD. Analysis of relative gene expression data using real-time quantitative PCR and the 2- $\Delta\Delta$ CT method. *Methods.* 2001;25(4):402-408. doi:10.1006/meth.2001.1262
 29. Lenas P, Moos M, Luyten FP. *Developmental Engineering: A New Paradigm for the Design and Manufacturing of Cell-Based Products. Part I: From Three-Dimensional Cell Growth to Biomimetics of In Vivo Development.* www.liebertpub.com
 30. Carter DR, Wong M. *Mechanical Stresses and Endochondral Ossification in the Chondroepiphysis.* Raven Press
 31. Prein C, Warmbold N, Farkas Z, Schieker M, Aszodi A, Clausen-Schaumann H. Structural and mechanical properties of the proliferative zone of the developing murine growth plate cartilage assessed by atomic force microscopy. *Matrix Biol.* 2016;50:1-15. doi:10.1016/j.matbio.2015.10.001
 32. Nowlan NC, Prendergast PJ, Murphy P. Identification of mechanosensitive genes during embryonic bone formation. *PLoS Comput Biol.* 2008;4(12). doi:10.1371/journal.pcbi.1000250
 33. Zhang X, Prasadam I, Fang W, Crawford R, Xiao Y. Chondromodulin-1 ameliorates osteoarthritis progression by inhibiting HIF-2 α activity. *Osteoarthr Cartil.* 2016;24(11):1970-1980. doi:10.1016/j.joca.2016.06.005
 34. Miura S, Kondo J, Takimoto A, et al. The n-terminal cleavage of chondromodulin-i in growth-plate cartilage at the hypertrophic and calcified zones during bone development. *PLoS One.* 2014;9(4):3-10. doi:10.1371/journal.pone.0094239
 35. McDermott AM, Eastburn EA, Kelly DJ, Boerckel JD. Effects of chondrogenic priming duration on mechanoregulation of engineered cartilage. *J Biomech.* 2021;125. doi:10.1016/j.jbiomech.2021.110580
 36. Borys BS, Dang T, So T, et al. Overcoming bioprocess bottlenecks in the large-scale expansion of high-quality hiPSC aggregates in vertical-wheel stirred suspension

- bioreactors. *Stem Cell Res Ther.* 2021;12(1). doi:10.1186/s13287-020-02109-4
37. Shafa M, Panchalingam KM, Walsh T, Richardson T, Ahmadian Baghbaderani B. Computational fluid dynamics modeling, a novel, and effective approach for developing scalable cell therapy manufacturing processes. Published online 2019. doi:10.1002/bit.27159
 38. Egger D, Schwedhelm I, Hansmann J, Kasper C. Hypoxic three-dimensional scaffold-free aggregate cultivation of mesenchymal stem cells in a stirred tank reactor. *Bioengineering.* 2017;4(2). doi:10.3390/bioengineering4020047
 39. Nahir AM. *Aerobic Glycolysis: A Study of Human Articular Cartilage.* Vol 5.; 1987.
 40. Pattappa G, Heywood HK, de Bruijn JD, Lee DA. The metabolism of human mesenchymal stem cells during proliferation and differentiation. *J Cell Physiol.* 2011;226(10):2562-2570. doi:10.1002/jcp.22605
 41. Salinas D, Minor CA, Carlson RP, McCutchen CN, Mumey BM, June RK. Combining targeted metabolomic data with a model of glucose metabolism: Toward progress in chondrocyte mechanotransduction. *PLoS One.* 2017;12(1). doi:10.1371/journal.pone.0168326
 42. Ghani QP, Wagner S, Zamirul Hussain ; M. *Role of ADP-Ribosylation in Wound Repair. The Contributions of Thomas K. Hunt, MD.*
 43. Olivares O, Mayers JR, Gouirand V, et al. Collagen-derived proline promotes pancreatic ductal adenocarcinoma cell survival under nutrient limited conditions. *Nat Commun.* 2017;8. doi:10.1038/ncomms16031
 44. Huynh TYL, Zareba I, Baszanowska W, Lewoniewska S, Palka J. Understanding the role of key amino acids in regulation of proline dehydrogenase/proline oxidase (prodh/pox)-dependent apoptosis/autophagy as an approach to targeted cancer therapy. *Mol Cell Biochem.* 2020;466(1-2):35-44. doi:10.1007/s11010-020-03685-y
 45. Loeser RF, Olex AL, McNulty MA, et al. Microarray analysis reveals age-related differences in gene expression during the development of osteoarthritis in mice. *Arthritis Rheum.* 2012;64(3):705-717. doi:10.1002/art.33388
 46. Zheng K, Shen N, Chen H, et al. Global and targeted metabolomics of synovial fluid discovers special osteoarthritis metabolites. *J Orthop Res.* 2017;35(9):1973-1981. doi:10.1002/jor.23482
 47. Piepoli T, Mennuni L, Zerbi S, Lanza M, Rovati LC, Caselli G. Glutamate signaling in chondrocytes and the potential involvement of NMDA receptors in cell proliferation and inflammatory gene expression. *Osteoarthr Cartil.* 2009;17(8):1076-1083. doi:10.1016/j
 48. Stegen S, Laperre K, Eelen G, et al. HHS Public Access. Vol 565.; 2020. doi:10.1038/s41586-019-0874-3.HIF-1 doi:10.1016/j.joca.2009.02.002

49. Tournaire G, Loopmans S, Stegen S, et al. Skeletal progenitors preserve proliferation and self-renewal upon inhibition of mitochondrial respiration by rerouting the TCA cycle. *Cell Rep.* 2022;40(4). doi:10.1016/j.celrep.2022.111105

Chapter 5. General Discussion

5.1 Main conclusions and contributions

This chapter summarizes the main results of the thesis and the main conclusions of the work, placing the work in the broader context of bioprocess engineering for tissue engineering applications, and ends with suggestions for further work.

Bone has the remarkable ability to regenerate without the formation of scar tissue. However, up to 10 % of all fractures result in delayed or non-union. Skeletal tissue engineering inspired by recapitulation of developmental processes, is a promising approach to generate clinically relevant bone and cartilage regeneration, thus offering a solution to the abovementioned unmet clinical need. Although this approach is currently gaining momentum, the lack of critical quality attributes, being able to predict the final product functionality impedes the translation into the clinic. Additionally, there are limited studies examining the scaling up of such processes, necessary for the production of the necessary amounts for cell-based bone and cartilage regeneration in humans.

In this PhD project, we explored the use of metabolomics for the identification of molecular signatures of cartilaginous microtissues during their differentiation *in vitro* and their dynamic culture using an in-house developed stirred tank microbioreactor. We first characterized the metabolic profile during the cascade of the chondrogenic differentiation, from proliferative to prehypertrophic stage using stable isotope tracer analysis (Chapter 3). Our findings further motivated us to investigate the role of glucose dependent *de novo* fatty acid synthesis in chondrogenic differentiation *in vitro* and the bone formation capacity of the tissue-engineered constructs *in vivo*. (Chapter 3). Finally, we provided a proof of concept for the dynamic culture of cartilaginous microtissues in a stirred tank in-house developed microbioreactor system. We characterized the mechanical environment of the bioreactor culture using computational modeling and we investigated the effect of dynamic culture on gene expression and exometabolome of the cartilaginous microtissues. These findings increase our knowledge of the bioenergetics during chondrogenic differentiation and the potential link of metabolic profiles *in vitro* with the bone formation capacity *in vivo*. Additionally, these findings provide novel insights into the dynamic culture of cartilaginous microtissues, proposing an integrated toolbox of computational modeling and exometabolomics for thorough characterization of their production (Chapter 4). Taken together, these findings propose the use of metabolic profiling together with other omics data in the exploration of novel critical quality attributes in the context of Quality Cell Therapy by Design concept.

5.1.1 Metabolic profiling of callus microtissues during their chondrogenic differentiation *in vitro*.

The main goal of this PhD project was the metabolic characterization of the callus microtissue modules generated by subjecting microaggregates of human periosteum-derived cells (hPDCs) to chondrogenic differentiation *in vitro*. This in-house developed process has shown promising results of regeneration of critical size tibial defects in mice. We anticipated that the metabolic characterization of the callus microtissues is a critical step towards identifying molecular signatures used as critical quality attributes for the clinical translation of the process developed in the lab.

At the start of this PhD, only limited exploration of the skeletal cell metabolism had taken place, yet during recent years, the metabolic understanding of skeletal cells and their chondrogenic differentiation in particular, has progressively increased^{1,2,3,4}. Most of these research efforts focused on the role of glucose⁵, but only a few of those studies were conducted on periosteum-derived cells^{6,7,8}. Additionally, many studies have been conducted in 2D culture conditions, which significantly limits their accuracy in reflecting the *in vivo* microenvironment and cell-cell interactions. Another important aspect is that most of our current knowledge is derived from metabolic studies in mouse models. Although valuable knowledge has been generated in these models, there is a clear need for validation of these findings in human cells which will be used for future clinical applications. An important contribution of this thesis is the characterization of metabolism in a 3D cell culture model of hPDC-based cartilaginous microtissues, mimicking as closely as possible the *in vivo* cell state. Addressing the above-mentioned challenges, our findings also add to the current body of knowledge on the metabolism of hPDCs during microtissue-based chondrogenic differentiation *in vitro*.

Stable tracer analysis and exometabolomics revealed metabolic profiles of the human cartilaginous microtissues that are coherent with what is known to date on the metabolism of growth plate chondrocytes. We identified enrichment of glutamine in proline and hydroxyproline and we showed that glutamine metabolism was linked to ECM production in the early stages of the *in vitro* differentiation, followed by matrix remodeling in the later stages, aligning with a mechanistic study by Stegen et al⁸., carried out in murine cells. These findings are also important from a developmental engineering point of view, pointing towards the recapitulation of metabolic features of the native tissue (i.e. transient cartilage). Notably, this thesis also revealed alterations in a metabolic pathway largely unexplored in the context of chondrogenic differentiation. We identified a progressive increase in glucose-dependent *de novo* fatty acid synthesis from the proliferative towards the (pre)hypertrophic stage of the microtissue differentiation process. These results were further explored by studying in more

detail the role of this metabolic pathway during the *in vitro* differentiation of the microtissues and the functionality of the microtissues-based construct *in vivo*.

Overall, this thesis proposed the integration of metabolomics in developmental bone tissue engineering strategies. This research approach adds valuable information on the phenotypic characterization of cartilaginous microtissues and therefore can contribute to the relevance of such systems as drug screening platforms. It is important to note that this phenotypic characterization may contribute to the development of strategies enhancing the differentiation process of cartilaginous microtissues as discussed in further detail in the *perspectives and future research* section.

5.1.2 Investigating the role of *de novo* fatty acid synthesis during cartilaginous microtissue differentiation *in vitro* and the functionality of microtissue-based constructs *in vivo*.

To study the role of the glucose dependent *de novo* fatty acid synthesis in the cartilaginous microtissues during their differentiation, we performed chemical inhibition of Fatty Acid Synthase (FASN), using tetrahydro-4-methylene-2R-octyl-5-oxo-3S-furancarboxylic acid (C75), an inhibitor widely used in cancer metabolism studies^{9,10}. We observed no significant difference in cell viability and proliferation in the C75 treated microtissues on Day 21 compared to the control group. ones. Transcriptomic profiling identified significant downregulation of important regulators of endochondral ossification including chondrocyte hypertrophy activators, as well as downregulation of gene expression of collagens, and signaling factors of hypertrophy and angiogenesis. Interestingly, transcriptomic profiling demonstrated ferroptosis as an enriched pathway of the C75-driven inhibition. Further research is required to verify if fatty acid synthesis induces ferroptosis and whether this metabolic pathway may contribute to the survival mechanisms of the chondrocytes, escaping ferroptosis, as has been shown in cancer cells. Evaluating the effect of c75-driven FASN inhibition on *in vivo* bone forming capacity, we concluded that it led to poor survival of the C75 treated microtissue-based constructs as opposed to the control ones.

5.1.3 Stirred culture of cartilaginous microtissues promotes chondrogenic hypertrophy through exposure to intermittent shear stress.

In the second part of this PhD, we investigated the impact of dynamic culture conditions on the process of cartilaginous differentiation of microtissues using a novel in house developed microbioreactor system. This was carried out in order to develop a suspension process where the metabolomics analysis could be used as a non-destructive monitoring approach for microtissue quality. Moreover, suspension culture in bioreactors can be easily scaled up in the future to larger volumes following established scalability principles. We characterized the mechanical environment to which the cartilaginous microtissues were exposed to during mixing, using a center-based model (CBM) coupled with a computational fluid dynamics (CFD) solver. This combined *in vitro- in silico* approach provided a more accurate estimate of the microtissue shear stress exposure enabling individual module assessment. We identified operating conditions where suspension of the microtissue dispersion was obtained while avoiding shear damage. As hPDCs are mechanosensitive cells¹¹, we aimed to understand the impact of shear stress in the microtissues' chondrogenic capacity. Shear stress was found to be a factor accelerating chondrogenic differentiation with enhanced hypertrophy as indicated by the upregulation of relevant gene markers. This is important for the formation of bone through endochondral ossification upon implantation of the microtissue-based construct. Additionally, exometabolomics revealed distinct metabolic readouts for the dynamic process. These findings form the starting point of a future in-depth endometabolomics characterization, using said readouts as critical quality attributes of the biomanufacturing process.

5.2 Perspectives and future research.

In this section, we make different suggestions to extend the impact of the current research.

5.2.1 The need of recapitulating the *in vivo* metabolic profile

In this dissertation, we performed stable-isotope tracer analysis in a 3D cell culture platform of cartilaginous microtissues, following a developmental engineering approach. Although this platform offers a unique opportunity of mimicking steps occurring during endochondral ossification (production of cartilage tissue intermediate), it is important that a biomimetic approach is followed regarding other aspects of the process. More specifically, the aim should be to recapitulate the metabolic characteristics of the *in vivo* microenvironment as closely as possible, including the use of physiological tension¹² and appropriate culture media¹³.

Currently, the commercially available medium that has been used in the study contains suprphysiologic levels of certain metabolites (for example, amino acids). In the context of the cartilage tissue environment, given its avascular nature, the use of physiologic media that better recapitulates the nutrient composition of different micro and macro cell environments that the microtissues will experience *in vivo* (from proliferation towards prehypertrophy) becomes essential to improve the physiological relevance of *in vitro* metabolic studies.

5.2.2 Towards a more comprehensive understanding of metabolism of chondrogenic differentiation

Despite the exponential progress that has been made in the last 7 years, our knowledge of skeletal cell metabolism and, more specifically, the metabolic changes during chondrogenic differentiation, is still limited. In this PhD project, the metabolic profile of different stages of chondrogenic differentiation of hPDC-based microtissues was defined. Linked with the heterogeneous nature of periosteum, the initial cell population of hPDCs may contain different progenitor cells and therefore it is also expected to generate different cellular phenotypes within each microtissue. scRNAseq^{14,15} will provide better identification of different cell populations within microtissues. Although in its infancy, technological advances in the field of single cell metabolomics^{16,17} and spatial metabolomics¹⁸ together with single cell transcriptomics will deepen our understanding of the metabolic identity of different cell populations, thus defining how metabolism can control the shift from proliferation to prehypertrophic state during chondrogenic differentiation.

5.2.3 Role of Fatty Acid Synthesis on chondrogenic differentiation and endochondral bone formation

The use of stable isotope tracer analysis in this dissertation (Chapter 3) underscored the importance of de novo fatty acid synthesis for the chondrogenic differentiation and the bone forming capacity of the cartilaginous microtissues.

Further work is required to fully understand the effect of the pharmacological inhibition of FASN during the microtissue differentiation *in vitro* and the resulting bone formation *in vivo*. Our findings provide new insight into the effect of fatty acid synthesis inhibition on the transcriptome level *in vitro*. However, additional information from histology would be required to validate further the effect of FASN inhibition on the resulting phenotype of the microtissues. Furthermore, transcriptomic analysis showed upregulation of metabolic genes, suggesting

activation of metabolic pathways to compensate as a response to fatty acid synthesis inhibition. Stable isotope tracer analysis of C75 treated microtissues versus the vehicle control can provide us with improved insights into the effect of the inhibition on the metabolic level. Furthermore, given the complexity of fatty acid metabolism, the use of labeled palmitate is necessary to reveal its fate and thus advanced insight into the role of de novo lipogenesis for chondrogenic differentiation. Blocking FASN revealed ferroptosis as one of the upregulated pathways using RNAseq analysis. Further research includes the use of lipid peroxidation assays for the *in vitro* culture to validate this indication of ferroptosis in the C75 treated microtissues, as shown by the transcriptomics results.

Our *in vivo* findings demonstrated that pharmacological inhibition of fatty acid synthesis led to poor survival of the *in vivo* constructs as opposed to the control ones. As we chose to implant the constructs for a period of 4 weeks, it would be of great interest, though, to investigate the impact of the FASN inhibition in earlier time points, to investigate in which phase of the endochondral ossification progress FASN is crucial. These studies would identify the cause of potential delays in the endochondral ossification process *in vivo* in the C75 treated microtissues as compared to the vehicle control ones as the stage of the process that is affected.

Our findings raise the question whether enhancing fatty acid synthesis can be beneficial for the outcome of our process *in vitro* and *in vivo*. The enhancement of fatty acid synthesis using metabolic engineering¹⁹ methods may be an interesting strategy, although not yet implemented in a regeneration setting. The use of exogenous fatty acids/lipids needs further investigation to see whether it can support the survival and boost the chondrogenic hypertrophy of the callus microtissues. Lipid supplementation can be technically challenging though as lipotoxicity^{20,21} phenomenon should be avoided by appropriate dosing. Subsequent studies include the examination of whether supplementation of fatty acids can improve chondrogenic differentiation *in vitro* and the functional outcome of engineered constructs after ectopic implantation in mice. On that aspect data from mechanistic studies are highly valuable, where the metabolism of the native tissue is characterized in depth.

5.2.4 Further investigation of the effect of dynamic culture conditions

In Chapter 4, we provided a proof of concept for scalable production of callus microtissues using a mini bioreactor system. This study improved our understanding of the impact of dynamic culture conditions in the chondrogenic differentiation process *in vitro* but further

experiments are needed to describe in a more accurate way the effect on the phenotype of the microtissues. More specifically the dynamic culture conditions showed enhanced hypertrophy, as indicated by upregulation of relevant gene markers. Suggested next steps include histological assessment of hypertrophy as well as (bulk) transcriptomics to provide new information about other aspects of the effect of the dynamic culture in the chondrogenic differentiation *in vitro*. The latter, coupled with an in-depth characterization of the metabolism, is essential for the identification of molecular signature linked to the differentiation capacity under dynamic conditions. The comparison of metabolic data obtained in the dynamic condition with the thorough study of metabolic features of the static conditions (Chapter 3) is a starting point towards this direction. In particular, it is of great interest to understand the effect of fatty acid synthesis (investigated in Chapter 3) in dynamic conditions. Further validation of the importance of this pathway for *in vitro* bioreactor conditions could be the basis for the confirmation of this metabolic feature as one novel critical quality attribute for chondrogenic differentiation of the callus microtissues. Future work should also look into the effects of scaling up the bioreactor culture process, ensuring the controlled size of the microtissues and homogeneous size distribution and differentiation capacity. Moreover, scaling up should include the integration of automation and controllability elements in the bioreactor process.

5.3 General perspectives

5.3.1 Towards integration of metabolomics in manufacturing of cartilaginous microtissues

The identification of CQAs related to ATMP potency is critical to address one of the biggest challenges that hinders clinical translation in cell therapy. Metabolomics approaches together with other omics data coupled with computational modeling can identify correlations to functional *in vivo* outcomes (*in vivo* bone formation) as shown in studies of other cell therapy applications. Metabolomics data such as those produced in this thesis offer a great potential to provide a panel of potency markers, given the proximity of metabolome to the cell phenotype. Intracellular metabolite data can serve as ‘at process’ data and together with extracellular metabolite data – (‘in process’ data), can be integrated into machine learning models. These models can help us in the identification of multivariate parameters that are predictive of the final manufacturing product phenotype. An example of a machine learning model used to identify the molecular signature of stem cells is the CellNet platform. CellNet uses RNAseq data to train machine learning models to classify cell types. Similarly to the CellNet platform, our metabolic data can be used for the development of a quantitative control system in the context of developmental tissue engineering. Additionally, future studies

including the use of single cell metabolomics together with single cell RNAseq data as refined data sets in relevant machine learning models, can reveal information regarding the heterogeneity of cartilaginous microtissues-and their spatiotemporal regulation.

An important aspect of clinically relevant biomanufacturing in autologous cell therapy is mapping and understanding donor to donor variation in process efficiency and product quality. Given its sensitivity, metabolomic analyses can reveal differences in the molecular signature of different donors and correlate this information with *in vivo* bone formation in a robust way.

5.3.2 Incorporation of metabolomics in the standardized PAT of microtissue-based bioprocess-Opportunities and Challenges

Metabolomics analysis, due to its sensitivity and high throughput nature, has the potential to be integrated into the Quality by Design (QbD) approach to maintain product quality in a bioprocess. There is significant potential in combining machine learning methods and large metabolome data sets²², as also discussed in the previous section. It remains a challenge though to contextualize the biological information obtained from metabolomics to its relevance to specific parameters in the bioprocess performance. A nice example of integration of metabolomics is described in the study of Zucker et al, where a multivariate analysis of intracellular and extracellular metabolome data led to the development of an improved predictive model of glycosylation in CHO cultures²³. Finally, metabolomics analysis offers the unique opportunity to integrate intracellular mechanisms in macroscopic models used in online bioprocess control. As shown by Nimmegeers et al²⁴., this kind of models built on actual metabolomics data pave the way for the future of model predictive control in bioprocess development via the use of soft sensors.

5.4 Conclusion

To conclude, during this PhD project, we pushed one step forward in the characterization of quality attributes for the in-house established developmental engineering strategy. Additionally, we explored suspension culture as a means to switch to a more scalable culture platform, using said quality attributes for a better understanding of the process. The prime focus of this PhD project was the characterization of metabolic profiles of cartilaginous microtissues differentiation *in vitro*. By using tracer analysis, we identified several pathways in alignment to the current knowledge of cartilage metabolism. Interestingly, our study underscored the importance of the largely unexplored, in the context of chondrocyte

metabolism, glucose dependent de novo fatty acid synthesis for the differentiation *in vitro*, and the bone forming capacity of cartilaginous microtissues after implantation *in vivo*. These findings add significantly to the phenotypic characterization of microtissue-based chondrogenic differentiation. Therefore, this can potentially act as the starting point of defining critical quality attributes, necessary for the clinical translation. As an additional important part of the clinical translation in the long run, in the second part of this PhD, we provided proof of concept of production of cartilage microtissues in a stirred tank mini bioreactor. We investigated the exometabolome, as a starting point to integrate metabolic profiling as an added layer of phenotypic information during the bioreactor culture. Eventually, we anticipate that these insights can pave the way for implementing metabolomics in the pipeline of scaled up production of cartilaginous microtissues possessing robust bone formation functionality upon *in vivo* implantation.

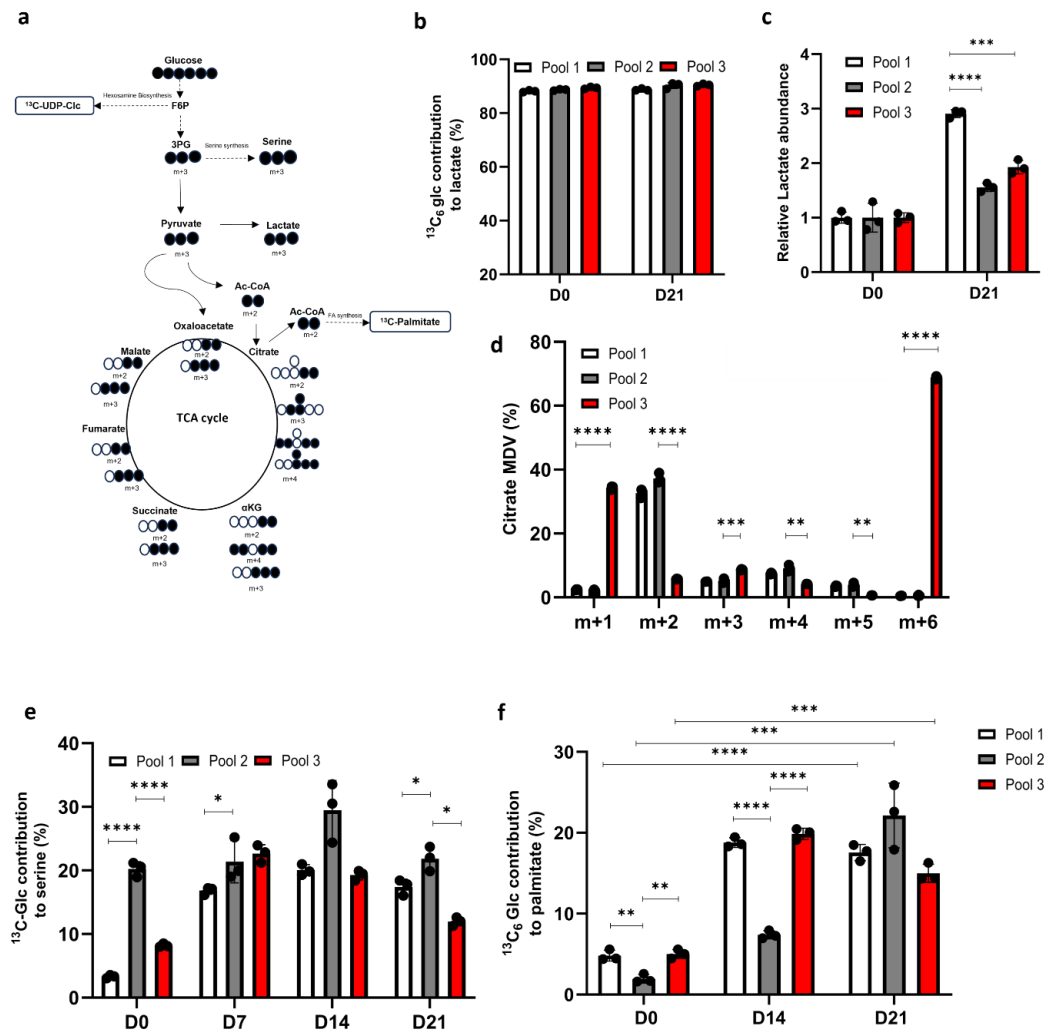
5.5 References

1. van Gastel, N. & Carmeliet, G. Metabolic regulation of skeletal cell fate and function in physiology and disease. *Nat. Metab.* 3, 11–20 (2021).
2. Devignes, C. S., Carmeliet, G. & Stegen, S. Amino acid metabolism in skeletal cells. *Bone Reports* 17, 101620 (2022).
3. Karsenty, G. & Khosla, S. The crosstalk between bone remodeling and energy metabolism: A translational perspective. *Cell Metab.* 34, 805–817 (2022).
4. Stegen, S. & Carmeliet, G. Metabolic regulation of skeletal cell fate and function. *Nat. Rev. Endocrinol.* (2024) doi:10.1038/s41574-024-00969-x.
5. Lee, S. Y., Abel, E. D. & Long, F. Glucose metabolism induced by Bmp signaling is essential for murine skeletal development. *Nat. Commun.* 9, 1–11 (2018).
6. Stegen, S. et al. Glutamine Metabolism Controls Chondrocyte Identity and Function. *Dev. Cell* 53, 530-544.e8 (2020).
7. Stegen, S. et al. De novo serine synthesis regulates chondrocyte proliferation during bone development and repair. *Bone Res.* 10, (2022).
8. Stegen, S. et al. HIF-1 α metabolically controls collagen synthesis and modification in chondrocytes. *Nature* 565, 511–515 (2019).
9. Kuhajda, F. P. et al. Synthesis and antitumor activity of an inhibitor of fatty acid synthase. *Proc. Natl. Acad. Sci. U. S. A.* 97, 3450–3454 (2000).
10. Koundouros, N. & Poulogiannis, G. Reprogramming of fatty acid metabolism in cancer. *Br. J. Cancer* 122, 4–22 (2020).
11. Moore, E. R., Zhu, Y. X., Ryu, H. S. & Jacobs, C. R. Correction to: Periosteal progenitors contribute to load-induced bone formation in adult mice and require primary cilia to sense mechanical stimulation (*Stem Cell Research & Therapy* (2018) 9 (190) DOI: 10.1186/s13287-018-0930-1). *Stem Cell Res. Ther.* 9, 1–15 (2018).
12. Ast, T. & Mootha, V. K. Oxygen and mammalian cell culture: are we repeating the experiment of Dr. Ox? *Nat. Metab.* 1, 858–860 (2019).
13. Lagziel, S., Gottlieb, E. & Shlomi, T. Mind your media. *Nat. Metab.* 2, 1369–1372 (2020).
14. Chan, C. K. F. et al. Identification of the Human Skeletal Stem Cell. *Cell* 175, 43-56.e21 (2018).
15. Chan, C. K. F. et al. Identification and specification of the mouse skeletal stem cell. *Cell* 160, 285–298 (2015).
16. Alexandrov, T. the Age of Artificial Intelligence. 61–87 (2020).
17. Hartmann, F. J. et al. Single-cell metabolic profiling of human cytotoxic T cells. *Nat. Biotechnol.* 39, 186–197 (2021).

18. Wang, G. et al. Spatial dynamic metabolomics identifies metabolic cell fate trajectories in human kidney differentiation. *Cell Stem Cell* 29, 1580-1593.e7 (2022).
19. Liu, J., Mandlaa, Wang, J., Sun, Z. & Chen, Z. A strategy to enhance and modify fatty acid synthesis in *Corynebacterium glutamicum* and *Escherichia coli*: overexpression of acyl-CoA thioesterases. *Microb. Cell Fact.* 22, 1–15 (2023).
20. Stanley, W. C., Recchia, F. A. & Lopaschuk, G. D. Myocardial substrate metabolism in the normal and failing heart. *Physiol. Rev.* 85, 1093–1129 (2005).
21. Alsabeeh, N. et al. HHS Public Access. 1863, 143–151 (2019).
22. Shimizu, H. & Toya, Y. Recent advances in metabolic engineering—integration of in silico design and experimental analysis of metabolic pathways. *J. Biosci. Bioeng.* 132, 429–436 (2021).
23. Zürcher, P. et al. Cell culture process metabolomics together with multivariate data analysis tools opens new routes for bioprocess development and glycosylation prediction. *Biotechnol. Prog.* 36, 1–11 (2020).
24. Nimmegeers, P., Vercammen, D., Bhonsale, S., Logist, F. & Van Impe, J. Metabolic reaction network-based model predictive control of bioprocesses. *Appl. Sci.* 11, (2021).

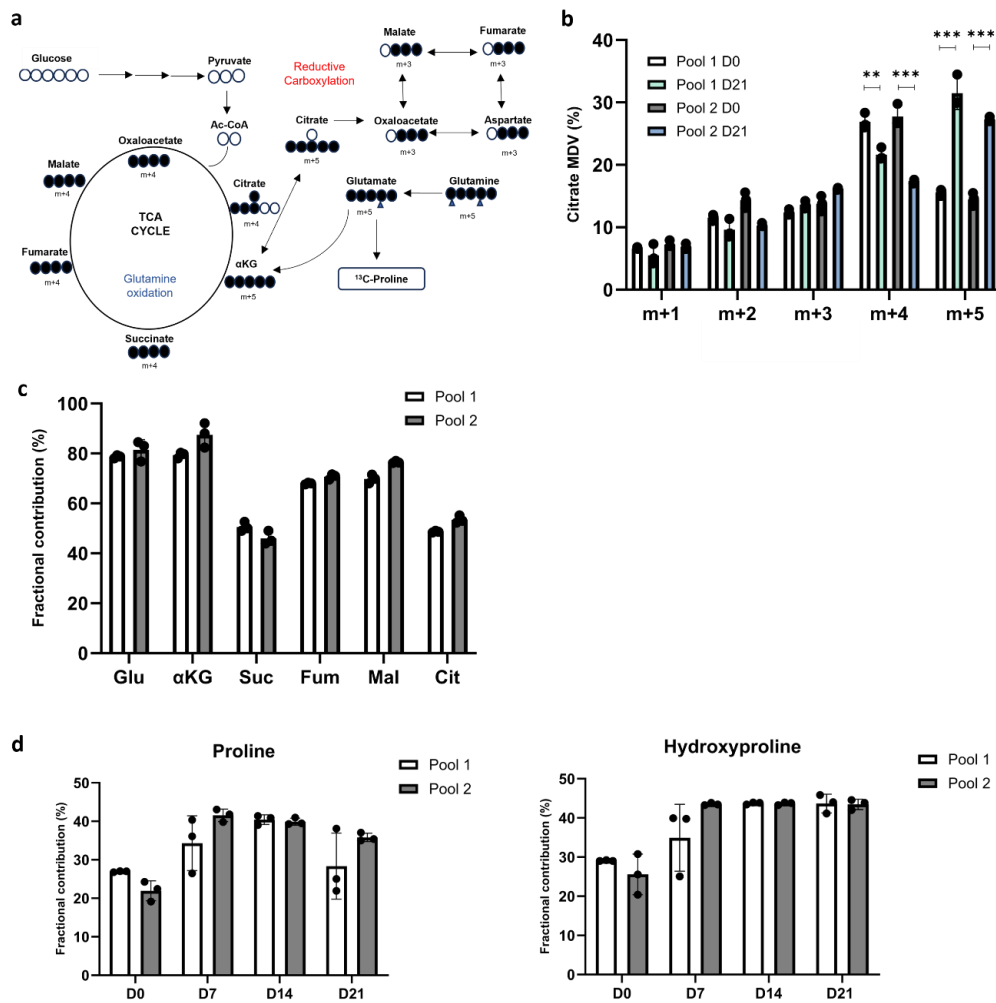
Appendix A

Supporting Information of Chapter 3



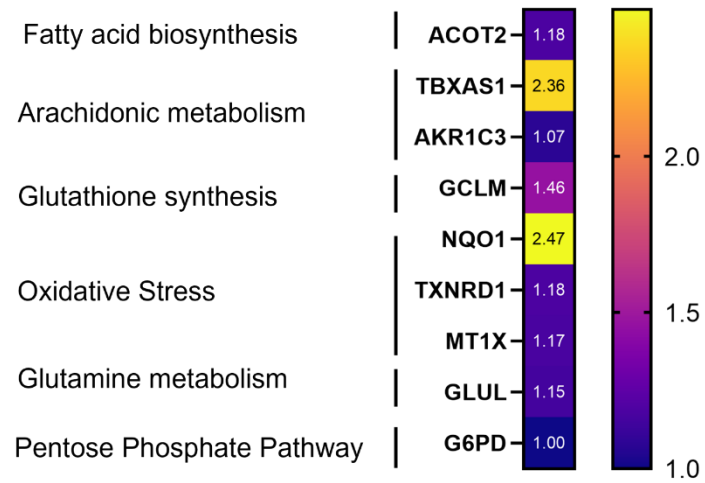
Extended Data Figure 1. Use of glucose carbon in cartilaginous microtissues assembled from different hPDCs cell pools during their differentiation

a) Schematic of carbon atom (circles) transitions of $^{13}\text{C}_6\text{Glc}$ used to detect label incorporation into indicated metabolites. Black filled circles represent ^{13}C , whereas white circles represent ^{12}C . F6P is fructose-6-phosphate, 3PG is 3-phosphoglycerate. Ac-Coa is Acetyl-CoA, αKG is α -ketoglutarate. b) Fractional contribution of $^{13}\text{C}_6\text{Glc}$ to lactate of D0 and D21 microtissues, assembled from cells of pool 1 (white), pool 2 (grey) and pool 3 (red) ($n=3$). c) Relative intracellular abundance of lactate of D0 and D21 microtissues, ($n=3$). d) Citrate labelling from $^{13}\text{C}_6\text{Glc}$ glucose at D21 microtissues assembled from the different cell pools. e) $^{13}\text{C}_6\text{Glc}$ incorporation to serine over in vitro culture time for microtissues assembled from different cell pools. ($n=3$). f) $^{13}\text{C}_6\text{Glc}$ incorporation to palmitate over in vitro culture time for microtissues assembled from different cell pools, ($n=3$). The data are represented as means \pm SEM. * $p < 0.05$, ** $p < 0.01$, *** $p < 0.001$, one way ANOVA followed by Tukey's multiple comparison test. Relevant mass distribution vectors (MDVs) are shown in d.



Extended Data Figure 2. Glutamine tracing analysis during differentiation of cartilaginous microtissues of different hPDCs cell pools.

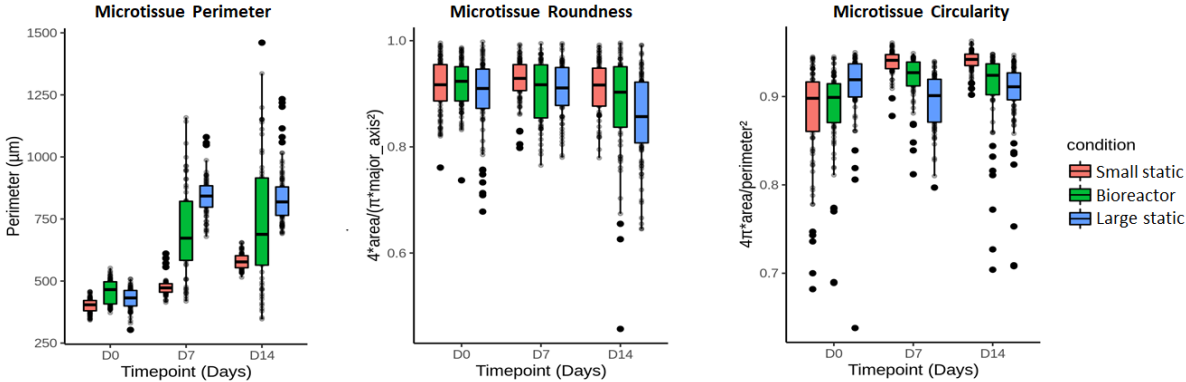
a) Schematic of carbon (circles) and nitrogen (triangles) atom transitions of $^{13}\text{C}_5$ Gln used to detect label incorporation into indicated metabolites. Black filled circles represent ^{13}C , whereas white circles represent ^{12}C . b) Citrate labelling from $^{13}\text{C}_5$ Gln at D0 and D21 microtissues via glutamine oxidation (m+4) and via reductive carboxylation (m+5), assembled from cell pool 1 (white and green respectively) and cell pool 2 (gray and blue respectively), (n=3) c) Fractional contribution of $^{13}\text{C}_5$ Gln of D21 microtissues to TCA cycle metabolites in cell pool 1 (white) and cell pool 2 (gray). d) $^{13}\text{C}_5$ Gln incorporation to proline and hydroxyproline during differentiation of cartilaginous microtissues showed similar trend between the two different cell pools (cell pool 1 in white, cell pool 2 in gray) , (n=3), The data are represented as means \pm SEM *p< 0.05, **p< 0.01, ***p< 0.001, one way ANOVA followed by Tukey's multiple comparison test.



Extended data Figure 3 .Significantly upregulated metabolic genes of D21 C75 treated microtissues versus the vehicle control ones. The scale refers to log2foldchange.

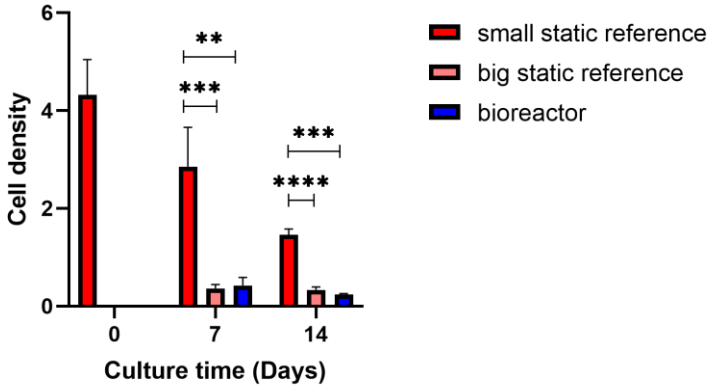
Appendix B

Supporting Information of Chapter 4



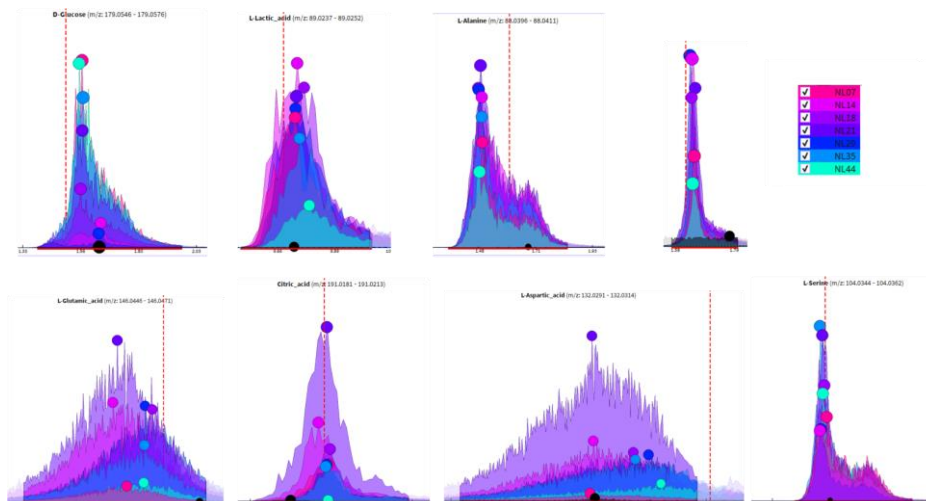
Supplementary Figure S1. Microtissue perimeter, roundness and circularity for static and dynamic conditions over time.

Red represents the small static reference, blue the large static and green the bioreactor condition. The biggest variations in tissue morphology characteristics were observed in bioreactor condition at the end of the in vitro process (Day 14).



Supplementary Figure S2. Cell density (cell number/volume aggregate) for static and bioreactor conditions over time.

Blue color represents the dynamic condition, pink the static big microtissues and red the static small microtissues. *p < 0.05, **p < 0.01, ***p < 0.001, one way ANOVA followed by Tukey's multiple comparison test. Blue color represents the dynamic condition, pink the static big microtissues and red the static small microtissues.



Supplementary Figure S3. Representative chromatograms of the metabolites analyzed in the medium.

The different colors (see legends) represent conditions (static and bioreactor) over time. Cell density

Scientific acknowledgement

Research presented in this thesis was funded by the Fonds Nationale de la Recherche Scientifique (FRS-FNRS, FRIA mandate), the special Research Fund from KULeuven (C24/17/077) and European Union's Horizon 2020 research and innovation programme under grant agreement No 772418 (European Research Council CoG INSITE) and the European Union's Horizon 2020 research and innovation programme under grant agreement No 874837.

Curriculum Vitae

Personal information

Niki Loverdou	Date of birth: February 14 th 1990
Paparrigopoulou 39-41	Place of birth: Athens, Greece
153 43 Athens, Greece	Nationality: Greek
Tel.: +32 4 85 98 59 52	niki.loverdou@kuleuven.be

Education

Doctoral school of Engineering Science

2015-2024, KU Leuven, Leuven, Belgium

University of Liège, Liège, Belgium

Promoters: Prof. Liesbet Geris, Prof. Kristel Bernaerts, Prof. Ioannis Papantoniou

Diploma in Chemical Engineering (Msc)

2009-2014, Department of Chemical Engineering, University of Patras, Patras, Greece

Diploma thesis: Metabolomic analysis of heart under adult onset hypothyroidism in a mouse model

Promoter: Dr. Maria. I. Klapa, Metabolic Engineering and Systems Biology Laboratory, ICE-HT/FORTH, Patras, Greece

Fellowships and awards

FRIA-FNRS doctoral mandate

December 2016-December 2019

Young Investigator Travel Grant

ESACT course for animal cell technology 2017

Young Investigator Travel Grant

Herbert Fleisch Workshop 2019 ASBMR/IBMS travel grant

Young Investigator Travel Grant

ESACT course for Bioprocessing and Manufacturing of Gene and Cell Therapy products 2022

Mentoring

Master thesis Chemical Engineering, KU Leuven

Maarten Croonen, September 2017-June 2017

Master thesis Chemical Engineering, KU Leuven

An-Sofie Christaens, September 2017-June 2018

Master thesis Chemical Engineering, KU Leuven

Giulia de Dorlodot, September 2018-June 2019

Master thesis Biomedical Engineering, KU Leuven

Bjorn Kenis, September 2018-June 2019

Publications

Loverdou N., Nilsson-Hall G., Cuvelier M., Christiaens A.S., Bernaerts K., Smeets B., Ramon, H., Luyten, F.P. Geris, L., Papantoniou, I. “Stirred culture of cartilaginous microtissues promotes chondrogenic hypertrophy through exposure to intermittent shear stress.”, 2022, Bioengineering and Translational Medicine

Papantoniou I., Nilsson-Hall G. **Loverdou N.**, Lesage R., Herpelinck T., Mendes L., Geris L., “Turning Nature’s own processes into design strategies for living bone implant biomanufacturing: a decade of Developmental Engineering”, 2020, Advanced Drug delivery reviews

Ioannis Papantoniou, Toon Lambrechts, Priyanka Gupta, Sébastien de Bourmonville, **Niki Loverdou**, Liesbet Geris, Jean-Marie Aerts (2017). Bioreactor Sensing and Monitoring for Cell Therapy Manufacturing Bioreactors for Stem Cell Expansion and Differentiation, Taylor and Francis Publishing group (book chapter)

Loverdou N., Nilsson-Hall, G., Stegen S., Bernaerts K., Garcia Caballero M., Ghesquiere B. , Carmeliet P., Carmeliet G., Papantoniou I., Geris L “Metabolic alterations during chondrogenic differentiation in spheroids: towards identification of metabolic markers for endochondral ossification.”, manuscript in preparation

Conferences

N.Loverdou, G.Nillson Hall, I.Papantoniou, L.Geris “Exometabolomics profiling as a quality control for chondrogenic differentiation in spheroids” In :“BSMS 2017”, XXth annual meeting in Leuven at KULeuven, 8 February 2017, Leuven, Belgium (oral presentation)

N.Loverdou, G.Nillson Hall, I.Papantoniou, L.Geris “Developing a metabolomics protocol for chondrogenic microtissues” In :“BSTE 2017”, 5TH Belgian Symposium on Tissue Engineering, 4-5 May 2017, Leuven, Belgium (poster presentation)

N.Loverdou, G.Nillson Hall, K.Bernaerts, B.Ghesquiere, G.Carmeliet, I.Papantoniou, L.Geris “Metabolomics as a high sensitivity quality control tool for the characterization of chondrogenic microtissues”, Metabolic Engineering 12, 24-28 June 2018, Munich, Germany (poster presentation)

N.Loverdou, G.Nillson Hall, K.Bernaerts, B.Ghesquiere, G.Carmeliet,I.Papantoniou, L.Geris
“Stable isotope resolved metabolomics identified metabolic alteration of periosteal cells cultures as spheroids”, ESBES 2018, 9-12 September 2018, Lisbon, Portugal (oral presentation)

N.Loverdou, G.Nillson Hall, K.Bernaerts, B.Ghesquiere, G.Carmeliet,I.Papantoniou, L.Geris
“Metabolomics as a High sensitivity quality control tool for the characterization of chondrogenic microtissues, Metabolism in Cancer and Stromal Cells (2nd Edition), Leuven, 26-27 November 2018 (poster presentation)

N.Loverdou, G.Nillson Hall, K.Bernaerts, B.Ghesquiere, G.Carmeliet,I.Papantoniou, L.Geris
“Identifying metabolic alterations during chondrogenic differentiation of periosteal cells cultured in spheroids” 26th ESACT meeting, May 5-8 2019, Copenhagen, Denmark (poster presentation)

N.Loverdou, G.Nillson Hall, K.Bernaerts, B.Ghesquiere, G.Carmeliet,I.Papantoniou, L.Geris,
“Metabolomics as a quality control for the production of chondrogenic microtissues. Towards characterized endochondral bone regeneration”, 15th Annual Conference of the Metabolomics Society, Metabolomics 2019, June 23-27 2019, The Hague, Netherlands (oral presentation)

N.Loverdou, G.Nillson Hall, K.Bernaerts, B.Ghesquiere, G.Carmeliet,I.Papantoniou, L.Geris,
“Identifying metabolic alterations during chondrogenic differentiation of periosteal cells cultured in spheroids”, 7th International conference on Stem Cell Bioengineering, 11-13 December, 2019, Barcelona, Spain (oral presentation)

N.Loverdou, G.Nillson Hall, S.Stegen, K.Bernaerts, B.Ghesquiere, M. Caballero, P.Carmeliet, G.Carmeliet, I.Papantoniou, L.Geris, “Metabolic alterations during chondrogenic differentiation in spheroids: Towards identification of metabolic markers for endochondral ossification”, 6th WORLD TERMIS, 15-19 November 2021, online, (oral presentation)

N.Loverdou, G.Nillson Hall, S.Stegen, K.Bernaerts, B.Ghesquiere, M. Caballero, P.Carmeliet, G.Carmeliet, I.Papantoniou, L.Geris, “Stirred culture of cartilaginous microtissues promotes chondrogenic hypertrophy through exposure to intermittent shear stress.”, TERMIS EU-Chapter, 28-06/1-07 2022, Krakow, Poland (oral presentation)